BPC-01-300-3
Revision 0
January 1984

HOPE CREEK GENERATING STATION
PLANT UNIQUE ANALYSIS REPORT
VOLUME 3
VENT SYSTEM ANALYSIS

Prepared for:
Public Service Electric and Gas Company

Prepared by:
NUTECH Engineers, Inc.
San Jose, California

Prepared by:

Robert S. Quinn

R. D. Quinn, P.E.
Senior Engineer

Reviewed by:

Y. C. Yiu

Y. C. Yiu, P.E.
Group Leader

Approved by:

N. W. Edwards

N. W. Edwards, P.E.
President

Issued by:

Robert A Lehnert

R. A. Lehnert, P.E.
Project Manager

nutech ENGINEERS

REVISION CONTROL SHEET

TITLE: Hope Creek Generating Station
Plant Unique Analysis Report
Volume 3

DOCUMENT FILE NUMBER: BPC-01-300-3
Revision 0

H. Fatehi/Specialist	HKF Initials
M. C. Hsieh/Consultant I	MCH Initials
L. R. Hussar/Engineer	LRH Initials
A. Imandoust/Consultant I	A.I. Initials
R. A. Lehnert/Project Manager	RAL Initials
G. S. Ma/Consultant II	GSM Initials
R. D. Quinn/Senior Engineer	RDQ Initials
M. Shamszad/Senior Engineer	MS Initials
J. A. Treiber/Associate Engineer	JAT Initials
C. S. Wu/Consultant I	CSW Initials
Y. C. Yiu/Group Leader	YCY Initials

REVISION CONTROL SHEET

(CONTINUATION)

TITLE: Hope Creek Generating Station Plant Unique Analysis Report, Volume 3

DOCUMENT FILE NUMBER: BPC-01-300-3 Revision 0

AFFECTED PAGE(S)	DOC REV	PREPARED BY / DATE	ACCURACY CHECK BY / DATE	CRITERIA CHECK BY / DATE	REMARKS
ii	0	RDD/1-30-84	ycy/1-30-84	RAL/1-30-84	
iii	0				
iv	0				
v	0				
vi	0				
vii	0				
viii	0				
ix	0				
x	0				
xi	0				
xii	0				
3-1.1	0				
3-1.2	0				
3-1.3	0				
3-1.4	0		ycy/1-30-84	RAL/1-30-84	
3-2.1	0		LRH/1-30-84	ycy/1-30-84	
3-2.2	0				
3-2.3	0				
3-2.4	0				
3-2.5	0				
3-2.6	0				
3-2.7	0				
3-2.8	0				
3-2.9	0				
3-2.10	0				
3-2.11	0				
3-2.12	0				
3-2.13	0				
3-2.14	0				
3-2.15	0				
3-2.16	0				
3-2.17	0				
3-2.18	0				
3-2.19	0	RDD/1-30-84	LRH/1-30-84	ycy/1-30-84	

REVISION CONTROL SHEET (CONTINUATION)

TITLE: Hope Creek Generating Station Plant Unique Analysis Report, Volume 3

DOCUMENT FILE NUMBER: BPC-01-300-3 Revision 0

AFFECTED PAGE(S)	DOC REV	PREPARED BY / DATE	ACCURACY CHECK BY / DATE	CRITERIA CHECK BY / DATE	REMARKS
3-2.20	0	ROQ/1-30-84	LRH/1-30-84	ycy/1-30-84	
3-2.21	0				
3-2.22	0				
3-2.23	0				
3-2.24	0				
3-2.25	0				
3-2.26	0				
3-2.27	0				
3-2.28	0				
3-2.29	0				
3-2.30	0				
3-2.31	0				
3-2.32	0				
3-2.33	0				
3-2.34	0				
3-2.35	0				
3-2.36	0				
3-2.37	0				
3-2.38	0				
3-2.39	0				
3-2.40	0				
3-2.41	0				
3-2.42	0				
3-2.43	0				
3-2.44	0				
3-2.45	0				
3-2.46	0				
3-2.47	0				
3-2.48	0				
3-2.49	0				
3-2.50	0				
3-2.51	0				
3-2.52	0	ROQ/1-30-84	LRH/1-30-84	ycy/1-30-84	

REVISION CONTROL SHEET
(CONTINUATION)

TITLE: Hope Creek Generating Station Plant Unique Analysis Report, Volume 3

DOCUMENT FILE NUMBER: BPC-01-300-3 Revision 0

AFFECTED PAGE(S)	DOC REV	PREPARED BY / DATE	ACCURACY CHECK BY / DATE	CRITERIA CHECK BY / DATE	REMARKS
3-2.53	0	RDQ/1-30-84	LRH/1-30-84	ycy/1-30-84	
3-2.54	0	↓	↓	↓	
3-2.55	0	RDQ/1-30-84	LRH/1-30-84		
3-2.56	0	LRH/1-30-84	HKF/1-30-84		
3-2.57	0	HKF/1-30-84	LRH/1-30-84	ycy/1-30-84	
3-2.58	0	ycy/1-30-84	HKF/1-30-84	RAL/1-30-84	
3-2.59	0	LRH/1-30-84	HKF/1-30-84	RAL/1-30-84	
3-2.60	0	HKF/1-30-84	LRH/1-30-84	ycy/1-30-84	
3-2.61	0	HKF/1-30-84	↓	↓	
3-2.62	0	RDQ/1-30-84			
3-2.63	0	HKF/1-30-84	LRH/1-30-84		
3-2.64	0	LRH/1-30-84	HKF/1-30-84		
3-2.65	0	RDQ/1-30-84	LRH/1-30-84		
3-2.66	0	RDQ/1-30-84	↓	↓	
3-2.67	0	HKF/1-30-84	LRH/1-30-84	ycy/1-30-84	
3-2.68	0	ycy/1-30-84	HKF/1-30-84	RAL/1-30-84	
3-2.69	0	RAL/1-30-84	HKF/1-30-84	ycy/1-30-84	
3-2.70	0	RDQ/1-30-84	LRH/1-30-84		
3-2.71	0				
3-2.72	0				
3-2.73	0				
3-2.74	0				
3-2.75	0				
3-2.76	0				
3-2.77	0				
3-2.78	0				
3-2.79	0				
3-2.80	0				
3-2.81	0				
3-2.82	0				
3-2.83	0				
3-2.84	0	↓	↓	↓	
3-2.85	0	RDQ/1-30-84	LRH/1-30-84	ycy/1-30-84	

REVISION CONTROL SHEET
(CONTINUATION)

TITLE: Hope Creek Generating Station Plant Unique Analysis Report, Volume 3

DOCUMENT FILE NUMBER: BPC-01-300-3 Revision 0

AFFECTED PAGE(S)	DOC REV	PREPARED BY / DATE	ACCURACY CHECK BY / DATE	CRITERIA CHECK BY / DATE	REMARKS
3-2.86	0	RDQ/1-30-84	LRH/1-30-84	ycy/1-30-84	
3-2.87	0				
3-2.88	0				
3-2.89	0				
3-2.90	0				
3-2.91	0				
3-2.92	0				
3-2.93	0		LRH/1-30-84		
3-2.94	0		GSM/1-30-84		
3-2.95	0		LRH/1-30-84		
3-2.96	0				
3-2.97	0				
3-2.98	0				
3-2.99	0				
3-2.100	0				
3-2.101	0				
3-2.102	0				
3-2.103	0				
3-2.104	0				
3-2.105	0				
3-2.106	0				
3-2.107	0				
3-2.108	0				
3-2.109	0				
3-2.110	0				
3-2.111	0				
3-2.112	0				
3-2.113	0				
3-2.114	0				
3-2.115	0		LRH/1-30-84		
3-2.116	0		HKF/1-30-84		
3-2.117	0				
3-2.118	0	RDQ/1-30-84	HKF/1-30-84	ycy/1-30-84	

REVISION CONTROL SHEET (CONTINUATION)

TITLE: Hope Creek Generating Station Plant Unique Analysis Report, Volume 3

DOCUMENT FILE NUMBER: BPC-01-300-3 Revision 0

AFFECTED PAGE(S)	DOC REV	PREPARED BY / DATE	ACCURACY CHECK BY / DATE	CRITERIA CHECK BY / DATE	REMARKS
3-2.119	0	RDQ/1-30-84	HKF/1-30-84	ycy/1-30-84	
3-2.120	0				
3-2.121	0				
3-2.122	0				
3-2.123	0	RDQ/1-30-84			
3-2.124	0	LRH/1-30-84	HKF/1-30-84		
3-2.125	0	HKF/1-30-84	LRH/1-30-84		
3-2.126	0	RDQ/1-30-84			
3-2.127	0				
3-2.128	0				
3-2.129	0	RDQ/1-30-84			
3-2.130	0	CSW/1-30-84			
3-2.131	0	RDQ/1-30-84			
3-2.132	0				
3-2.133	0				
3-2.134	0				
3-2.135	0				
3-2.136	0		LRH/1-30-84		
3-2.137	0	RDQ/1-30-84	CSW/1-30-84		
3-2.138	0	CSW/1-30-8	LRH/1-30-84		
3-2.139	0	RDQ/1-30-84			
3-2.140	0				
3-2.141	0				
3-2.142	0				
3-2.143	0	RDQ/1-30-84		ycy/1-30-84	
3-2.144	0	ycy/1-30-84		RDQ/1-30-84	
3-2.145	0	RDQ/1-30-84		ycy/1-30-84	
3-2.146	0				
3-2.147	0				
3-2.148	0				
3-2.149	0				
3-2.150	0				
3-2.151	0	RDQ/1-30-84	LRH/1-30-84		
3-2.152	0	HKF/1-30-84	JAT/1-30-84	ycy/1-30-84	

REVISION CONTROL SHEET
(CONTINUATION)

TITLE: Hope Creek Generating Station Plant Unique Analysis Report, Volume 3

DOCUMENT FILE NUMBER: BPC-01-300-3 Revision 0

AFFECTED PAGE(S)	DOC REV	PREPARED BY / DATE	ACCURACY CHECK BY / DATE	CRITERIA CHECK BY / DATE	REMARKS
3-2.153	0	AI/1-30-84	MS/1-30-84	yzy/1-30-84	
3-2.154	0	LRH/1-30-84	JAT/1-30-84		
3-2.155	0	CSW/1-30-84	HKF/1-30-84		
3-2.156	0	GSH/1-30-84	CSW/1-30-84		
3-2.157	0	MCH/1-30-84	MS/1-30-84		
3-2.158	0	LRH/1-30-84	HKF/1-30-84		
3-2.159	0	HKF/1-30-84	LRH/1-30-84		
3-2.160	0	HKF/1-30-84			
3-2.161	0	RDQ/1-30-84			
3-2.162	0				
3-2.163	0				
3-2.164	0				
3-2.165	0				
3-3.1	0	RDQ/1-30-84	LRH/1-30-84	yzy/1-30-84	

ABSTRACT

The primary containment for the Hope Creek Generating Station was designed, erected, pressure-tested, and N-stamped in accordance with the ASME Boiler and Pressure Vessel Code, Section III, 1974 Edition with addenda up to and including Winter 1974. These activities were performed for the Public Service Electric and Gas Company (PSE&G) by the Pittsburgh-Des Moines Steel Company. Since then, new requirements which affect the design and operation of the primary containment system have been established. These requirements are defined in the Nuclear Regulatory Commission's (NRC) Safety Evaluation Report, NUREG-0661. The NUREG-0661 requirements define revised containment design loads postulated to occur during a loss-of-coolant accident or a safety-relief valve discharge event which are to be evaluated. In addition, NUREG-0661 requires that an assessment of the effects that these postulated events have on the operation of the containment system be performed.

This plant unique analysis report (PUAR) documents the efforts undertaken to address and resolve each of the applicable NUREG-0661 requirements for Hope Creek. It demonstrates, in accordance with NUREG-0661 acceptance criteria, that the design of the primary containment system is adequate and that original design safety margins have been restored. The Hope Creek PUAR is composed of the following six volumes:

- o Volume 1 - GENERAL CRITERIA AND LOADS METHODOLOGY
- o Volume 2 - SUPPRESSION CHAMBER ANALYSIS
- o Volume 3 - VENT SYSTEM ANALYSIS
- o Volume 4 - INTERNAL STRUCTURES ANALYSIS
- o Volume 5 - SAFETY RELIEF VALVE DISCHARGE PIPING ANALYSIS
- o Volume 6 - TORUS ATTACHED PIPING AND SUPPRESSION CHAMBER PENETRATION ANALYSES

Major portions of all volumes of this report have been prepared by NUTECH Engineers, Incorporated (NUTECH), acting as a consultant responsible to the Public Service Electric and Gas Company. Selected sections of Volumes 5 and 6 have been prepared by the Bechtel Power Corporation acting as an agent responsible to the Public Service Electric and Gas Company. This volume, Volume 3, documents the evaluation of the vent system.

NOTE: Identification of the volume number precedes each page, section, subsection, table, and figure number.

TABLE OF CONTENTS

LIST OF ACRONYMS

ACI	American Concrete Institute
ADS	Automatic Depressurization System
AISC	American Institute of Steel Construction
ASME	American Society of Mechanical Engineers
ATWS	Anticipated Transients Without Scram
BDC	Bottom Dead Center
BWR	Boiling Water Reactor
CDF	Cumulative Distribution Function
CO	Condensation Oscillation
DBA	Design Basis Accident
DC	Downcomer
DLF	Dynamic Load Factor
ECCS	Emergency Core Cooling System
FSAR	Final Safety Analysis Report
FSI	Fluid-Structure Interaction
FSTF	Full-Scale Test Facility
HNWL	High Normal Water Level
HPCI	High Pressure Coolant Injection
IBA	Intermediate Break Accident
I&C	Instrumentation and Control
ID	Inside Diameter
IR	Inside Radius
LDR	Load Definition Report
LOCA	Loss-of-Coolant Accident

LIST OF ACRONYMS
(Continued)

LPCI	Low Pressure Coolant Injection
LTP	Long-Term Program
MC	Midcylinder
MCF	Modal Correction Factor
MJ	Mitered Joint
MVA	Multiple Valve Actuation
NEP	Non-Exceedance Probability
NOC	Normal Operating Conditions
NRC	Nuclear Regulatory Commission
NSSS	Nuclear Steam Supply System
NVB	Non-Vent Line Bay
OBE	Operating Basis Earthquake
OD	Outside Diameter
PSD	Power Spectral Density
PSE&G	Public Service Electric and Gas Company
PUA	Plant Unique Analysis
PUAAG	Plant Unique Analysis Application Guide
PUAR	Plant Unique Analysis Report
PULD	Plant Unique Load Definition
QSTF	Quarter-Scale Test Facility
RCIC	Reactor Core Isolation Cooling
RHR	Residual Heat Removal
RPV	Reactor Pressure Vessel

LIST OF ACRONYMS
(Concluded)

RSEL	Resultant Static-Equivalent Load
SBA	Small Break Accident
SBP	Small Bore Piping
SER	Safety Evaluation Report
SORV	Stuck-Open Safety Relief Valve
SRSS	Square Root of the Sum of the Squares
SRV	Safety Relief Valve
SRVDL	Safety Relief Valve Discharge Line
SSE	Safe Shutdown Earthquake
STP	Short-Term Program
SVA	Single Valve Actuation
TAP	Torus Attached Piping
VB	Vent Line Bay
VH	Vent Header
VL	Vent Line
VPP	Vent Pipe Penetration
ZPA	Zero Period Acceleration

LIST OF TABLES

LIST OF TABLES
(Concluded)

LIST OF FIGURES

LIST OF FIGURES
(Continued)

LIST OF FIGURES
(Concluded)

3-1.0 INTRODUCTION

In conjunction with Volume 1 of the Plant Unique Analysis Report (PUAR), this volume documents the efforts undertaken to address the requirements defined in NUREG-0661 which affect the Hope Creek vent system. The vent system PUAR is organized as follows:

- o INTRODUCTION
  - Scope of Analysis
- o VENT SYSTEM ANALYSIS
  - Component Description
  - Loads and Load Combinations
  - Analysis Acceptance Criteria
  - Method of Analysis
  - Analysis Results and Conclusions

The INTRODUCTION section contains an overview discussion of the scope of the vent system evaluation. The VENT SYSTEM ANALYSIS section contains a comprehensive discussion of the vent system loads and load combinations, and a description of the component parts of the vent system affected by these loads. The section also contains a discussion of the methodology used to evaluate the effects of these loads, the associated

evaluation results, and the acceptance limits to which the results are compared. A summary of the conclusions derived from the vent system evaluation is also included.

3-1.1 Scope of Analysis

The general criteria presented in Volume 1 are used as the basis for the Hope Creek vent system evaluation. The vent system is evaluated for the effects of LOCA related loads and SRV discharge related loads discussed in Volume 1 and defined by the NRC Safety Evaluation Report NUREG-0661 (Reference 1) and the Mark I Containment Program Load Definition Report (LDR) (Reference 2).

The LOCA and SRV discharge loads used in this evaluation are developed using the plant unique geometry, operating parameters, and test results contained in the Mark I Containment Program Plant Unique Load Definition (PULD) (Reference 3). The effects of increased suppression pool temperatures which occur during SRV discharge events are also evaluated. These temperatures are taken from the plant's suppression pool temperature response analysis. Other loads and methodology, such as the evaluation for seismic loads, are taken from the plant's original design basis evaluation documented in the Final Safety Analysis Report (FSAR) (Reference 4).

The evaluation includes a structural analysis of the vent system for the effects of LOCA and SRV discharge related loads to confirm that the design of the vent system is adequate. Rigorous analytical techniques are used in this evaluation, including use of detailed analytical models for computing the dynamic response of the vent system. Effects such as local penetration and intersection flexibilities are considered in the vent system analysis.

The results of the structural evaluation for each load are used to evaluate load combinations and fatigue effects for the vent system in accordance with the Mark I Containment Program Structural Acceptance Criteria Plant Unique Analysis Application Guide (PUAAG) (Reference 5). The analysis results are compared with the acceptance limits specified by the PUAAG and the applicable sections of the American Society of Mechanical Engineers (ASME) Code (Reference 6).

3-2.0 VENT SYSTEM ANALYSIS

An evaluation of each of the NUREG-0661 requirements which affect the design adequacy of the Hope Creek vent system is presented in the sections which follow. The criteria used in this evaluation are contained in Volume 1 of this report.

The component parts of the vent system which are examined are described in Section 3-2.1. The loads and load combinations for which the vent system is evaluated are described and presented in Section 3-2.2. The analysis methodology used to evaluate the effects of these loads and load combinations on the vent system is discussed in Section 3-2.4. The acceptance limits to which the analysis results are compared are discussed and presented in Section 3-2.3. The analysis results and the corresponding vent system design margins are presented in Section 3-2.5.

3-2.1 Component Description

The Hope Creek vent system is constructed from cylindrical shell segments joined together to form a manifold-like structure which connects the drywell to the suppression chamber. The configuration of the vent system is illustrated in Figures 3-2.1-1 and 3-2.1-2. The major components of the vent system include the vent lines, vent header, and downcomers. The proximity of the vent system to other components of the containment is shown in Figures 3-2.1-3 through 3-2.1-6.

The eight vent lines connect the drywell to the vent header in alternate mitered cylinders of the suppression chamber. The vent lines are nominally 9/16" thick and have an inside diameter of 6'-2". The upper ends of the vent lines are 2" thick and include a conical transition segment at the penetration to the drywell, as shown in Figure 3-2.1-7. The drywell shell at each vent line-drywell penetration is reinforced by a 3" thick insert plate. The vent line is connected to the drywell by full penetration welds. The vent lines are shielded from jet impingement loads at each vent line-drywell penetration location by jet deflectors which span the openings of the vent lines. The portions of the vent lines within the suppression

chamber, as shown in Figure 3-2.2-3, are 1-1/2" thick, except for the lower 7'-3" of the vent lines which are 2" thick. The end of each vent line is capped with a 3" thick flat plate.

The vent header is an assembly of mitered cylindrical shell segments joined together to form a ring header, as shown in Figure 3-2.1-1. The vent header is nominally 9/16" thick and has an inside diameter of 4'-3". The vent header is continuous between adjacent vent lines. The vent header is connected to each vent line by a 3/8" partial penetration weld with a 1/2" cover fillet weld outside the vent line and a 1/2" fillet weld inside the vent line.

A total of eighty downcomers penetrate the vent header in pairs, as shown in Figures 3-2.1-1, 3-2.1-3, and 3-2.1-6. Two downcomer pairs are located in each vent line bay and three pairs are located in each non-vent line bay. Each downcomer consists of an inclined segment which penetrates the vent header and a vertical segment which terminates below the surface of the suppression pool, as shown in Figure 3-2.1-9. Each downcomer is nominally 3/8" thick and has an outside diameter of 2'-0". The downcomers are attached to the

vent header by 1/2" fillet welds inside and outside the vent header.

The intersections of the downcomers and the vent header are reinforced with a system of stiffener plates and bracing members, as shown in Figures 3-2.1-6, 3-2.1-9, and 3-2.1-10. In the plane of the downcomers, the intersections are stiffened by a 1-5/8" thick crotch plate located between downcomers in a pair. The connection of the top side of each downcomer to the vent header is reinforced by 1-5/8" thick outer stiffener plates. Downcomer ring plates which are 1-5/8" thick connect the associated crotch plate and the outer stiffener plates. This system of stiffener plates is designed to reduce local intersection stresses caused by loads acting on the submerged portion of the downcomers.

In the direction normal to the plane of the downcomer pair, the intersections are braced by 4" diameter Schedule 120 pipes. One pipe member is located on each side of the vent header. The upper ends of these pipe members are connected to a 1-5/8" thick built-up tee-section and 7/8" thick pad plates attached to the vent header. The lower ends of the pipe members are connected to the downcomer ring plates. The ring

plates are stiffened locally with a 3/4" thick gusset plate and pad plate assembly. In addition, the adjacent downcomer pairs in the non-vent line bay are joined by 2-1/2" diameter rods, one on either side of the vent header. The ends of these rods are connected to the downcomer rings. The bracing system provides an additional load path for the transfer of loads acting on the submerged portion of the downcomers and results in reduced intersection local stresses. The system of downcomer-vent header intersection stiffener plates and bracing members provides a highly redundant mechanism for the transfer of loads which act on the downcomers, thus reducing the magnitude of loads which pass directly through the intersection.

A bellows assembly is provided at the penetration of the vent line to the suppression chamber as shown in Figure 3-2.1-7. The bellows allow differential movement of the vent system and suppression chamber to occur without developing significant interaction loads. The bellows assemblies consist of a tandem bellows unit with a nominal outside diameter of 6'-8". A 1/2" thick annular plate connects the upper end of the bellows assembly to the vent line. The lower end of the bellows assembly is connected to the suppression chamber by a 2-1/2" thick nozzle. Each of the two

bellows units in the assembly contains a section with five convolutions which are alternately connected to 1/2" thick cylindrical sleeves. The total length of the bellows assembly is 4'-2 1/2". The annular plates are attached to the vent lines by 1/2" fillet welds.

The SRV piping is routed from the drywell down the vent lines and penetrate the vent lines inside the suppression chamber, as shown in Figures 3-2.1-3 and 3-2.1-8. The vent lines and SRV piping nozzles are reinforced at each vent line-SRV piping penetration location by a 2-1/2" thick insert plate and four 2" thick gusset plates. The vent line-SRV piping penetration assembly provides an effective means of transferring loads which act on the SRV piping to the vent line.

The drywell/wetwell vacuum breakers (not shown) are twenty-four inches in size and extend from mounting flanges attached to the vacuum breaker support nozzles. The 2'-0" diameter, 0.438" thick support nozzles penetrate the vent line end plate, as shown in Figure 3-2.1-3.

The vent system is supported within the suppression chamber by two column members at each mitered joint location, one column member at each midcylinder

location, and by an overhead truss system, as shown in Figures 3-2.1-3 through 3-2.1-6. The support column and overhead truss members are constructed from 10" diameter Schedule 120 pipe with built-up clevis assemblies attached to each end, as shown in Figure 3-2.1-14. The upper ends of the mitered joint support columns are attached to 1-1/2" thick vent header support rings, shown in Figure 3-2.1-12. The support rings are attached to the vent header with 5/16" fillet welds. The lower ends of the mitered joint support columns are attached to 2" thick ring beam pin plates. Each vent line is supported by a single support column member and two overhead truss members. The supp rt column is connected to a 2" thick pin plate on the vent line and a 1-3/4" thick pin plate on the midcylinder ring beam. The overhead truss members in the vent line bay are connected to a 2-1/4" thick pin plate on the vent line and to 1-3/4" thick pin plates at top dead center on the mitered joint ring beams. Details of the support column and overhead truss member connections on the vent line are shown in Figure 3-2.1-13.

The midcylinder non-vent bay location is reinforced by two 1-1/2" thick vent header ring plates each located 1'-10" from midcylinder. Two 1-1/2" thick longitudinal plates span between the two ring plates. Two 1-3/4"

thick pin plates are attached to the lower longitudinal plate, and a 2-1/4" thick pin plate is attached to the face of each vent header ring plate at top dead center. The details of the connections at midcylinder non-vent bay are shown in Figure 3-2.1-11. The midcylinder non-vent bay support column is attached to the two 1-3/4" thick pin plates at its upper end and to a 1-3/4" thick pin plate on the midcylinder ring beam. The two overhead truss members in the non-vent bay are each attached to the 2-1/4" thick pin plates at the vent header ring plate and to a 1-3/4" thick pin plate at top dead center on the mitered joint ring beams.

The support columns and overhead truss members provide an effective means of transferring vertical loads acting on the vent system to the suppression chamber. The overhead truss members also effectively transfer horizontal vent system loads to the suppression chamber. The vent lines provide additional support for the vent system, although primary vertical support is provided by the vent system support columns and overhead truss members. The support offered by the vent line bellows is negligible, since the relative stiffness of the bellows with respect to other vent system components is small.

The vent system also provides support for a portion of the SRV piping inside the vent line and suppression chamber, as shown in Figure 3-2.1-3. Loads which act on the SRV piping are transferred to the vent system by the penetration assembly on the vent line, and by 4" diameter Schedule 80 support members attached to pad plates on the vent header near the mitered joint. Conversely, loads acting on the vent system cause motions to be transferred to the SRV piping at these same penetration and support locations.

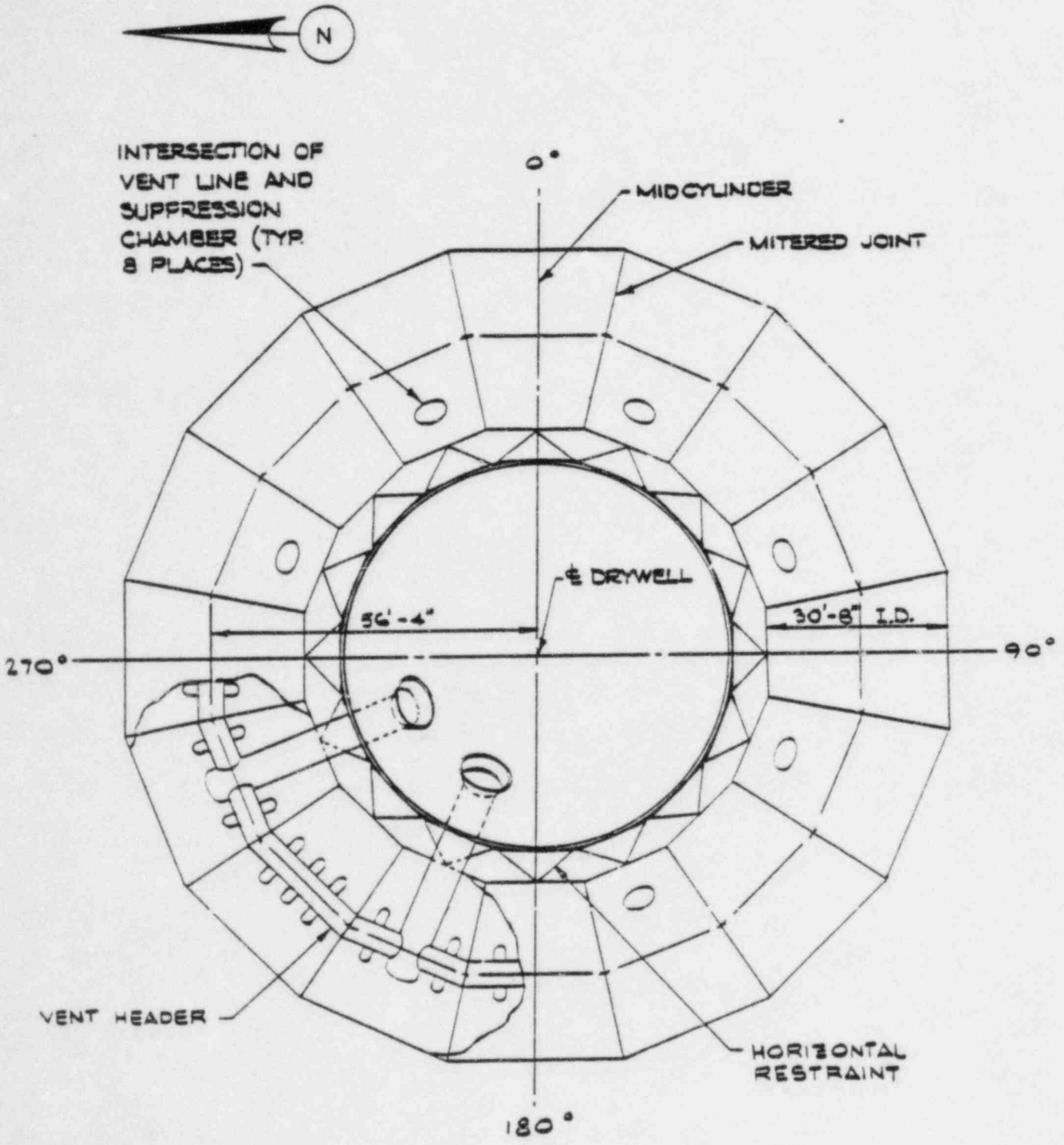

Figure 3-2.1-1

PLAN VIEW OF CONTAINMENT

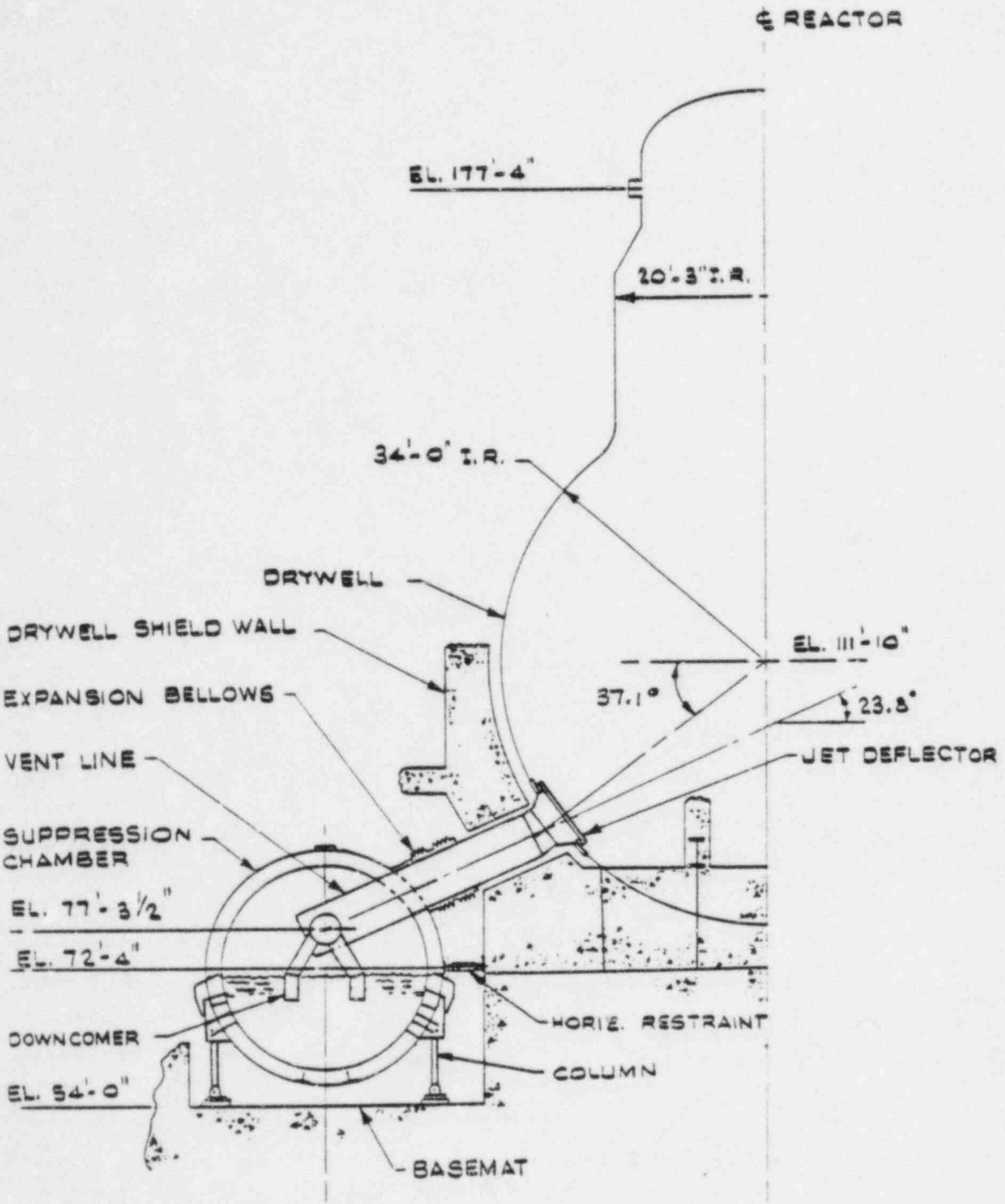

Figure 3-2.1-2

ELEVATION VIEW OF CONTAINMENT

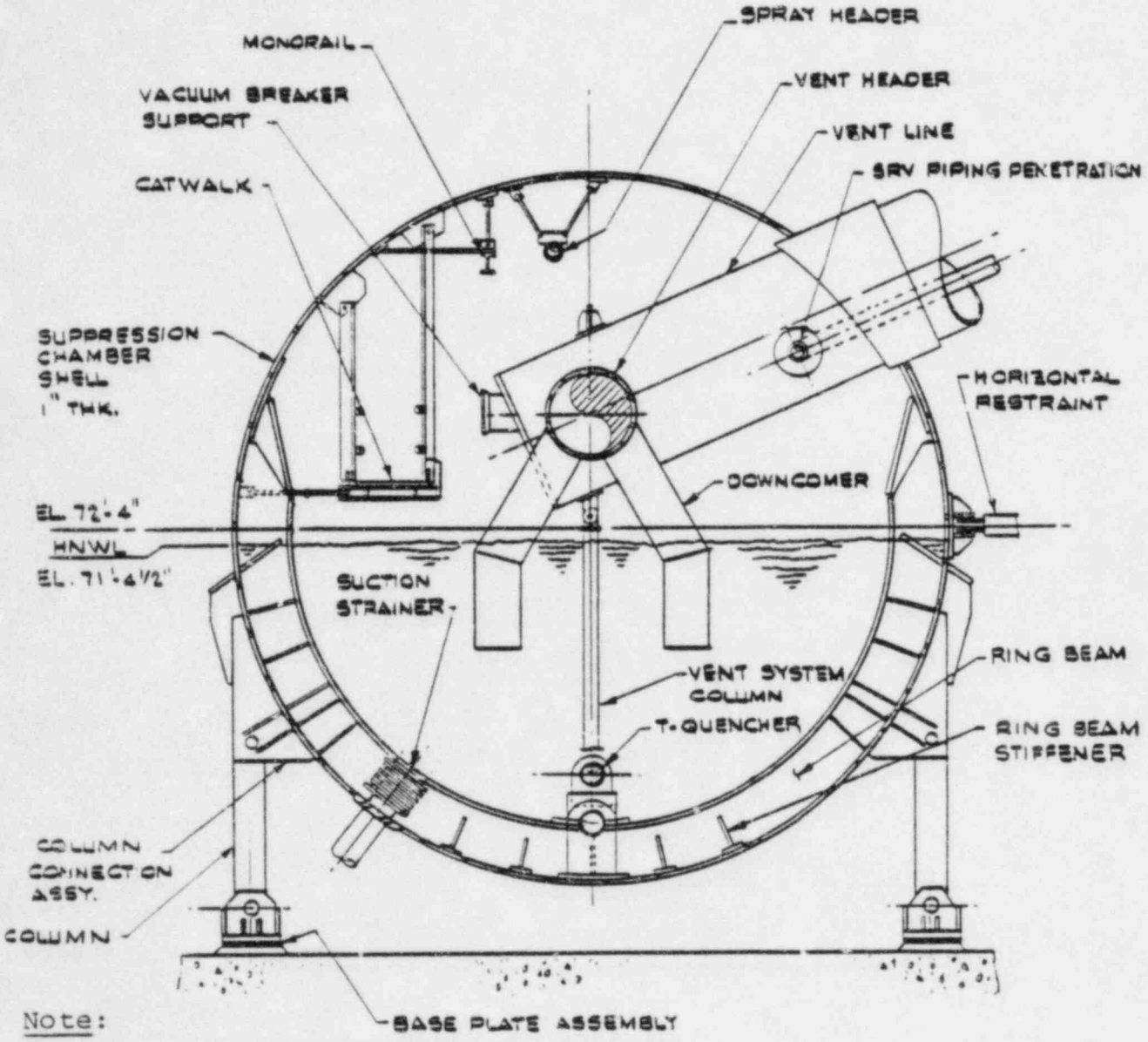

Note:

1. Downcomer stiffener plates not shown for clarity.

Figure 3-2.1-3

SUPPRESSION CHAMBER SECTION - MIDCYLINDER VENT LINE BAY

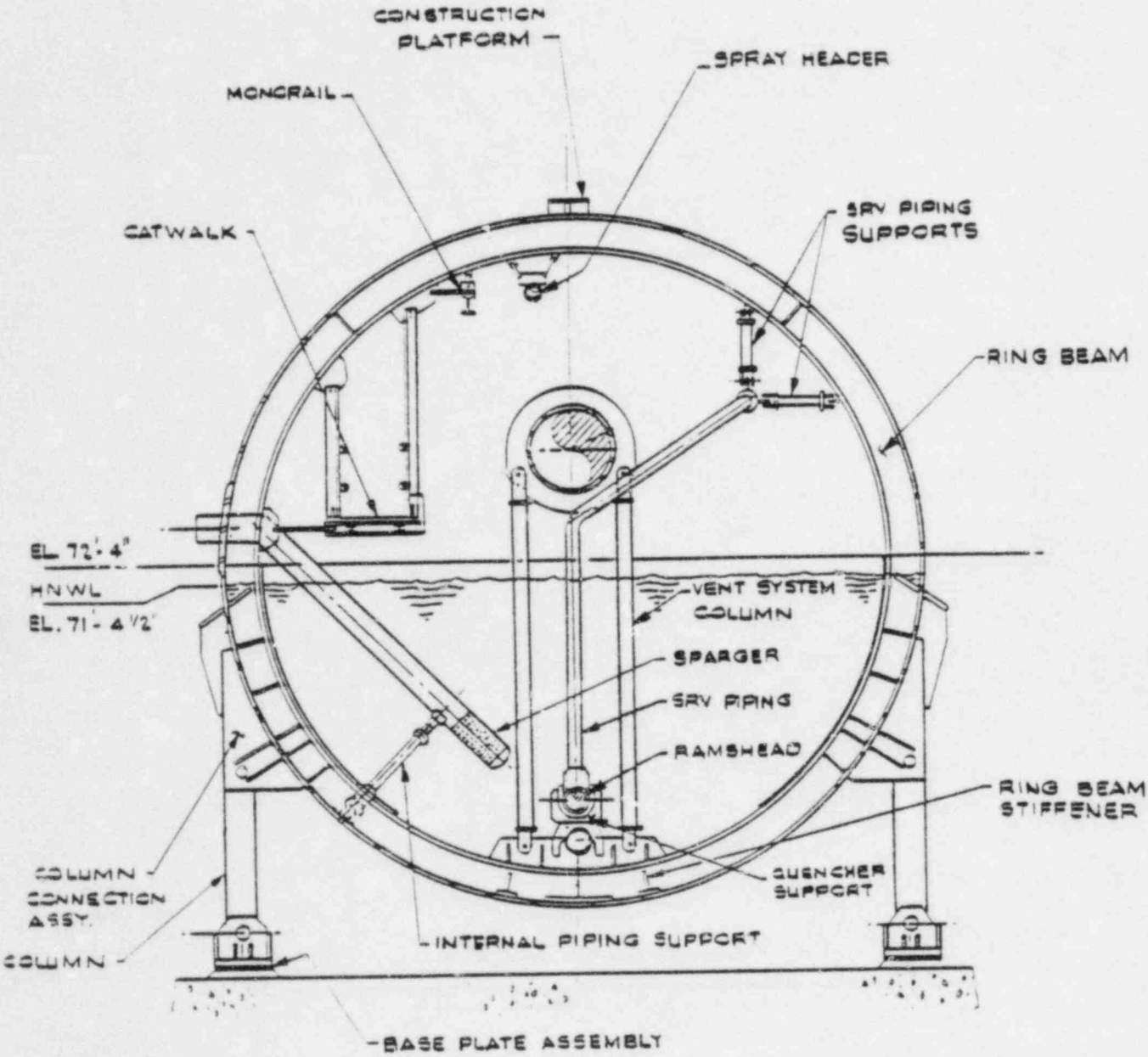

Figure 3-2.1-4

SUPPRESSION CHAMBER SECTION - MITERED JOINT

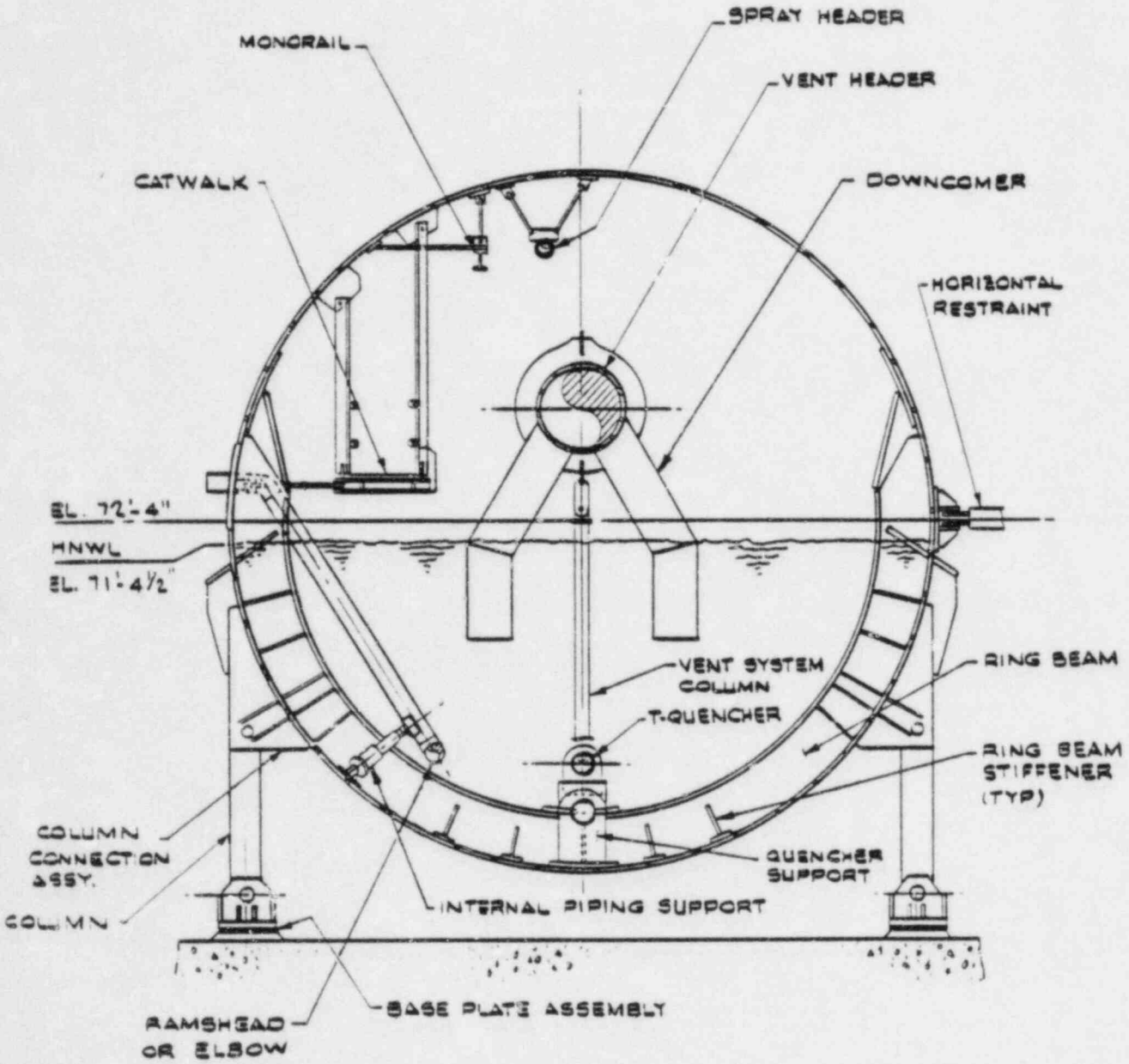

Note:

1. Downcomer stiffener plates not shown for clarity.

Figure 3-2.1-5

SUPPRESSION CHAMBER SECTION - MIDCYLINDER NON-VENT BAY

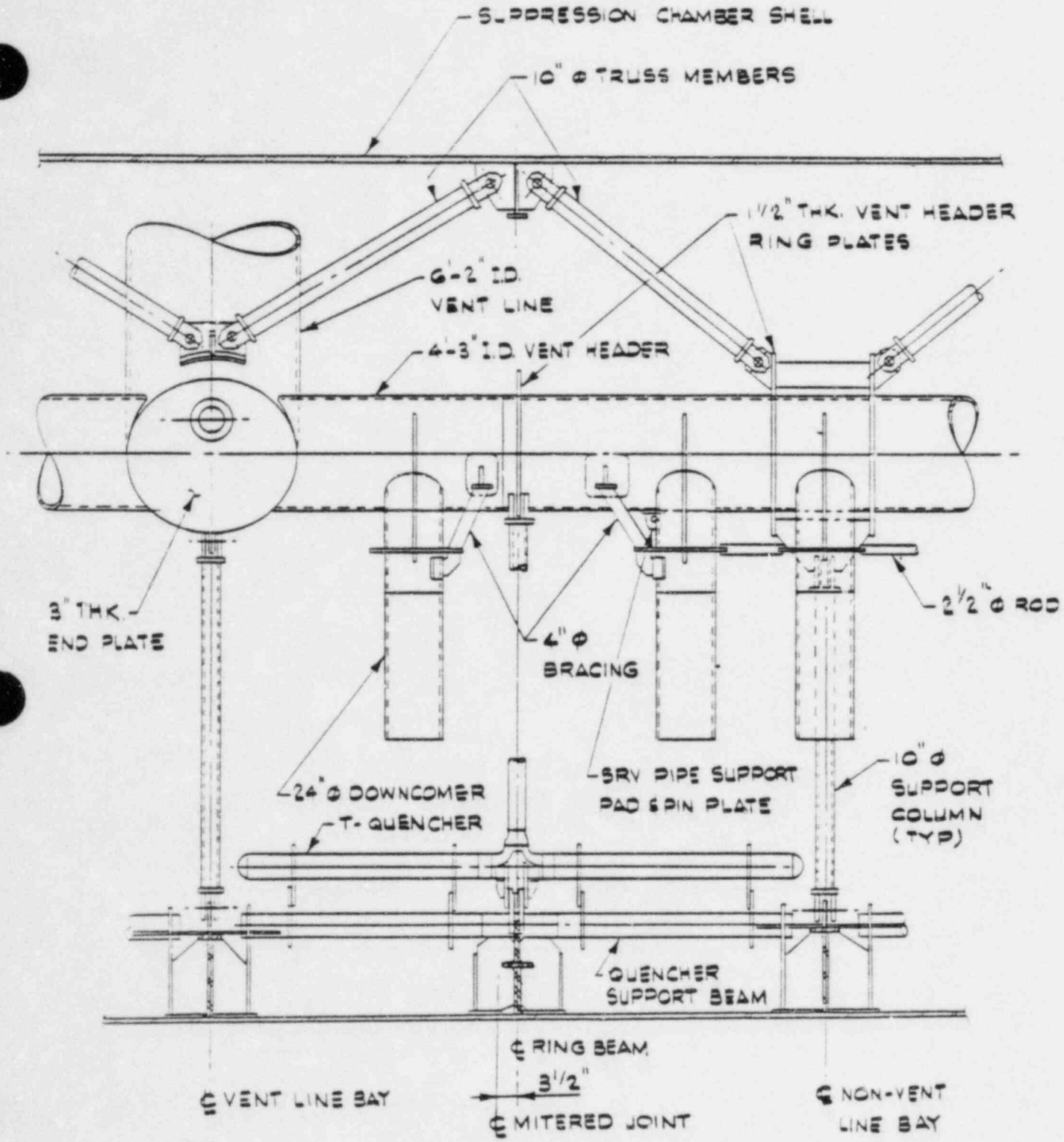

Figure 3-2.1-6

DEVELOPED VIEW OF SUPPRESSION CHAMBER SEGMENT

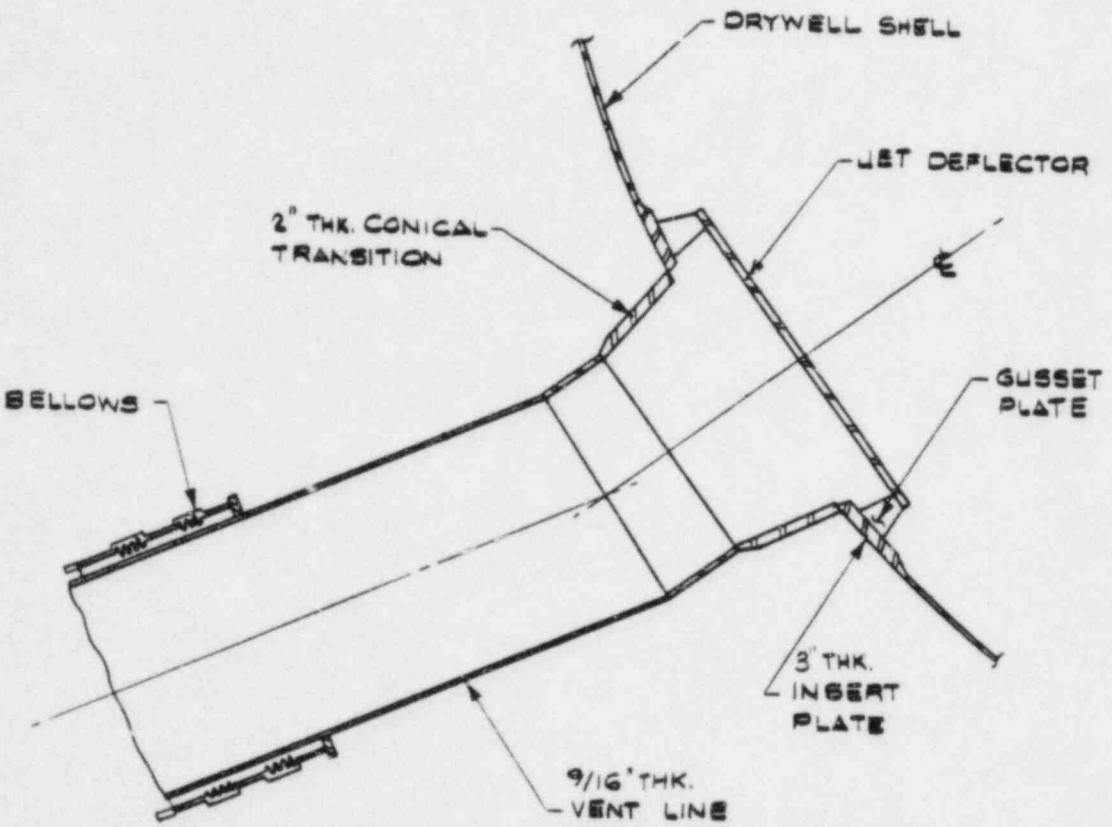

Figure 3-2.1-7

DRYWELL VENT LINE PENETRATION DETAILS

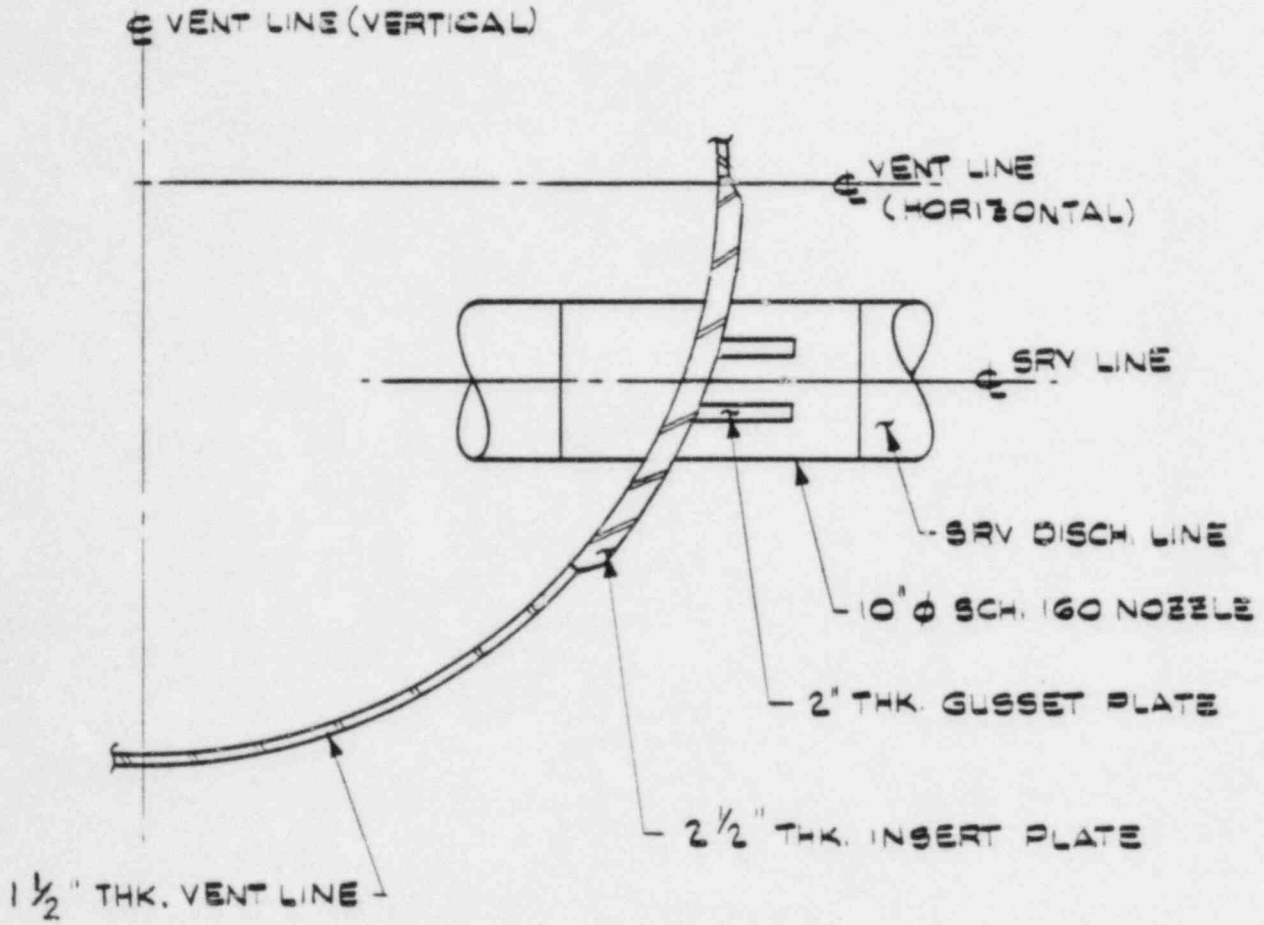

Figure 3-2.1-8

SRV PIPING VENT LINE PENETRATION DETAILS

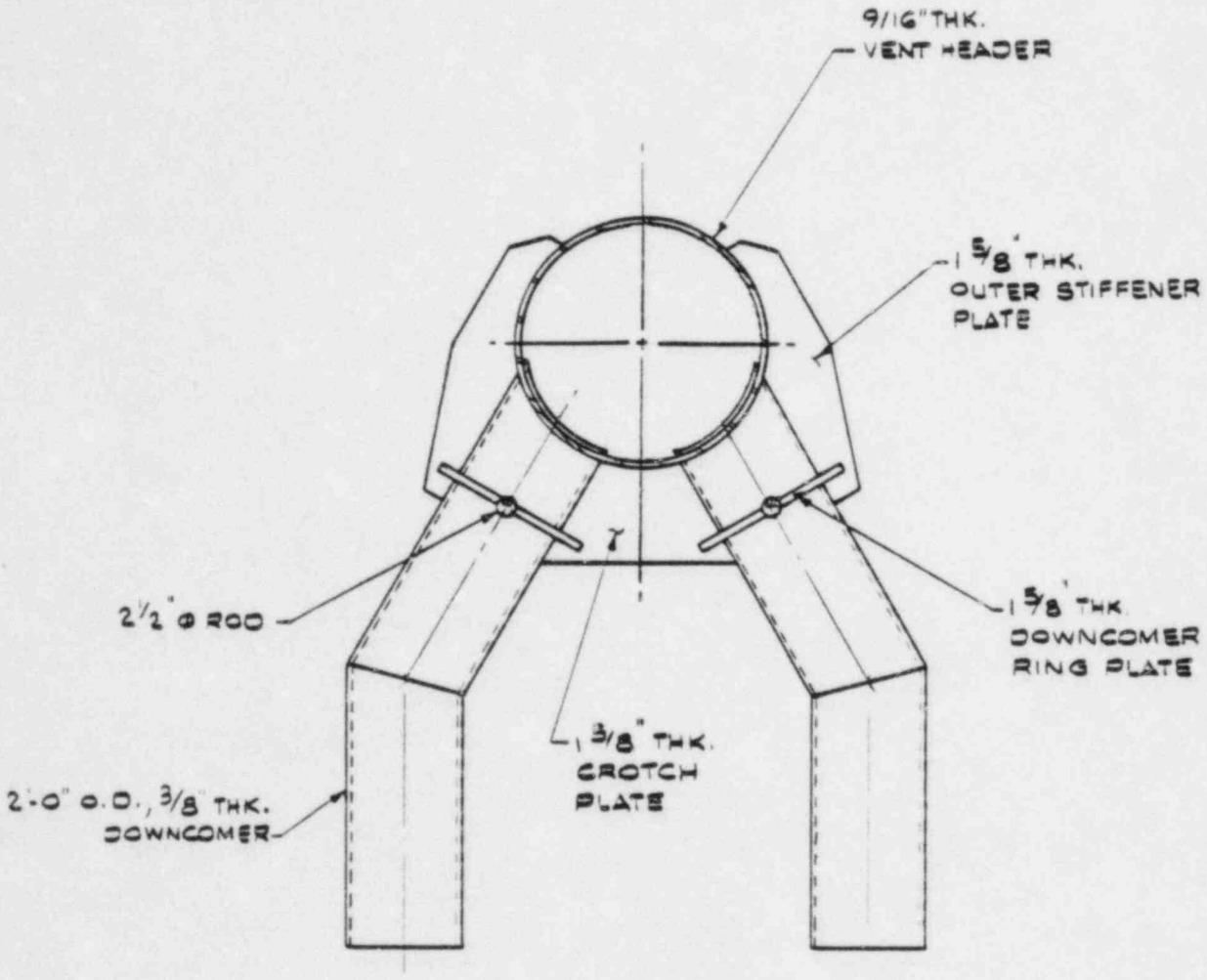

Figure 3-2.1-9

VENT HEADER-DOWNCOMER INTERSECTION DETAIL

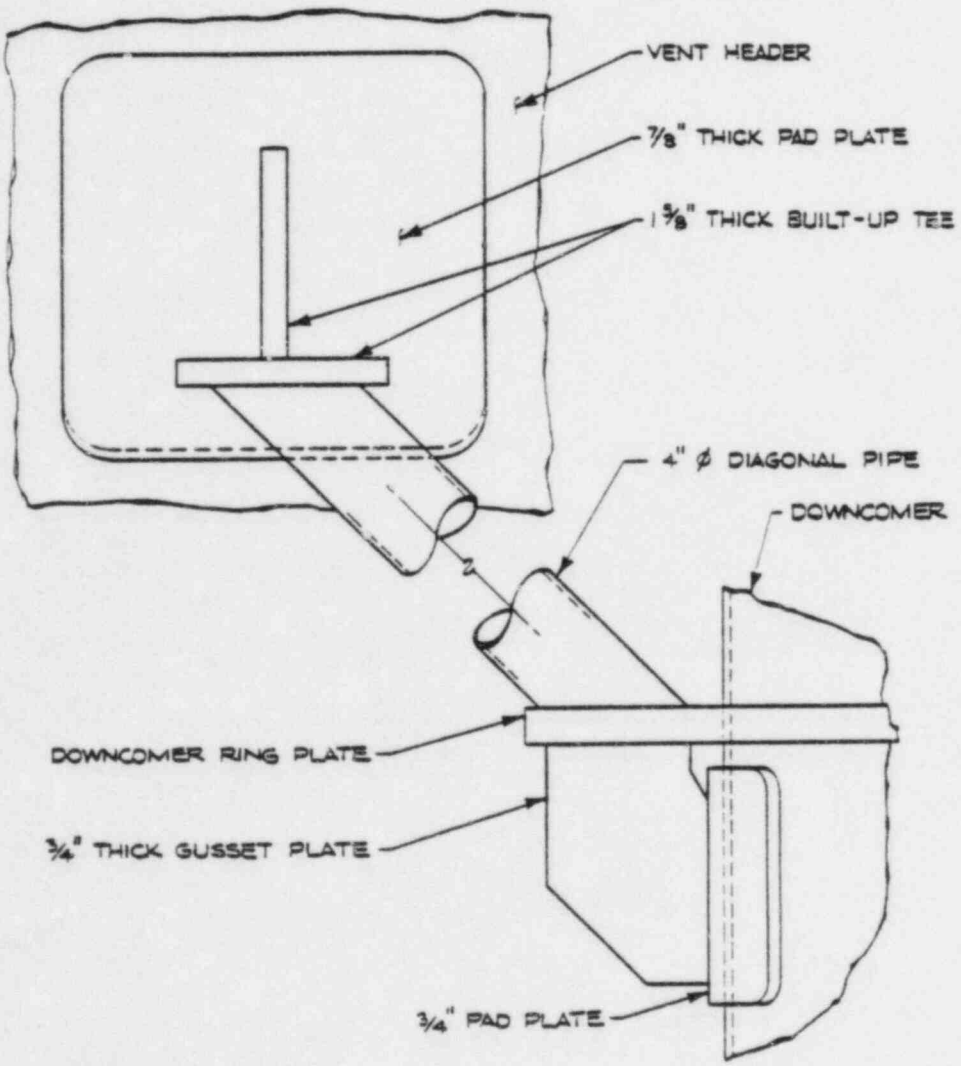

Figure 3-2.1-10

DOWNCOMER BRACING SYSTEM DETAILS

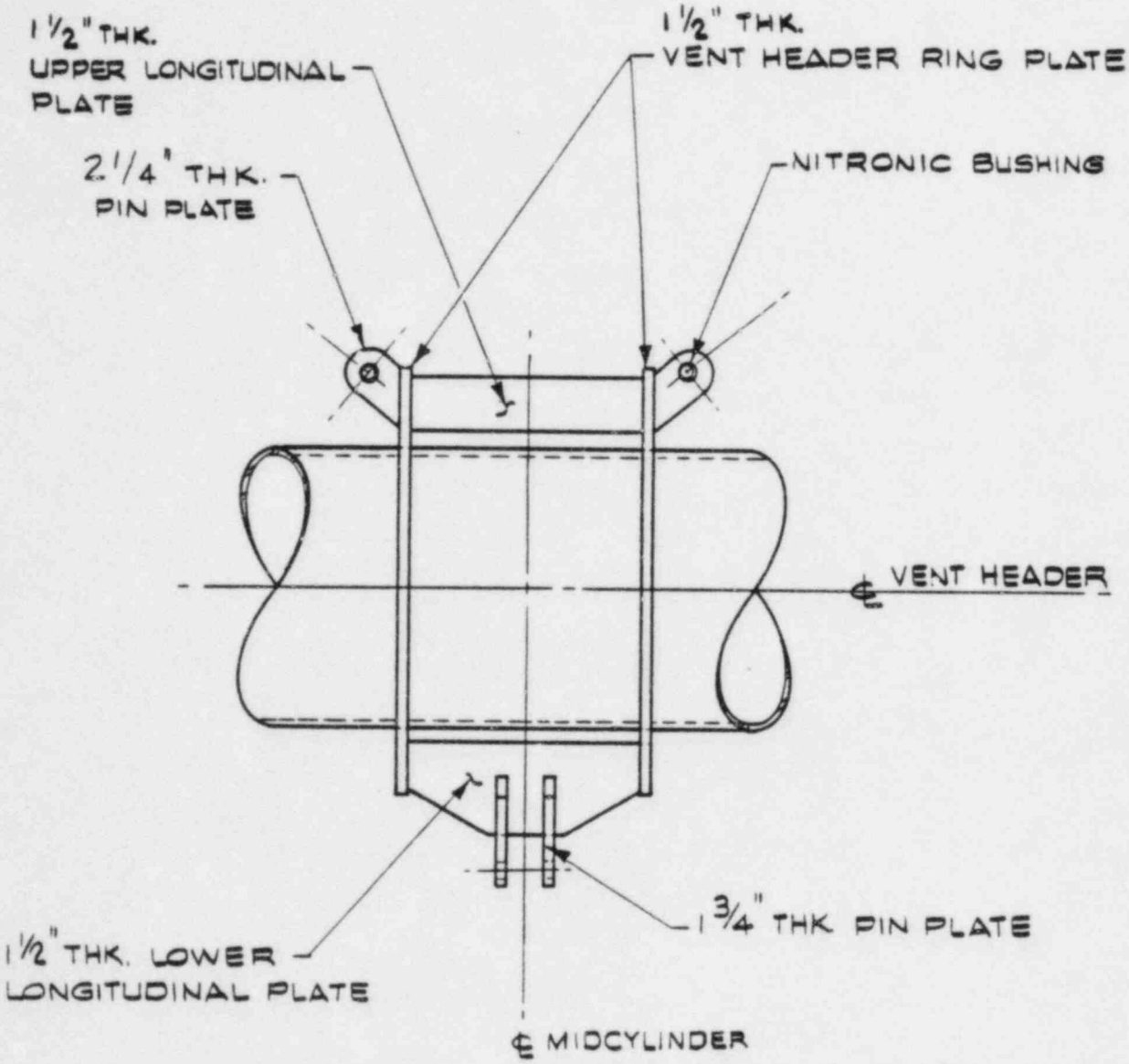

Figure 3-2.1-11

COLUMN CONNECTION DETAILS - MIDCYLINDER NON-VENT BAY

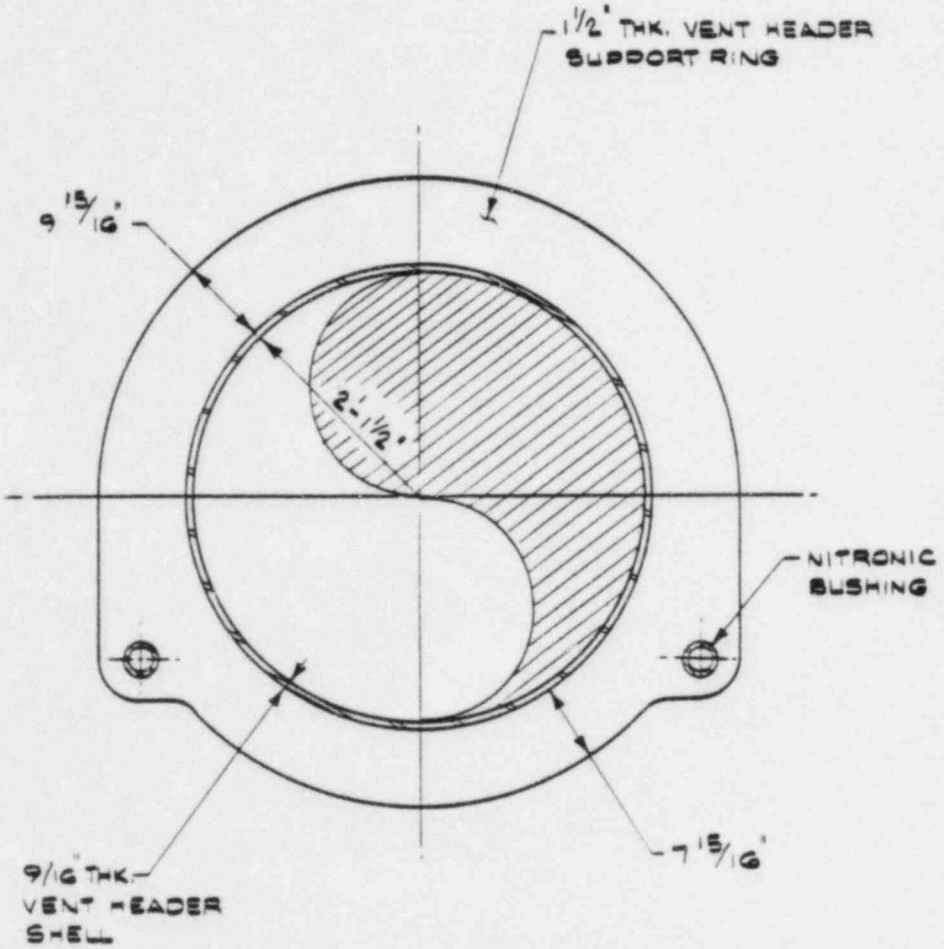

Figure 3-2.1-12

VENT HEADER MITERED JOINT SUPPORT RING DETAILS

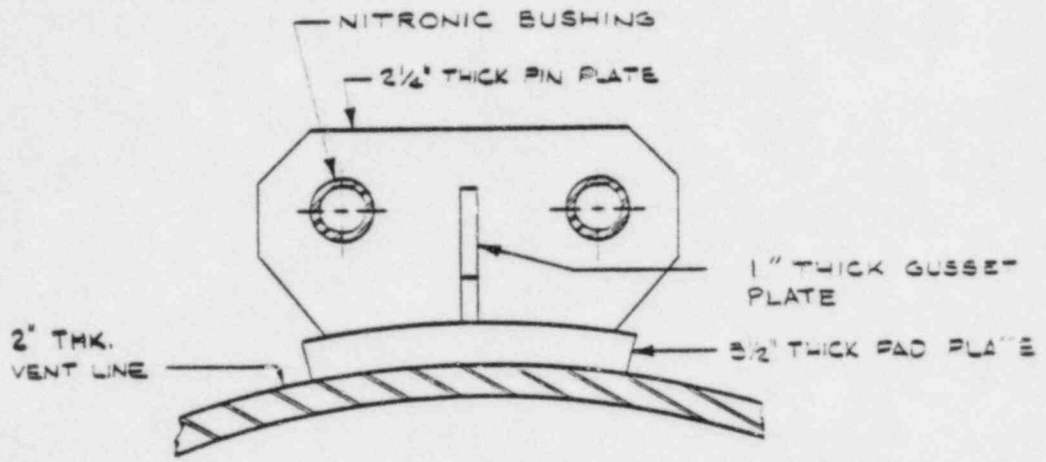

UPPER CONNECTION

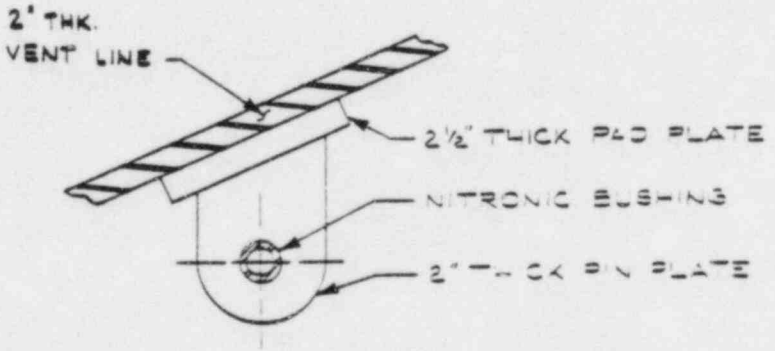

LOWER CONNECTION

Figure 3-2.1-13

COLUMN CONNECTION DETAILS - MIDCYLINDER VENT LINE BAY

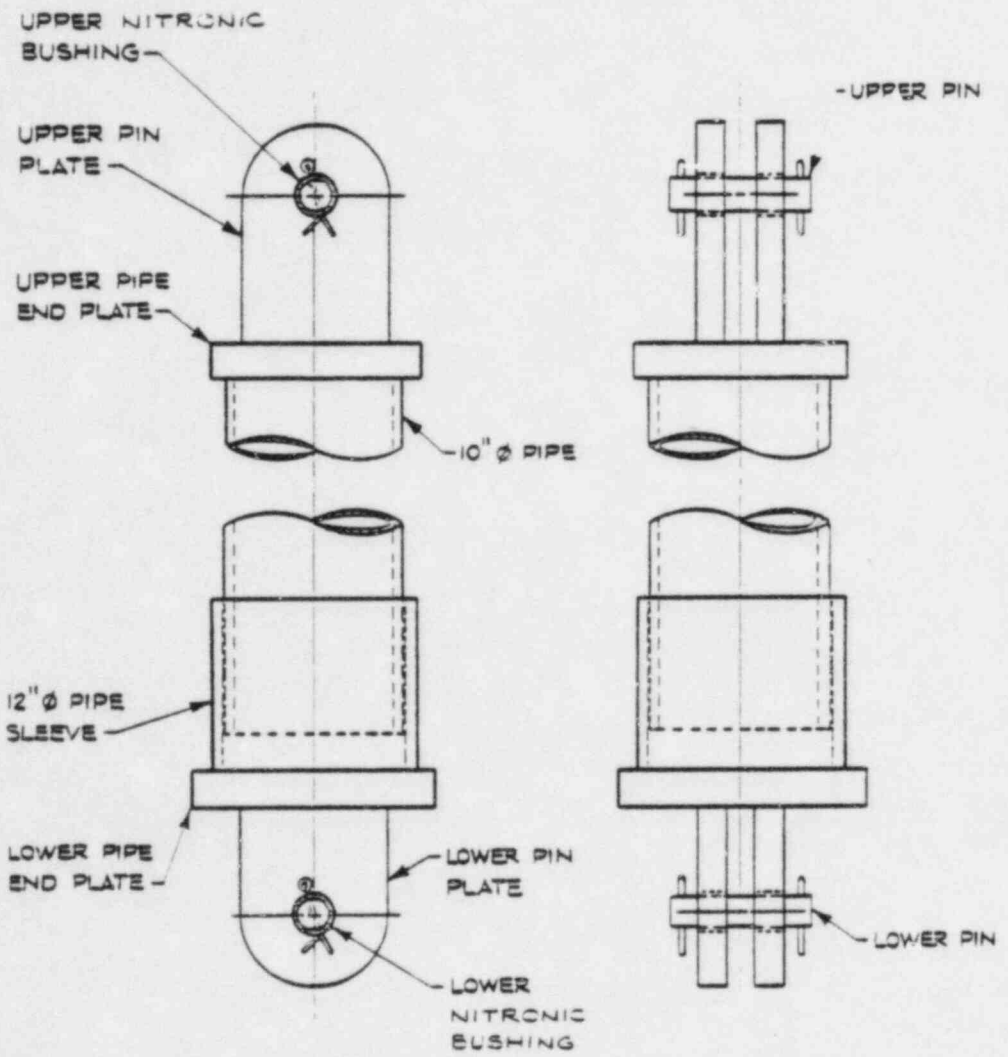

Figure 3-2.1-14

SUPPORT COLUMN DETAILS

3-2.2 Loads and Load Combinations

The loads for which the Hope Creek vent system is evaluated are defined in NUREG-0661 on a generic basis for all Mark I plants. The methodology used to develop plant unique vent system loads for each load defined in NUREG-0661 is discussed in Section 1-4.0. The results of applying the methodology to develop specific values for each of the governing loads which act on the vent system are discussed and presented in Section 3-2.2.1.

Using the event combinations and event sequencing defined in NUREG-0661 and discussed in Sections 1-3.2 and 1-4.3, the controlling load combinations which affect the vent system are formulated. The controlling vent system load combinations are discussed and presented in Section 3-2.2.2.

3-2.2.1 Loads

The loads acting on the vent system are categorized as follows:

1. Dead Weight Loads
2. Seismic Loads
3. Pressure and Temperature Loads
4. Vent System Discharge Loads
5. Pool Swell Loads
6. Condensation Oscillation Loads
7. Chugging Loads
8. Safety Relief Valve Discharge Loads
9. Piping Reaction Loads
10. Containment Interaction Loads

Loads in categories 1 through 3 are defined in the original containment design as documented in the plant's FSAR. Revised category 3 pressure and temperature loads result from postulated LOCA and SRV discharge events. Loads in categories 4 through 7 result from postulated LOCA events; loads in category 8 result from SRV discharge events; loads in category 9 are reactions which result from loads acting on SRV piping systems; loads in category 10 are motions which result from loads acting on other containment-related structures.

Not all of the loads defined in NUREG-0661 are evaluated in detail since some are enveloped by others or have a negligible effect on the vent system. Only those loads which maximize the vent system response and lead to controlling stresses are fully evaluated and discussed. These loads are referred to as governing loads in subsequent discussions.

Table 3-2.2-1 shows the specific vent system components which are affected by each of the loadings defined in NUREG-0661. The table also lists the section in Volume 1 in which the methodology for developing values for each loading is discussed. The magnitudes and characteristics of each governing vent system load in each load category are identified and presented in the paragraphs which follow.

1. Dead Weight Loads

   a. Dead Weight of Steel: The weight of steel used to construct the vent system and its supports is considered. The dead weight of steel is determined based on nominal component dimensions and a density of steel of 490 lb/ft^3.

2. Seismic Loads

a. OBE Loads: The vent system is subjected to horizontal and vertical accelerations during an Operating Basis Earthquake (OBE). This loading is taken from the original design basis for the containment documented in the plant's FSAR.

b. SSE Loads: The vent system is subjected to horizontal and vertical accelerations during a Safe Shutdown Earthquake (SSE). This loading is taken from the original design basis for the containment documented in the plant's FSAR.

3. Pressure and Temperature Loads

a. Normal Operating Internal Pressure Loads: The vent system is subjected to internal pressure loads during Normal Operating conditions. This loading is taken from the original design basis for the containment documented in the plant's FSAR. The range of normal operating internal pressures specified is 0.0 to 2.0 psi.

b. LOCA Internal Pressure Loads: The vent system is subjected to internal pressure loads during a Small Break Accident (SBA), Intermediate Break Accident (IBA), and Design Basis Accident (DBA) event. The procedure used to develop LOCA internal pressures for the containment is discussed in Section 1-4.1.1. The resulting vent system internal pressure magnitudes at key times during the SBA, IBA, and DBA events are presented in Table 3-2.2-2.

The vent system internal pressures for each event are conservatively assumed to be equal to the corresponding drywell internal pressures, neglecting reductions due to losses. The net internal pressures acting on the components of the vent system inside the suppression chamber are taken as the difference in pressures between the vent system and suppression chamber.

The pressures specified are assumed to act uniformly over the vent line, vent header, and downcomer shell surfaces. The external or secondary containment pressure for the

vent system components outside the suppression chamber for all events is assumed to be 0.0 psig. The effects of internal pressure on the vent system for the DBA event are included in the pressurization and thrust loads discussed in load case 4a.

c. Normal Operating Temperature Loads: The vent system is subjected to the thermal expansion loads associated with normal operating conditions. This loading is taken from the original design basis for the containment documented in the plant's FSAR. The range of normal operating temperatures for the vent system with a concurrent SRV discharge event is 50 to 150°F. The temperature of the SRV piping with a concurrent SRV discharge event is conservatively taken as 380°F for the submerged portion of the piping and 407°F for the portion in the suppression chamber airspace.

Additional normal operating temperatures for the vent system inside the suppression chamber are taken from the suppression pool temperature response analysis contained in the plant's FSAR.

d. LOCA Temperature Loads: The vent system is subjected to thermal expansion loads associated with the SBA, IBA, and DBA events. The procedure used to develop LOCA containment temperatures is discussed in Section 1-4.1.1. The resulting vent system temperature magnitudes at key times during the SBA, IBA, and DBA events are presented in Table 3-2.2-2.

Additional vent system temperatures are taken from the suppression pool temperature response analysis contained in the plant's FSAR. These temperatures are enveloped by the maximum LOCA temperatures and are not considered further.

The temperatures of the major components of the vent system, such as the vent line, vent header, and downcomers, are conservatively assumed to be equal to the corresponding drywell temperatures for the IBA and DBA events. For the SBA event, the temperature of the major components of the vent system is assumed to be equal to the maximum saturation temperature of the drywell, which is 266°F.

The temperatures of the external components of the vent system such as the support columns, downcomer bracing, and associated ring plates and stiffeners are assumed to be equal to the corresponding suppression chamber temperatures for each event.

The temperatures specified are assumed to be representative of the major component and external component metal temperatures throughout the vent system. The temperature of the SRV piping for those SBA, IBA, and DBA events which include SRV discharge loads is taken as 380°F for the submerged portion of the piping and 407°F for the portion in the suppression chamber airspace. The ambient temperature of the vent system for all events is assumed to be 70°F.

4. Vent System Discharge Loads

a. Pressurization and Thrust Loads: The vent system is subjected to pseudo-static pressurization and thrust loads during a DBA event. The procedure used to develop vent system pressurization and thrust forces,

applied to the unreacted areas of the major components of the vent system, is discussed in Section 1-4.1.2. The resulting maximum forces for each of the major component unreacted areas at key times during the DBA event are shown in Table 3-2.2-3. The pressurization loads acting on the vent line-drywell penetrations are obtained by multiplying the corresponding drywell internal pressures for the DBA event by the penetration unreacted area.

The vent system discharge loads shown in Table 3-2.2-3 correspond to a zero drywell/wetwell pressure differential. The vent system discharge loads specified for the DBA event include the effects of DBA internal pressure loads as discussed in load case 3a. The vent system discharge loads which occur during the SBA or IBA events are negligible.

5. Pool Swell Loads

a. Vent System Impact and Drag Loads: During the initial phase of a DBA event, transient impact and drag pressures are postulated to act on major components of the vent system

above the suppression pool. The major components affected include the vent line inside the suppression chamber below the maximum bulk pool height, the vent header, and the inclined portion of the downcomers below the downcomer rings. The upper portion of the downcomers is shielded from pool swell impact loads by the downcomer rings.

The procedure used to develop the transient forces and the spatial distribution of pool swell impact loads on these components is discussed in Section 1-4.1.4. The resulting maximum pool swell impact and drag pressures on the vent line and downcomers are summarized in Table 3-2.2-4. The resulting magnitudes and distribution of pool swell impact loads on the vent header are summarized in Figure 3-2.2-1. Typical vent header loading transients at selected locations on the vent header are provided in Table 3-2.2-5. The maximum pool swell impact pressures at bottom dead center of the vent header are shown in Figure 3-2.2-2. Typical vent line and downcomer pool swell pressure transients are shown in Figure 3-2.2-3. The

results shown are based on plant unique QSTF test data contained in the PULD (Reference 3) and include the effects of the main vent orifice tests. Pool swell loads do not occur during the SBA and IBA events.

b. Impact and Drag Loads on Other Structure : During the initial phase of a DBA event, transient impact and drag pressures are postulated to act on the components of the vent system other than the major components. The components affected include the downcomer bracing members and ring plates, the vacuum breakers and vacuum breaker supports, the vent header support columns, and the SRV piping and supports.

The procedure used to develop the transient forces and the spatial distribution of pool swell impact loads on these components is discussed in Section 1-4.1.4. The resulting maximum pool swell impact and drag pressures on the downcomer bracing members and ring plates, and the vacuum breakers and vacuum breaker supports are summarized in Table 3-2.2-4. Typical pool swell pressure

transients are shown in Figure 3-2.2-3. The pool swell impact loads on the SRV piping and supports are presented in Volume 5 of this report. The results shown are based on plant unique QSTF test data contained in the PULD which are used to determine the impact velocities and arrival times. Pool swell loads do not occur during the SBA and IBA events.

c. Froth Impingement and Fallback Loads: During the initial phase of a DBA event, transient impingement pressures are postulated to act on components of the vent system located in specified regions above the rising suppression pool. The components located in Region I which are affected include the downcomer bracing members, the vacuum breakers and vacuum breaker supports, and the SRV piping and supports. The components located in Region II which are affected include the vacuum breakers and vacuum breaker supports, the downcomer bracing members, the overhead truss members, and the SRV piping and supports. The plant unique QSTF test results adjusted for the vent line longitudinal

location show that froth impingement loads on the vent line are negligible.

The procedure used to develop the transient forces and spatial distribution of froth impingement and fallback loads on these components is discussed in Section 1-4.1.4. The resulting maximum froth impingement pressures on the downcomer bracing members, and the vacuum breakers and vacuum breaker supports are summarized in Table 3-2.2-4. Froth fallback pressures are negligible. Typical froth impingement and fallback pressure transients are shown in Figure 3-2.2-3. The froth impingement loads acting on the SRV piping and supports are presented in Volume 5 of this report. Pool swell loads do not occur during the SBA and IBA events.

d. Pool Fallback Loads: During the later portion of the pool swell event, transient drag pressures are postulated to act on selected components of the vent system located between the maximum bulk pool height and the downcomer exit. The components affected include the downcomer bracing

members and ring plates, the support columns, and the SRV piping and supports. The procedure used to develop transient drag pressures and spatial distribution of pool fallback loads on these components is discussed in Section 1-4.1.4.

The resulting maximum pool fallback loads on the downcomer bracing members and ring plates are summarized in Table 3-2.2-4. A typical pool fallback pressure transient is shown in Figure 3-2.2-3. The pool fallback loads on the SRV piping and supports are presented in Volume 5 of this report. The results shown include the effects of maximum pool displacements measured in plant unique QSTF tests. Pool swell loads do not occur during the SBA and IBA events.

e. LOCA Air Clearing Submerged Structure Loads: Transient drag pressures are postulated to act on the submerged components of the vent system during the air clearing phase of a DBA event. The components affected include the downcomers, the support columns, the submerged portion of the SRV piping, the

T-quenchers, and the T-quencher supports. The procedure used to develop the transient forces and spatial distribution of DBA air clearing drag loads on these components is discussed in Section 1-4.1.6.

The resulting maximum drag pressures acting on the downcomers and the vent system support columns for the controlling DBA air clearing load case are shown in Table 3-2.2-6. The controlling DBA air clearing loads on the submerged portion of the SRV piping, T-quenchers and supports are presented in Volume 5 of this report. The results shown include the effects of velocity drag, acceleration drag, and interference effects. The LOCA air clearing submerged structure loads which occur during the SBA and IBA events are negligible.

6. Condensation Oscillation Loads

   a. IBA Condensation Oscillation Downcomer Loads: Harmonic internal pressure loads are postulated to act on the downcomers during the condensation oscillation phase of an IBA event. The procedure used to develop the

harmonic pressures and spatial distribution of IBA condensation oscillation downcomer loads is discussed in Section 1-4.1.7. The loading consists of a uniform internal pressure component acting on all downcomers and a differential internal pressure component acting on one downcomer in a downcomer pair. The resulting pressure amplitudes and associated frequency range for each of the three harmonics in the IBA condensation oscillation downcomer loading are shown in Table 3-2.2-7. The corresponding distribution of differential downcomer internal pressure loadings are shown in Figure 3-2.2-4.

The IBA condensation oscillation downcomer load harmonic in the range of the dominant downcomer frequency for the uniform and the differential pressure components is applied at the dominant downcomer frequency. The remaining two downcomer load harmonics are applied at frequencies which are multiples of the dominant frequency. The results of the three harmonics for the uniform and differ-

ential IBA condensation oscillation downcomer load components are combined.

b. DBA Condensation Oscillation Downcomer Loads: Harmonic internal pressure loads are postulated to act on the downcomers during the condensation oscillation phase of a DBA event. The procedure used to develop the harmonic pressures and spatial distribution of DBA condensation oscillation downcomer loads is the same as that discussed for IBA condensation oscillation downcomer loads in load case 6a. The resulting pressure amplitudes and associated frequency range for each of the three harmonics in the DBA condensation oscillation downcomer loading are shown in Table 3-2.2-8. The corresponding distribution of differential downcomer internal pressure loadings are shown in Figure 3-2.2-4.

c. IBA Condensation Oscillation Vent System Pressure Loads: Harmonic internal pressure loads are postulated to act on the vent system during the condensation oscillation phase of an IBA event. The components

affected include the vent line, the vent header, and the downcomers. The procedure used to develop the harmonic pressures and spatial distribution of IBA condensation oscillation vent system pressures is discussed in Section 1-4.1.7. The resulting pressure amplitudes and associated frequency range for the vent line and vent header are shown in Table 3-2.2-9. The loading is applied at the frequency within a specified range which maximizes the vent system response.

The effects of IBA condensation oscillation vent system pressures on the downcomers are included in the IBA condensation oscillation downcomer loads discussed in load case 6a. An additional static internal pressure of 1.5 psi is applied uniformly to the vent line, vent header, and downcomers to account for the effects of nominal downcomer submergence. The IBA condensation oscillation vent system pressures act in addition to the IBA containment internal pressures discussed in load case 3b.

d. DBA Condensation Oscillation Vent System Pressure Loads: Harmonic internal pressure loads are postulated to act on the vent system during the condensation oscillation phase of a DBA event. The components affected include the vent line, the vent header, and the downcomers. The procedure used to develop the harmonic pressures and spatial distribution of DBA condensation oscillation vent system pressures is the same as that discussed for IBA condensation oscillation vent system pressures in load case 6c. The resulting pressure amplitudes and associated frequency range for the vent line and vent header are shown in Table 3-2.2-9. The DBA condensation oscillation vent system pressures act in addition to the DBA vent system pressurization and thrust loads discussed in load case 4a.

e. IBA Condensation Oscillation Submerged Structure Loads: Harmonic pressure loads are postulated to act on the submerged components of the vent system during the condensation oscillation phase of an IBA event. In accordance with NUREG-0661, the submerged

structure loads specified for pre-chug are used in lieu of IBA condensation oscillation submerged structure loads. Pre-chug submerged structure loads are discussed in load case 7c.

f. DBA Condensation Oscillation Submerged Structure Loads: Harmonic drag pressures are postulated to act on the submerged components of the vent system during the condensation oscillation phase of a DBA event. The components affected include the support columns, the submerged portions of the SRV piping, the T-quenchers and the T-quencher supports. The procedure used to develop the harmonic forces and spatial distribution of DBA condensation oscillation drag loads on these components is discussed in Section 1-4.1.7.

Loads are developed for the case with the average source strength at all downcomers and the case with twice the average source strength at the nearest downcomer. The results of these two cases are evaluated to determine the controlling loads.

The resulting maximum drag pressure acting on the support columns for the controlling DBA condensation oscillation drag load case are shown in Table 3-2.2-6. The effects of DBA condensation oscillation submerged structure loads on the downcomers are included in the loads discussed in load case 6b.

The results shown in Table 3-2.2-6 include the effects of velocity drag, acceleration drag, torus shell FSI acceleration drag, and interference effects. A typical DBA condensation oscillation pool acceleration profile from which FSI accelerations are derived is shown in Figure 3-2.2-5. The results of each harmonic in the loading are combined using the methodology discussed in Section 1-4.1.7.

7. Chugging Loads

   a. Chugging Downcomer Lateral Loads: Lateral loads are postulated to act on the downcomers during the chugging phase of the SBA, IBA, and DBA events. The procedure used to develop chugging downcomer lateral loads is discussed in Section 1-4.1.8. The maximum

lateral load acting on any one downcomer in any direction is obtained using the maximum downcomer lateral load and chugging pulse duration measured at FSTF, the frequency of the tied downcomers for FSTF, and the plant unique downcomer frequency calculated for Hope Creek. This information is summarized in Table 3-2.2-10. The resulting ratic of Hope Creek to FSTF Dynamic Load Factors (DLF's) is used in subsequent calculations to determine the magnitude of multiple downcomer loads and to determine the load magnitude used for evaluating fatigue. The methodology used to determine the plant unique downcomer frequency is discussed in Section 3-2.4.1.

The magnitude of chugging lateral loads acting on multiple downcomers simultaneously is determined using the methodology described in Section 1-4.1.8. The methodology involves using 10^{-4} as the probability of exceeding a given downcomer load magnitude once per LOCA. The chugging load magnitudes, shown in Table 3-2.2-11, are determined using the above non-exceedance probability and the ratio of the DLF's taken for the maximum downcomer load

calculation. The distributions of chugging downcomer lateral loads which are considered include those cases which maximize local effects in the vent system and those cases which maximize overall effects in the vent system.

The maximum downcomer lateral load magnitude used for evaluating fatigue is obtained using the maximum downcomer lateral load measured at FSTF with a 95% NEP, and the ratio of DLF's taken from maximum downcomer load calculations. The stress reversal histograms provided for FSTF are converted to plant unique stress reversal histograms using the postulated plant unique chugging duration as shown in Table 3-2.2-12.

b. Chugging Vent System Pressures: Transient and harmonic internal pressures are postulated to act on the vent system during the chugging phase of the SBA, IBA, and DBA events. The components affected include the vent line, the vent header, and the downcomers. The procedure used to develop chugging vent system pressures is discussed

in Section 1-4.1.8. The load consists of a gross vent system pressure oscillation component, an acoustic vent system pressure oscillation component, and an acoustic downcomer pressure oscillation component. The resulting pressure magnitudes and characteristics of the chugging vent system pressure loading are shown in Table 3-2.2-13. The three load components are evaluated individually and are not combined.

The overall effects of chugging vent system pressures on the downcomers are included in the loads discussed in load case 7a. The downcomer pressures shown in Table 3-2.2-13 are used to evaluate downcomer hoop stresses. The chugging vent system pressures act in addition to the SBA and IBA containment internal pressures discussed in load case 3b and the DBA pressurization and thrust loads discussed in load case 4a.

c. Pre-Chug Submerged Structure Loads: During the chugging phase of SBA, IBA, and DBA events, harmonic drag pressures associated with the pre-chug portion of a chug cycle are

postulated to act on the submerged components of the vent system. The components affected include the support columns, the submerged portion of the SRV piping, the T-quenchers, and the T-quencher supports. The procedure used to develop the harmonic forces and spatial distribution of pre-chug drag loads on these components is discussed in Section 1-4.1.8.

Loads are developed for the case with the average source strength at all downcomers and the case with twice the average source strength at the nearest downcomer. The results of these two cases are evaluated to determine the controlling loads. The resulting maximum drag pressures acting on the support columns for the controlling pre-chug drag load case are shown in Table 3-2.2-6. The effects of pre-chug submerged structure loads on the downcomers are included in the loads discussed in load case 7a.

The results shown include the effects of velocity drag, acceleration drag, torus shell FSI acceleration drag, and interference

effects. As can be seen by examining Table 3-2.2-6, the submerged structure drag pressures due to pre-chug are bounded by post-chug. Therefore post-chug submerged structure loads (Case 7d) are used in the analysis in lieu of pre-chug submerged structure loads.

d. Post-Chug Submerged Structure Loads: During the chugging phase of SBA, IBA, and DBA events, harmonic drag pressures associated with the post-chug portion of a chug cycle are postulated to act on the submerged components of the vent system. The components affected include the support columns, the submerged portion of the SRV piping, the T-quenchers, and the T-quencher supports. The procedure used to develop the harmonic forces and spatial distribution of post-chug drag loads on these components is discussed in Section 1-4.1.8.

Loads are developed for the cases with the average source strength at the nearest two downcomers acting both in-phase and out-of-phase. The results of these cases are

evaluated to determine the controlling loads. The resulting maximum drag pressures acting on the vent system support columns for the controlling post-chug drag load case are shown in Table 3-2.2-6. The controlling post-chug drag loads on the submerged portion of the SRV piping, the T-quenchers, and the T-quencher supports are presented in Volume 5 of this report. The effects of post-chug submerged structure loads acting on the downcomers are included in the chugging downcomer lateral loads discussed in load case 7a.

The results shown include the effects of velocity drag, acceleration drag, torus shell FSI acceleration drag, and interference effects. A typical post-chug pool acceleration profile from which the FSI accelerations are derived is shown in Figure 3-2.2-6. The results of each harmonic are combined using the methodology described in Section 1-4.1.8.

8. Safety Relief Valve Discharge Loads

a. SRV Discharge Air Clearing Submerged Structure Loads: Transient drag pressures are

postulated to act on the submerged components of the vent system during the air clearing phase of an SRV discharge event. The components affected include the downcomers, support columns, the submerged portion of the SRV piping, the T-quenchers, and the T-quencher supports. The procedure used to develop the transient forces and spatial distribution of the SRV discharge air clearing drag loads on these components is discussed in Section 1-4.2.4.

Loads are developed for the case with three or four quenchers in consecutive bays acting in-phase and the case with three quenchers in adjacent bays acting out-of-phase. These results are evaluated to determine the controlling loads. The maximum drag pressures acting on the downcomers and the support columns for the controlling SRV discharge drag load case are shown in Table 3-2.2-6.

These results include the effects of velocity drag, acceleration drag, and interference effects.

9. Piping Reaction Loads

a. SRV Piping Reaction Loads: Reaction loads are induced on the vent system due to loads acting on the drywell and wetwell SRV piping systems. These reaction loads occur at the vent line-SRV piping penetrations and SRV piping support on the vent header. The SRV piping reaction loads consist of those caused by motions of the vent system and loads acting on the drywell and wetwell portions of the SRV piping systems. Loads acting on the SRV piping systems include pressurization and thrust loads, elevated structure loads, submerged structure loads, and other operating or design basis loads.

The effects of the SRV piping reaction loads on the vent system are included in the vent system analysis. The reaction loads from the drywell portion of the SRV piping are taken from Volume 5.

10. Containment Interaction Loads

a. Containment Structure Motions: Loads acting on the drywell, suppression chamber and vent system cause interaction effects between

these structures. The interaction effects result in vent system motions at the attachment points of the vent system to the drywell and the suppression chamber. The effects of these motions on the vent system are considered in the vent system analysis.

The values of the loads presented in the preceding paragraphs envelop those which could occur during the LOCA and SRV discharge events postulated. An evaluation for the effects of the above loads results in conservative estimates of the vent system responses and leads to bounding values of vent system stresses.

Table 3-2.2-1

VENT SYSTEM COMPONENT LOADING INFORMATION

Volume 3 Load Designation			PUAR Section Reference	Component Part Loaded							
Category	Load Type	Case Number		Drywell Penetration	Vent Line	Vent Line Bellows	Vent Header	Downcomers	Downcomer Bracing	Support Members	Vacuum Breaker and Support
Dead Weight Loads	Dead Weight of Steel	1a	1-3.1	X	X	X	X	X	X	X	X
Seismic Loads	OBE Seismic Loads	2a	1-3.1	X	X	X	X	X	X	X	X
	SSE Seismic Loads	2b	1-3.1	X	X	X	X	X	X	X	X
Pressure and Temperature Loads	Normal Operating Internal Pressure	3a	1-3.1	X	X	X	X	X			X
	LOCA Internal Pressure	3b	1-4.1.1	X	X	X	X	X			X
	Normal Operating Temperature Loads	3c	1-3.1	X	X	X	X	X	X	X	X
	LOCA Temperature Loads	3d	1-4.1.1	X	X	X	X	X	X	X	X
Vent System Discharge	Pressurization and Thrust Loads	4a	1-4.1.2	X	X		X	X			X
Pool Swell Loads	Vent System Impact and Drag Loads	5a	1-4.1.4.1		X		X	X			
	Impact and Drag Loads on Other Structures	5b	1-4.1.4.2						X	X	
	Froth Impingement & Fallback Loads	5c	1-4.1.4.3						X	X	X
	Pool Fallback Loads	5d	1-4.1.4.4						X	X	
	LOCA Water Clearing Submerged Structure Loads	N/A	1-4.1.5							X	
	LOCA Air Clearing Submerged Structure Loads	5e	1-4.1.6					X		X	
Condensation Oscillation Loads	IBA C.O. Downcomer Loads	6a	1-4.1.7.2					X			
	DBA C.O. Downcomer Loads	6b	1-4.1.7.2					X			
	IBA C.O. Vent System Pressure Loads	6c	1-4.1.7.2	X	X		X				X
	DBA C.O. Vent System Pressure Loads	6d	1-4.1.7.2	X	X		X				X
	IBA C.O. Submerged Structure Loads	6e	1-4.1.7.3							X	
	DBA C.O. Submerged Structure Loads	6f	1-4.1.7.3							X	
Chugging Loads	Chugging Downcomer Lateral Loads	7a	1-4.1.8.2					X			
	Chugging Vent System Pressures	7b	1-4.1.8.2	X	X		X	X			X
	Pre-Chug Submerged Structure Loads	7c	1-4.1.8.3							X	
	Post-Chug Submerged Structure Loads	7d	1-4.2.4							X	
SRV Discharge Loads	SRV Discharge Water Clearing Submerged Structure Loads	N/A	1-4.2.4							X	
	SRV Discharge Air Clearing Submerged Structure Loads	8a	1-4.2.4					X		X	
Piping Reaction Loads	SRV Piping Reaction Loads	9a	Vol. 5		X		X				
Containment Interaction Loads	Containment Structure Motions	10a	Vol. 2	X		X				X	

Table 3-2.2-2

VENT SYSTEM INTERNAL PRESSURES AND TEMPERATURES FOR LOCA EVENTS (1)

Event Description	Pressure, Temperature Designation	Time (sec)		Pressure (psig) (2)				Temperature (°F) (3)			
				Outside Torus		Inside Torus		Components		Externals	
		t_{min}	t_{max}	P_{min}	P_{max}	P_{min}	P_{max}	T_{min}	T_{max}	T_{min}	T_{max}
SBA LOCA											
Instant of Break to Onset of Chugging	P_1, T_1	0.	300.	0.75	12.0	0.0	2.0	266.	266.	95.	101.
Onset of Chugging to Initiation of ADS	P_2, T_2	300.	600.	12.0	21.3	1.4	2.0	266.	266.	101.	103.
Initiation of ADS to RPV Depressurization	P_3, T_3	600.	1200.	21.3	24.3	1.4	1.5	266.	266.	103.	135.
IBA LOCA											
Instant of Break to Onset of CO and Chugging	P_1, T_1	0.	5.	0.75	3.5	0.0	1.5	210.	220.	95.	95.
Onset of CO and Chugging to Initiation of ADS	P_2, T_2	5.	300.	3.5	22.1	1.4	1.5	220.	262.	95.	112.
Initiation of ADS to RPV Depressurization	P_3, T_3	300.	500.	22.1	33.7	1.4	2.0	262.	279.	112.	167.
DBA LOCA (4)											
Instant of Break to Termination of Pool Swell	P_1, T_1	0.	1.5	0.75	39.0	0.0	31.4	135.	270.	80.	82.
Termination of Pool Swell to Onset of CO	P_2, T_2	1.5	5.0	39.0	47.4	31.4	32.6	270.	292.	82.	87.
Onset of CO to Onset of Chugging	P_3, T_3	5.0	35.0	29.0	46.0	4.4	32.6	273.	292.	87.	118.
Onset of Chugging to RPV Depressurization	P_4, T_4	35.0	65.0	29.0	29.0	4.4	4.4	273.	273.	118.	118.

Notes:

1. LOCA pressure and temperature transients are contained in Hope Creek PULD (Reference 3).
2. Pressures for vent system components outside the torus are equal to absolute drywell pressure. Pressures for vent system components inside the torus are equal to the difference in drywell and suppression chamber absolute pressures. Initial pressures are assumed to be 0.0 psig.
3. Temperatures for the vent system components including the vent line, vent header, and downcomers are equal to the drywell temperatures. Temperatures for the vent system externals including the supports and downcomer bracing system are equal to the suppression chamber temperatures. Initial temperatures are assumed to be 70°F.
4. DBA vent system internal pressure loads are included in the vent system pressurization and thrust loads shown in Table 3-2.2-3.

Table 3-2.2-3

VENT SYSTEM PRESSURIZATION AND THRUST LOADS FOR

DBA EVENT

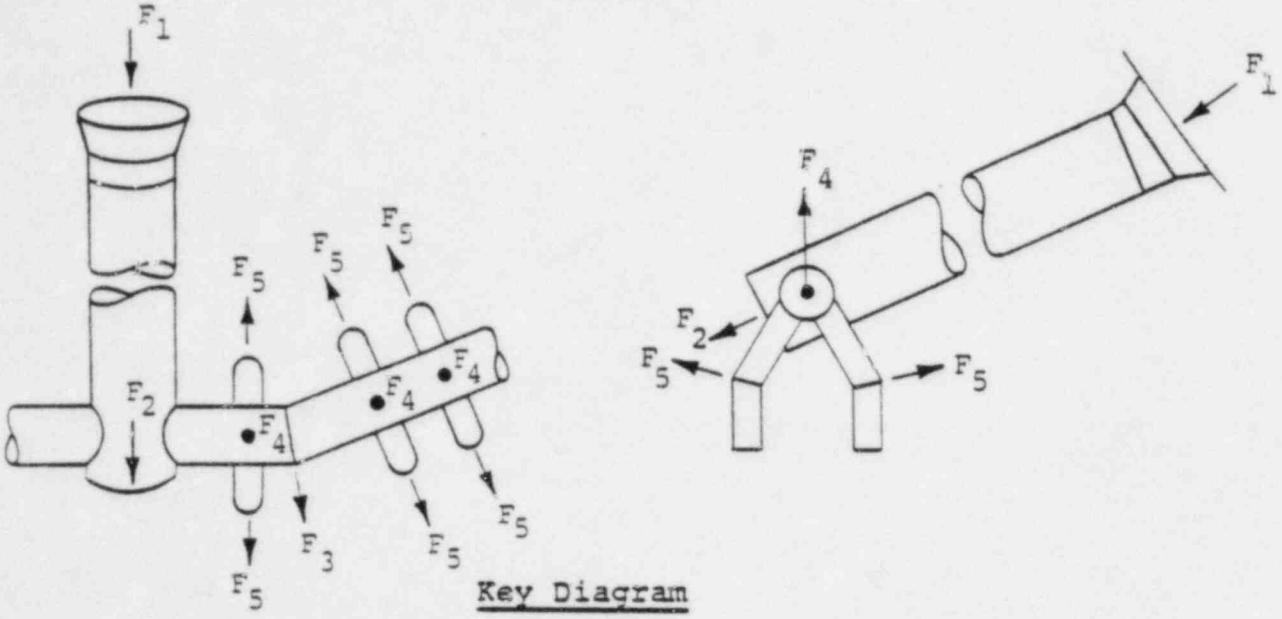

Key Diagram

Time During DBA Event (sec)	Maximum Component Force Magnitude (kips)				
	F_1 (1)	F_2	F_3	F_4	F_5
Pool Swell 0.0 to 1.5	67.45	139.89	19.70	19.16	3.93
Condensation Oscillation 5.0 to 35.0	81.98	129.61	17.74	17.44	3.52
Chugging 35.0 to 65.0	50.16	19.95	2.87	2.62	0.61

Notes:

1. Loads shown include the effects of the DBA internal pressures in Table 3-2.2-2.
2. Values shown are equal to product of penetration unreacted area and DBA internal pressure.

Table 3-2.2-4

MAXIMUM POOL SWELL ELEVATED STRUCTURE LOADS[1]

Component		Number of Segments[2]	Maximum Pressure (psi)[3]			
			Pool Impact (P_{max})	Pool Drag (P_d)	Pool Fallback (P_{pfb})	Froth Impingement (P_f)
Vent Line		2	13.21	2.649	-	1.388
Downcomer		4	-	8.0	-	-
Vacuum Breaker and Support		2	-	-	-	.704
Vent Bay Downcomer Bracing	Ring Plate	1	563.1	10.095	1.264	-
	4"Φ Pipe	3	14.21	2.44	.306	2.539
Non-Vent Bay Downcomer Bracing	2½"Φ Rod	2	42.67	7.312	.682	-
	Ring Plate	1	563.1	10.095	1.264	-
	4"Φ Pipe	3	14.21	2.44	.306	2.539

Notes:

1. See Table 3-2.2-5 and Figures 3-2.2-1 and 3-2.2-2 for vent header pool swell impact and drag loads.

2. Number of segments correspond to nodalization of structures for loads calculations.

3. See Figure 3-2.2-3 for typical pressure transient definitions.

4. Pressures are applied to vertical projected areas in a direction normal to structure.

5. Loads on vent line and vacuum breaker are symmetric with respect to the vertical centerline of the vent line. Loads on downcomers and downcomer bracing are symmetric with respect to the vertical centerline of the vent header.

Table 3-2.2-5

TYPICAL VENT HEADER POOL SWELL LOADING TRANSIENTS

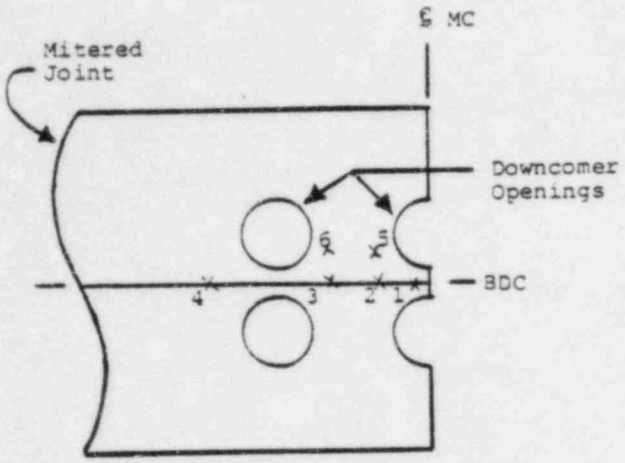

Developed View of NVB Vent Header

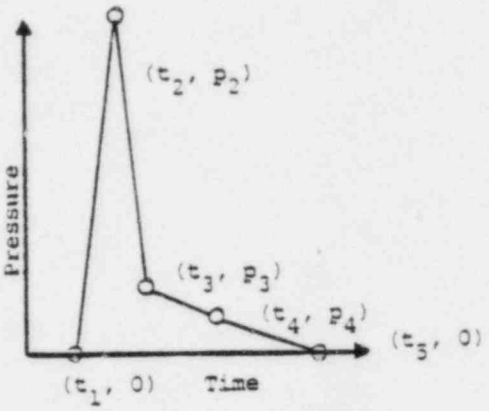

Typical Loading Transient

Location	t_1	t_2	P_2	t_3	P_3	t_4	P_4	t_5
1	0.366	2.194	174.3	3.869	23.6	27.17	1.99	107.2
2	1.975	3.532	115.5	6.119	32.8	25.31	1.96	88.3
3	4.301	6.064	87.7	8.876	29.1	27.65	1.86	95.9
4	8.950	10.981	80.0	13.971	25.8	34.04	1.57	103.6
5	4.020	8.155	60.3	14.120	18.4	38.76	1.03	100.4
6	6.432	9.390	38.5	15.021	14.9	35.74	1.04	101.7

Notes:

1. Pressure (p) in psi.
2. Time (t) in msec.

Table 3-2.2-6

MAXIMUM VENT SYSTEM SUBMERGED STRUCTURE LOADS

Loading[1]	Maximum Pressure (psi)	
	Downcomer[2]	Support Column[3]
LOCA Air Clearing	1.63	1.68
DBA Condensation Oscillation	N/A[4]	12.13
Pre-Chug	N/A[5]	1.47
Post-Chug	N/A[5]	44.61
SRV	20.13	37.24

Notes:

1. Loads shown include DLF's.
2. Downcomers are subdivided into two segments for loads calculations.
3. Support columns are subdivided into 13 segments for loads calculations.
4. Condensation oscillation loads on downcomers are provided in Tables 3-2.2-7 and 3-2.2-8.
5. Chugging loads on downcomers are provided in Table 3-2.2-11.

Table 3-2.2-7

IBA CONDENSATION OSCILLATION

DOWNCOMER LOADS

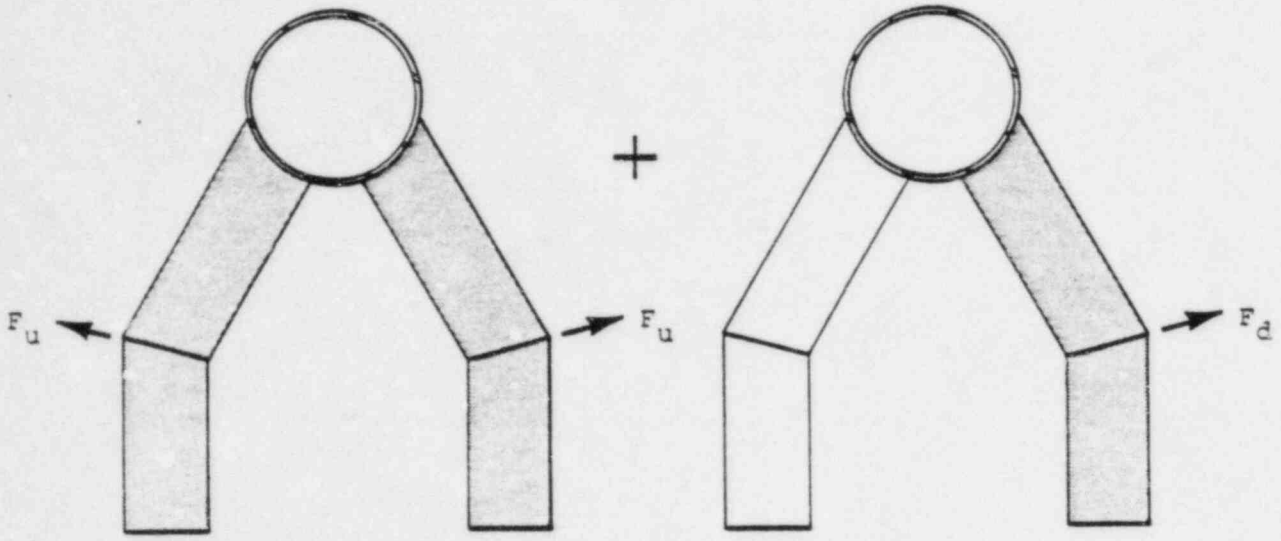

Uniform Pressure

Differential Pressure

Frequency Interval (Hz)	Downcomer Load Amplitudes (1)			
	Uniform (F_u)		Differential (F_d) (2)	
	Pressure (psi)	Force (lb)	Pressure (psi)	Force (lb)
6.0 - 10.0	1.10	241.75	0.20	43.95
12.0 - 20.0	0.80	175.82	0.20	43.95
18.0 - 30.0	0.20	43.95	0.20	43.95

Notes:

1. Effects of uniform and differential pressures summed to obtain total load.
2. See Figure 3-2.2-4 for downcomer differential pressure load distributions.

Table 3-2.2-8

DBA CONDENSATION OSCILLATION DOWNCOMER LOADS

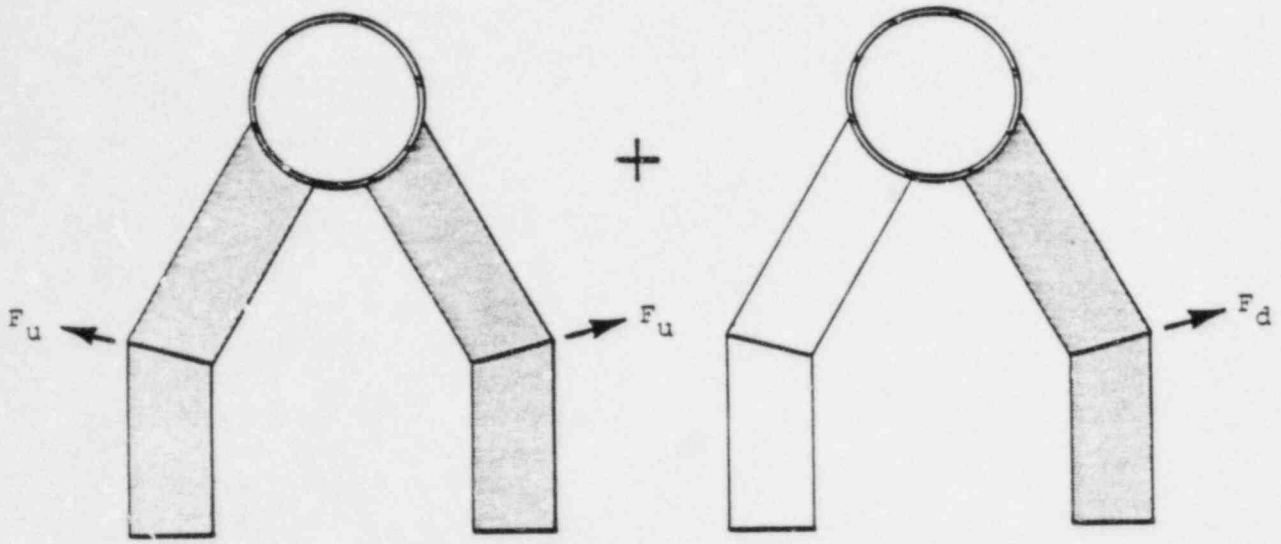

Uniform Pressure

Differential Pressure

Frequency Interval (Hz)	Downcomer Load Amplitudes (1)			
	Uniform (F_u)		Differential (F_d)(2)	
	Pressure (psi)	Force (lb)	Pressure (psi)	Force (lb)
4.0 - 8.0	3.60	791.16	2.85	626.34
8.0 - 16.0	1.30	285.70	2.60	571.39
12.0 - 24.0	0.60	131.86	1.20	263.72

Notes:

1. Effects of uniform and differential pressures summed to obtain total load.
2. See Figure 3-2.2-4 for downcomer differential pressure load distribution.

Table 3-2.2-9

IBA AND DBA CONDENSATION OSCILLATION
VENT SYSTEM INTERNAL PRESSURES

Load Characteristics	Component Load			
	Vent Line		Vent Header	
	IBA	DBA	IBA	DBA
Type	Single Harmonic	Single Harmonic	Single Harmonic	Single Harmonic
Magnitude (psi)	± 2.5	± 2.5	± 2.5	± 2.5
Distribution	Uniform	Uniform	Uniform	Uniform
Frequency Range (Hz)	6 - 10	4 - 8	6 - 10	4 - 8

Notes:

1. Downcomer CO internal pressure loads are included in loads shown in Tables 3-2.2-7 and 3-2.2-8.
2. Loads shown act in addition to vent system internal pressures in Table 3-2.2-2.
3. Additional static internal pressure of 1.5 psi applied to the entire vent system to account for nominal submergence of downcomers.

Table 3-2.2-10

MAXIMUM DOWNCOMER CHUGGING LOAD MAGNITUDE DETERMINATION

Maximum Chugging Load for Single Downcomer
FSTF Maximum Load Magnitude: P_1=3.046 kips Tied Downcomer Frequency: f_1=2.9 Hz Pulse Duration: t_d= 0.003 sec. Dynamic Load Factor: $DLF_1 = \pi f_1 t_d$=0.027
Hope Creek Downcomer Frequency: 13.92 Hz Dynamic Load Factor: $DLF=\pi f t_d$= .131 Maximum Load Magnitude (In any direction): $P_{max}=P_1(\frac{DLF}{DLF_1})=(3.046)(4.8)=$ 14.62 kips

Note:

1. See Table 3-2.4-3 for Hope Creek downcomer frequency.

nutech ENGINEERS

Table 3-2.2-11

DOWNCOMER CHUGGING LATERAL LOADS

Case Number	Number of Downcomers Loaded	Description/Distribution	Magnitude (kips)
1	10	Downcomers centered on one VL, perpendicular to VH, opposing directions, maximize VL bending	6.99
2	10	Downcomers centered on one VL, perpendicular to VH, same directions, maximize VL axial load	6.99
3	10	All downcomers between two VL's, perpendicular to VH, same direction, maximize VH bending	6.99
4	2	MC NVB downcomers, perpendicular to VH, opposing directions, maximize DC bending	13.49
5	2	MC NVB downcomers, perpendicular to VH, same directions, maximize DC swinging	13.49
6	2	MC NVB downcomers, parallel to VH, opposing directions, maximize DC bracing loads	13.49
7	2	MC NVB downcomers, parallel to VH, same directions, maximize DC bracing loads	13.49
8	1	MC NVB downcomers, parallel to VH, maximize effects on single DC	14.62
9	1	MC NVB downcomer, perpendicular to VH maximize effects on single DC	14.62

Table 3-2.2-12

LOAD REVERSAL HISTOGRAM FOR CHUGGING

DOWNCOMER LATERAL LOAD FATIGUE EVALUATION

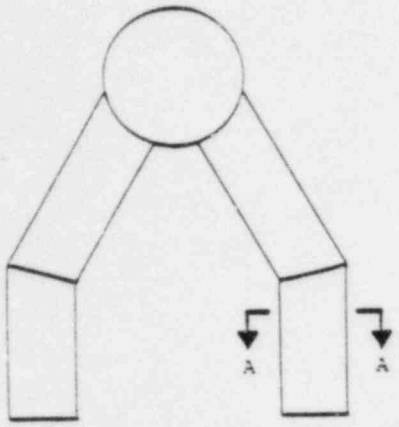

Elevation View

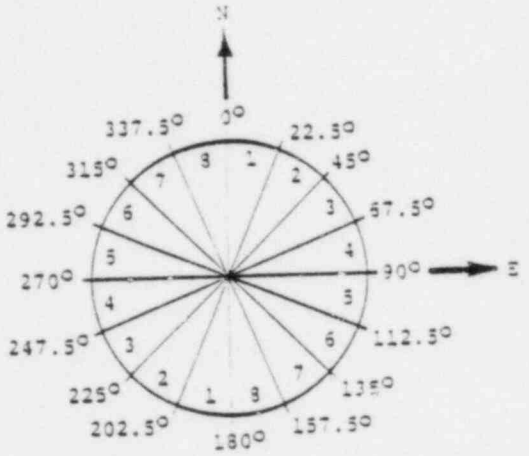

Section A-A

KEY DIAGRAM

Percent of Maximum Load Range[2]	Angular Sector Load Reversals (cycles)[1]							
	1	2	3	4	5	6	7	8
5 - 10	4706	2573	2839	3076	3168	2673	2563	4629
10 - 15	2696	1206	1100	1104	1096	1052	1163	2545
15 - 20	1399	727	653	572	709	708	679	1278
20 - 25	676	419	452	377	370	398	368	621
25 - 30	380	250	252	225	192	255	197	334
30 - 35	209	187	139	121	97	114	162	208
35 - 40	157	62	84	86	62	60	90	150
40 - 45	113	53	28	39	48	44	58	86
45 - 50	83	33	32	26	18	23	33	67
50 - 55	65	26	14	11	9	7	16	40
55 - 60	51	26	11	5	11	11	23	28
60 - 65	44	9	2	4	0	5	9	26
65 - 70	32	16	7	5	0	2	9	21
70 - 75	12	9	11	5	0	4	7	19
75 - 80	26	4	2	0	2	4	7	18
80 - 85	7	5	2	0	0	0	0	12
85 - 90	4	11	0	0	0	0	5	11
90 - 95	7	4	0	0	2	0	0	9
95 - 100	2	5	0	0	0	2	4	7

Notes:

1. Values shown are for chugging duration of 900 sec.
2. The maximum single downcomer load magnitude range used for fatigue is 3.936 x 4.8 = 18.9 kips (see Table 3-2.2-14).

Table 3-2.2-13

CHUGGING VENT SYSTEM INTERNAL PRESSURES

Load Type		Load Description	Component Load Magnitude (psi)		
Number	Description		Vent Line	Vent Header	Downcomer
1	Gross Vent System Pressure Oscillation	Transient pressure. Uniform distribution.	± 2.5	± 2.5	± 5.0
2	Acoustic Vent System Pressure Oscillation	Single harmonic in 6.9 to 9.5 Hz range. Uniform distribution.	± 2.5	± 3.0	± 3.5
3	Acoustic Downcomer Pressure Oscillation	Single harmonic in 40.0 to 50.0 Hz range. Uniform distribution.	N/A	N/A	± 13.0

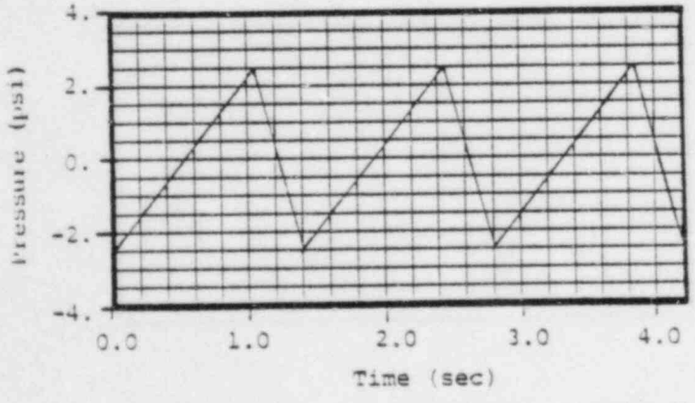

Forcing Function for Load Type 1

Loading Information
1. Downcomer loads shown used for hoop stress calculations only.
2. Loads act in addition to internal pressure loads shown in Table 3-2.2-2.

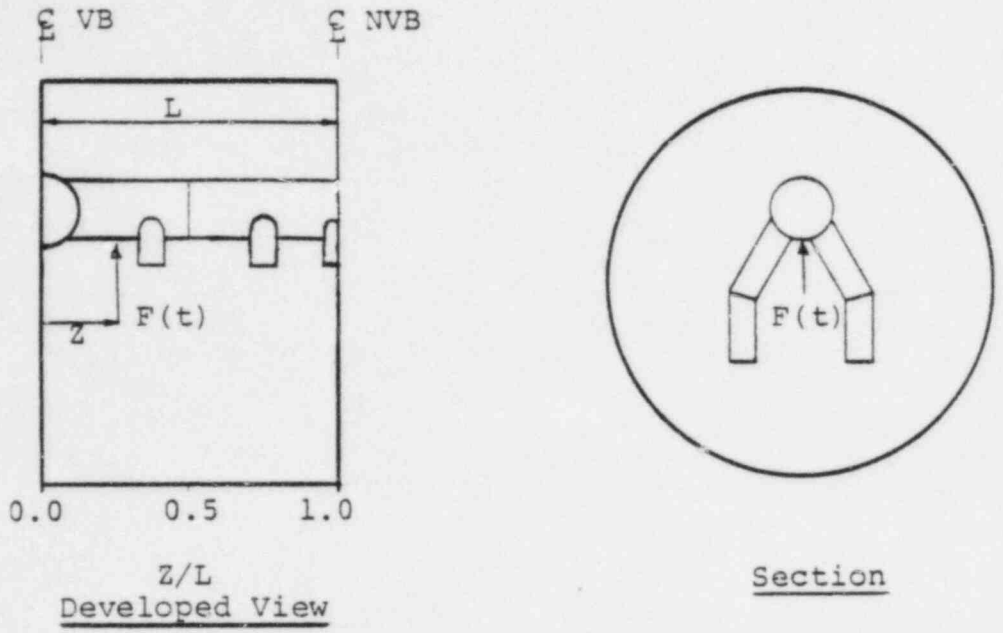

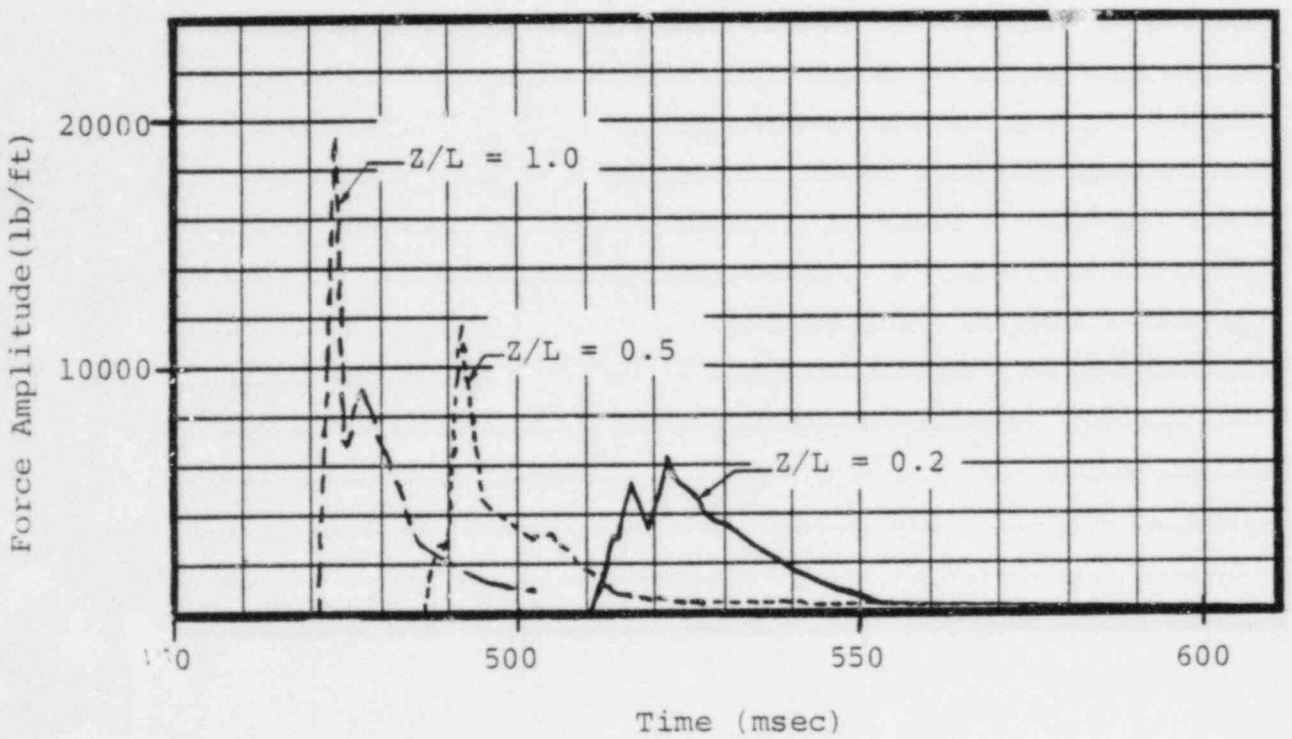

Figure 3-2.2-1

POOL SWELL IMPACT LOADS FOR VENT HEADER AT SELECTED LOCATIONS

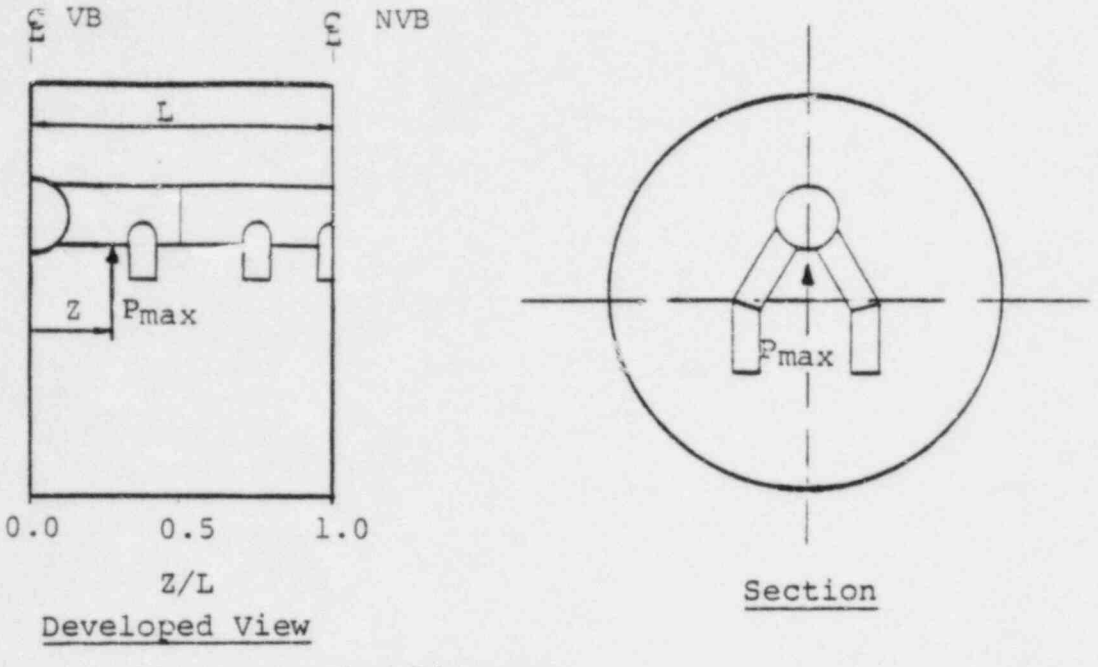

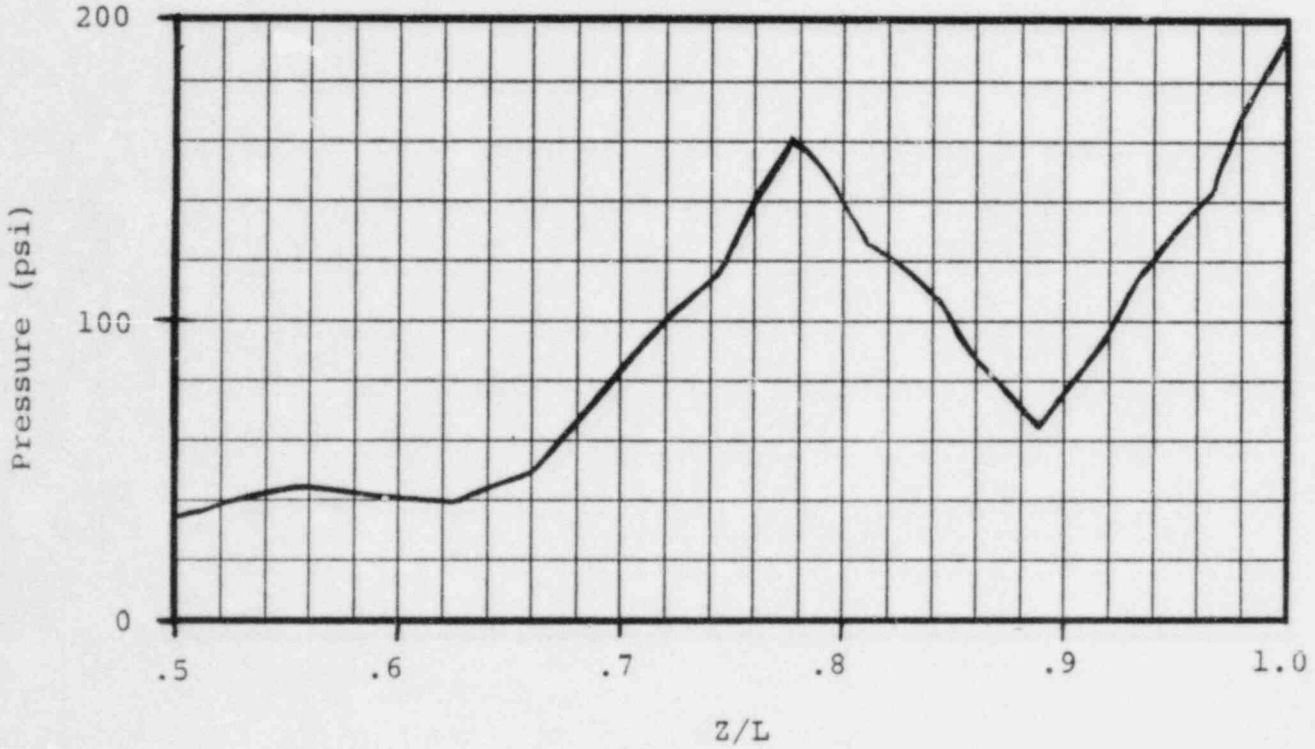

Figure 3-2.2-2

MAXIMUM POOL SWELL IMPACT PRESSURES
ON VENT HEADER AT BOTTOM DEAD CENTER

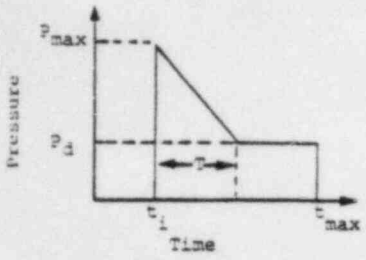

Pool Swell Impact - Cylindrical Structures

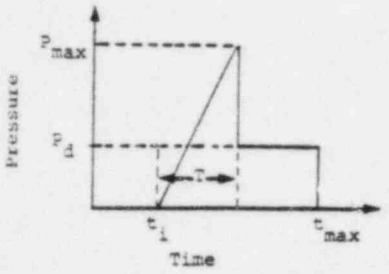

Pool Swell Impact - Flat Structures

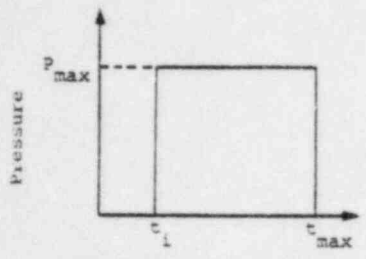

Pool Swell Impact - Downcomers

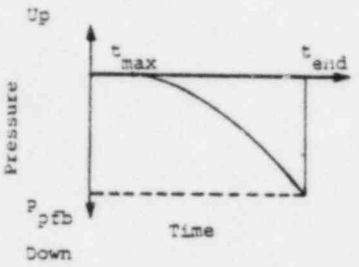

Pool Fallback

Pool Swell Impact and Pool Fallback

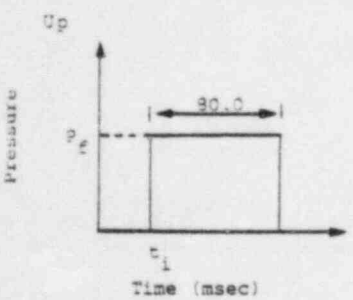

Region I Transient

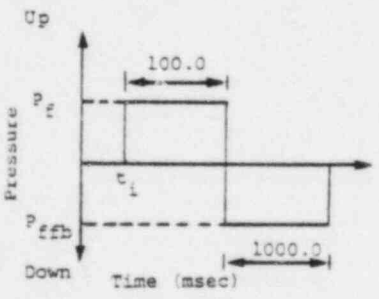

Region II Transient

Legend		
t_i	=	Arrival time
T	=	Impact duration
t_{max}	=	Time of maximum pool height
t_{end}	=	Time at end of pool fallback
P_{max}	=	Peak impact pressure
P_d	=	Drag pressure
P_f	=	Froth pressure
P_{ffb}	=	Froth fallback pressure
P_{pfb}	=	Pool fallback pressure

Froth Impingement and Fallback

Figure 3-2.2-3

TYPICAL POOL SWELL PRESSURE TRANSIENTS

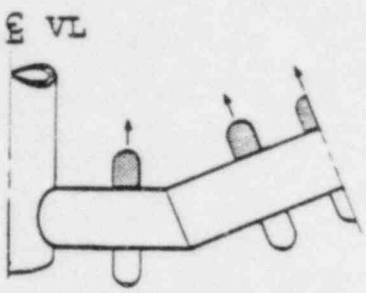

Case 1

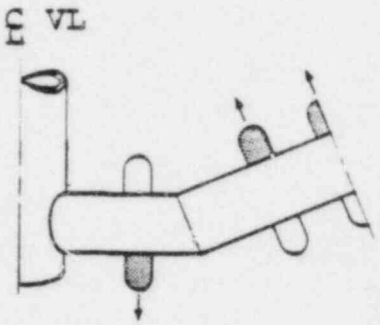

Case 2

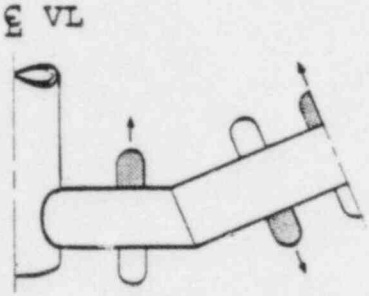

Case 3

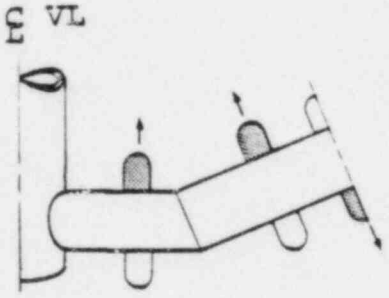

Case 4

Notes:

1. See Table 3-2.2-7 for IBA pressure amplitudes and frequencies.
2. See Table 3-2.2-8 for DBA pressure amplitudes and frequencies.
3. Four additional cases with pressures in downcomers opposite those shown are also specified.

Figure 3-2.2-4

IBA AND DBA CONDENSATION OSCILLATION DOWNCOMER DIFFERENTIAL PRESSURE LOAD DISTRIBUTION

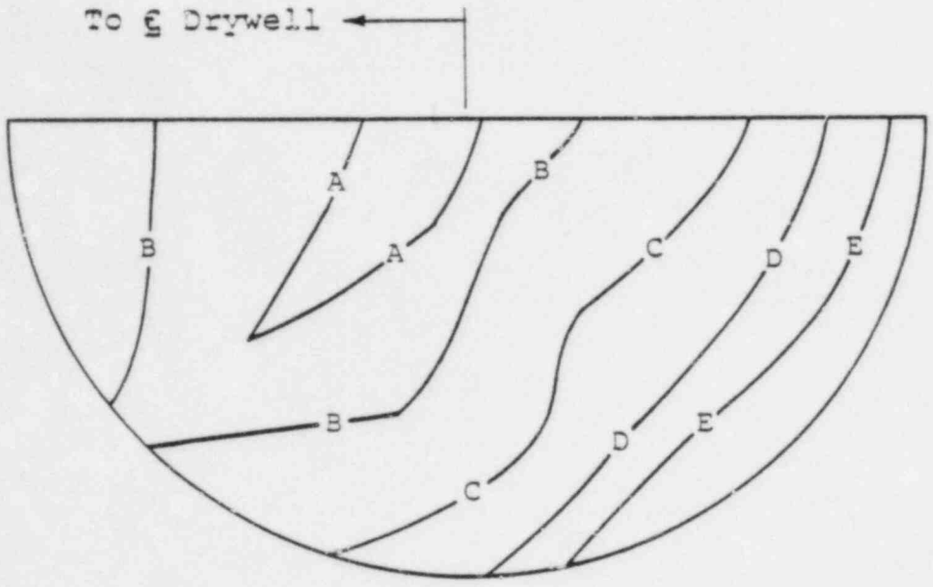

Key Diagram

Normalized Pool Accelerations	
Profile	Pool Acceleration (in/sec^2)
A	50.0
B	200.0
C	500.0
D	1000.0
E	1500.0
Pool accelerations due to harmonic application of torus shell pressures shown in Figure 2-2.2-3 and the Alternate 4 amplitudes shown in Table 2-2.2-4 (see PUAR Volume 2).	

Figure 3-2.2-5

POOL ACCELERATION PROFILE FOR DBA CONDENSATION OSCILLATION TORUS SHELL LOADS AT QUARTER-BAY LOCATION

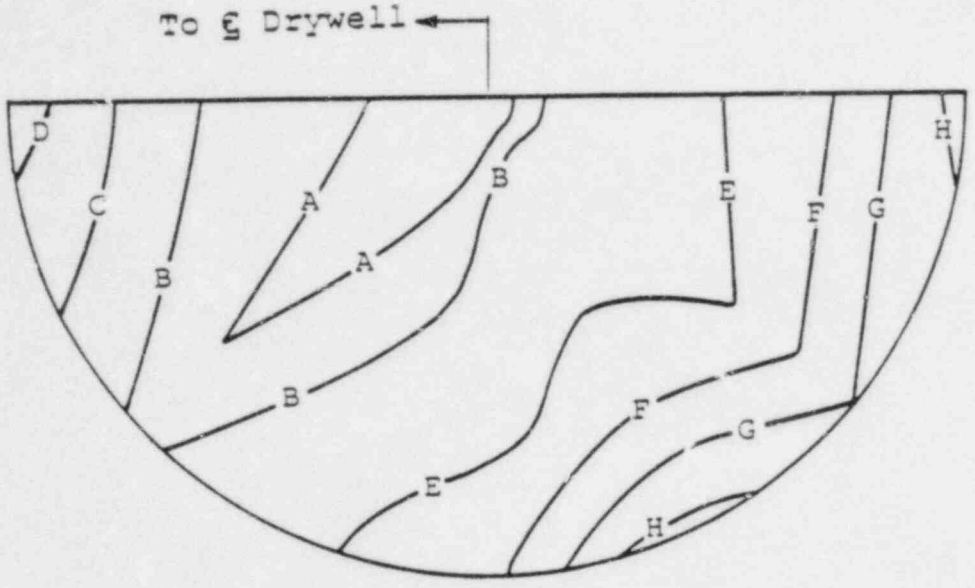

Key Diagram

Normalized Pool Accelerations	
Profile	Pool Acceleration (in/sec^2)
A	20.0
B	50.0
C	100.0
D	150.0
E	200.0
F	400.0
G	600.0
H	800.0
Pool accelerations due to harmonic application of torus shell pressures shown in Figure 2-2.2- 3 and the amplitudes shown in Table 2-2.2-5 (see PUAR Volume 2).	

Figure 3-2.2-6

POOL ACCELERATION PROFILE FOR POST-CHUG TORUS SHELL LOADS AT QUARTER-BAY LOCATION

3-2.2.2 Load Combinations

The load categories and associated load cases for which the vent system is evaluated are presented in Section 3-2.2.1. The general NUREG-0661 criteria for grouping the respective loads and load categories into event combinations are discussed in Section 1-3.2 and presented in Table 3-2.2-14.

The 27 general event combinations shown in Table 3-2.2-14 are expanded to form a total of 69 specific vent system load combinations for the Normal Operating, SBA, IBA, and DBA events. The specific load combinations reflect a greater level of detail than is contained in the general event combinations, including distinction between SBA and IBA, distinction between pre-chug and post-chug, and consideration of multiple cases of particular loadings. The total number of vent system load combinations consists of 3 for the Normal Operating event, 18 for the SBA event, 24 for the IBA event, and 24 for the DBA event. Several different service level limits and corresponding sets of allowable stresses are associated with these load combinations.

Not all of the possible vent system load combinations are evaluated since many are enveloped by others and do not lead to controlling vent system stresses. The enveloping load combinations are determined by examining the possible vent system load combinations and comparing the respective load cases and allowable stresses. The results of this examination are shown in Table 3-2.2-15, where each enveloping load combination is assigned a number for ease of identification.

The enveloping load combinations are reduced further by examining relative load magnitudes and individual load characteristics to determine which load combinations lead to controlling vent system stresses. The load combinations which have been found to produce controlling vent system stresses are separated into two groups. The SBA II, DBA II, and DBA III combinations are used to evaluate stresses in all vent system components except those associated with the vent line-SRV piping penetrations. The SBA II and DBA III combinations are used to evaluate stresses in the vent line-SRV piping penetrations. An explanation of the logic used to conclude that these are the controlling vent system load combinations is presented in the paragraphs which follow. Table 3-2.2-16 summarizes the controlling load combinations and identifies which load

combinations are enveloped by each of the controlling combinations.

Many of the general event combinations shown in Table 3-2.2-14 have the same allowable stresses and are enveloped by others which contain the same or additional load cases. There is no distinction between Service Level A and B conditions for the vent system, since the Service Level A and B allowable stress values are the same.

Many pairs of load combinations contain identical load cases except for seismic loads. One of the load combinations in the pair contains OBE loads and has Service Level A or B allowables, while the other contains SSE loads with Service Level C allowables. At the dominant vertical suppression chamber frequency, both the OBE and SSE vertical accelerations discussed in Section 3-2.2.1 are small compared to gravity. As a result, suppression chamber stresses and vertical support reactions due to vertical seismic loads are small compared to those caused by other loads in the load combination. The horizontal seismic accelerations for OBE and SSE at the dominant horizontal suppression chamber frequency are less than 50% of gravity and also result in small suppression chamber stresses compared

with those caused by other loads in the load combinations. The Service Level C primary stress allowables for the load combinations containing SSE loads are 33 to 75% higher than the Service Level B allowables for the corresponding load combination containing OBE loads. It is apparent, therefore, that the controlling load combinations for evaluation of vent system components are those containing OBE loads and Service Level B allowables.

By applying the above reasoning to the total number of vent system load combinations, a reduced number of enveloping load combinations for each event is obtained. The resulting vent system load combinations for the Normal Operating, SBA, IBA, and DBA events are shown in Table 3-2.2-15, along with the associated service level assignments. For ease of identification, each load combination in each event is assigned a number. The reduced number of enveloping load combinations shown in Table 3-2.2-15 consists of 1 for the Normal Operating event, 4 for the SBA event, 5 for the the IBA event, and 6 for the DBA event. The load case designations for the loads which make up the combinations are the same as those presented in Section 3-2.2.1.

It is evident from an examination of Table 3-2.2-15 that further reductions in the number of vent system load combinations requiring evaluation are possible. Any of the SBA or IBA combinations envelop the NOC I combination, since they contain the same loadings as the NOC I combination and, in addition, contain condensation oscillation or chugging loads. The effects of the number of load cycles specified for the NOC I combination are considered in the vent system fatigue evaluation.

The SBA II combination is the same as the IBA III combination except for negligible differences in internal pressure loads. Thus IBA III can be eliminated from consideration. The SBA II combination envelops the SBA I and IBA II combinations, since the submerged structure loads due to post-chug are more severe than those due to pre-chug. Similarly, the SBA II combination envelops the IBA I combination, since the downcomer lateral loads due to chugging are more severe than the downcomer loads due to IBA condensation oscillation. It also follows, from the reasoning presented earlier for OBE and SSE seismic loads, that the SBA II combination envelops the SBA III, SBA IV, IBA IV, and IBA V combinations. Similarly, the SBA II combination envelops the DBA V and DBA VI combinations,

except that these combinations contain vent system discharge loads which are somewhat larger than the pressure loads for the SBA II combination. This effect is accounted for by substituting the vent system discharge loads which occur during the chugging phase of a DBA event for the SBA II pressure loads when the SBA II load combination is evaluated.

The DBA II combination envelops the DBA IV combination, since the SRV discharge loads which occur late in the DBA event have a negligible effect on the vent system. The DBA II combination also has more restrictive allowables than the DBA IV combination.

The DBA III combination envelops the DBA I combination since the DBA III combination contains SSE seismic loads in addition to SRV loads, while the DBA 1 combination contains OBE seismic loads. However the DBA I combination has more restrictive allowables than the DBA III combination. Therefore the DBA III combination is evaluated using the allowable stresses associated with the DBA I combination for all components except the vent line-SRV piping penetration. The SBA II combination envelops the DBA I combination at the vent line-SRV piping penetration, since the DBA I combination does not include SRV discharge loads

which are a large contributor to loads on the penetration. The DBA III combination is evaluated using Service Level C allowables at the vent line-SRV piping penetration.

The controlling vent system load combinations evaluated in the remaining report sections can now be summarized. The SBA II, DBA II, and DBA III combinations are evaluated for all vent system components except those associated with the vent line-SRV piping penetration. The DBA II combination does not need to be examined when evaluating the vent line-SRV piping penetration, since it does not contain SRV discharge loads which are a large contributor to loads on the penetration. Thus, the SBA II and DBA III combinations are evaluated for the vent line-SRV piping penetration. As previously noted, the vent system discharge loads which occur during the chugging phase of the DBA event are conservatively substituted for the SBA pressure loads when evaluating the SBA II load combination.

To ensure that fatigue is not a concern for the vent system over the life of the plant, the combined effects of fatigue due to Normal Operating plus SBA events are evaluated. The relative sequencing and timing of each loading in the SBA, IBA, and DBA events used in this

evaluation are shown in Figures 3-2.2-7, 3-2.2-8 and 3-2.2-9. Since SBA combinations envelop IBA combinations, the fatigue effects for Normal Operating plus IBA events are enveloped by Normal Operating plus SBA events. The fatigue effects for Normal Operating plus DBA events are also enveloped by the Normal Operating plus SBA events, since the combined effects of SRV discharge loads and other loads for the SBA events are more severe than those for DBA. Additional information used in the vent system fatigue evaluation is summarized at the bottom of Table 3-2.2-15.

The load combinations and event sequencing described in the preceding paragraphs envelop those which could actually occur during a LOCA or SRV discharge event. An evaluation of these load combinations results in a conservative estimate of the vent system response and leads to bounding values of vent system stresses and fatigue effects.

Table 3-2.2-14

MARK I CONTAINMENT EVENT COMBINATIONS

	SRV	SRV + EQ		SBA IBA		SBA + EQ IBA + EQ				SBA+SRV IBA+SRV		SBA+SRV+EQ IBA+SRV+EQ				DBA		DBA + EQ				DBA+SRV		DBA+SRV+EQ			
Earthquake Type		O	S			O	S	O	S			O	S	O	S			O	S	O	S			O	S	O	S
LOADS	1	2	3	4	5	6	7	8	9	10	11	12	13	14	15	16	17	18	19	20	21	22	23	24	25	26	27
Normal	X	X	X	X	X	X	X	X	X	X	X	X	X	X	X	X	X	X	X	X	X	X	X	X	X	X	X
Earthquake		X	X			X	X	X	X			X	X	X	X			X	X	X	X			X	X	X	X
SRV Discharge	X	X	X							X	X	X	X	X	X							X	X	X	X	X	X
LOCA Thermal				X	X	X	X	X	X	X	X	X	X	X	X	X	X	X	X	X	X	X	X	X	X	X	X
LOCA Reactions				X	X	X	X	X	X	X	X	X	X	X	X	X	X	X	X	X	X	X	X	X	X	X	X
LOCA Quasi-Static Pressure				X	X	X	X	X	X	X	X	X	X	X	X	X	X	X	X	X	X	X	X	X	X	X	X
LOCA Pool Swell																X		X	X			X		X	X		
LOCA Condensation Oscillation					X			X	X		X			X	X		X			X	X		X			X	X
LOCA Chugging					X			X	X		X			X	X		X			X	X		X			X	X

Note:

1. See Section 1.3.2 for additional event combination information.

Table 3-2.2-15

CONTROLLING VENT SYSTEM LOAD COMBINATIONS

Section 3-2.2.1 Load Designation	Condition/Event	NOC	SBA				IBA					DBA					
	Volume 3 Load Combination Number	I	I	II	III	IV	I	II	III	IV	V	I	II	III	IV	V	VI
	Table 3-2.2-24 Load Combination Number	2	14	14	15	15	14	14	14	15	15	18	20	25	27	27	27
1) Dead Weight		1a ←															1a
2) Seismic	OBE	2a ←		→ 2a			2a ←		→ 2a			2a	2a				
	SSE				2b	2b				2b	2b			2b ←			→ 2b
3) Pressure[1]		P[2]	P_2,P_3	P_2,P_3	P_2,P_3	P_2,P_3	P_2,P_3	P_2,P_3	P_2,P_3	P_2,P_3	P_2,P_3	P_1	P_3	P_1	P_3	P_4	P_4
3) Temperature[3]		T[4]	T_2,T_3	T_2,T_3	T_2,T_3	T_2,T_3	T_2,T_3	T_2,T_3	T_2,T_3	T_2,T_3	T_2,T_3	T_1	T_3	T_1	T_3	T_4	T_4
4) Vent System Discharge												4a ←					→ 4a
5) Pool Swell												5a-5e		5a-5e			
6) Condensation Oscillation							6a,6c 6e						6b,6d 6f		6b,6d 6f		
7) Chugging	Pre-Chug		7a-7c		7a-7c			7a-7c		7a-7c						7a-7c	
	Post-Chug			7a,7b 7d		7a,7b 7d			7a,7b 7d		7a,7b 7d						7a,7b 7d
8) SRV Discharge		8a ←									→ 8a			8a	8a[5]	8a[5]	8a[5]
9) Piping Reactions		9a ←															→ 9a
10) Containment Interaction		10a ←															→ 10a
Service Level		B	B	B	C	C	B	B	B	C	C	B[6,7]	B[7]	C	C	C	C
Number of Event Occurences[8]		150	1 ←														→ 1
Number of SRV Actuations[9]		596	50 ←			→ 50	25 ←				→ 25	0	0	1 ←			→ 1

Table 3-2.2-15
(Concluded)

Notes:

1. See Table 3-2.2-2 for SBA, IBA, and DBA internal pressure values.
2. The range of normal operating internal pressures is 0.0 to 2.0 psi as specified by the FSAR.
3. See Table 3-2.2-2 for SBA. IBA, and DBA temperature values.
4. The range of normal operating temperatures is 50.0 to 150.0^{o}F as specified by the FSAR.
5. The SRV discharge loads which occur during this phase of the DBA event have a negligible effect on the vent system.
6. Evaluation of primary-plus-secondary stress range or fatigue not required.
7. The allowable stress value for local primary membrane stress at penetrations increased by 1.3.
8. The number of seismic load cycles used for fatigue is 1000.
9. The values shown are conservative estimates of the number of actuations expected for a BWR 4 plant with a reactor vessel diameter of 251 inches equipped with low-low set logic.

Table 3-2.2-16

ENVELOPING LOGIC FOR CONTROLLING
VENT SYSTEM LOAD COMBINATIONS

Condition/Event			NOC	SBA				IBA					DBA					
Table 3-2.2-24 Enveloping Load Combinations			2	14	14	15	15	14	14	14	15	15	18	20	25	27	27	27
Table 3-2.2-24 Load Combinations Enveloped			1	4-6 8, 10-12	4-6 8, 10-12	3,7 9, 13	3,7, 9, 13	4-6 8, 10-12	4-6 8, 10-12	3,7, 8, 10-12	3,7, 9, 13	3,7, 9, 13	16	17	19, 22, 24	21, 23, 26	21, 23, 26	21, 23, 26
Volume 3 Load Combination Designation			1	I	II	III	IV	I	II	III	IV	V	I	II	III	IV	V	VI
Controlling Load Combinations Evaluated	Vent System Components and Supports	SBA II (1)	X	X		X	X	X	X	X	X	X					X	X
		DBA II														X		
		DBA III (2)											X					
	Vent Line-SRV Piping Penetration	SBA II (1)	X	X		X	X	X	X	X	X	X					X	X
		DBA III (2)											X	X		X		

Notes:

1. DBA pressurization and thrust loads are substituted for SBA II internal pressure loads when evaluating the SBA II load combination.
2. The allowables associated with the DBA I combination are used when evaluating the DBA III load combination.
3. The number of load cycles associated with the NOC I combination are used with SBA II stresses when evaluating vent line SRV piping penetration fatigue effects.

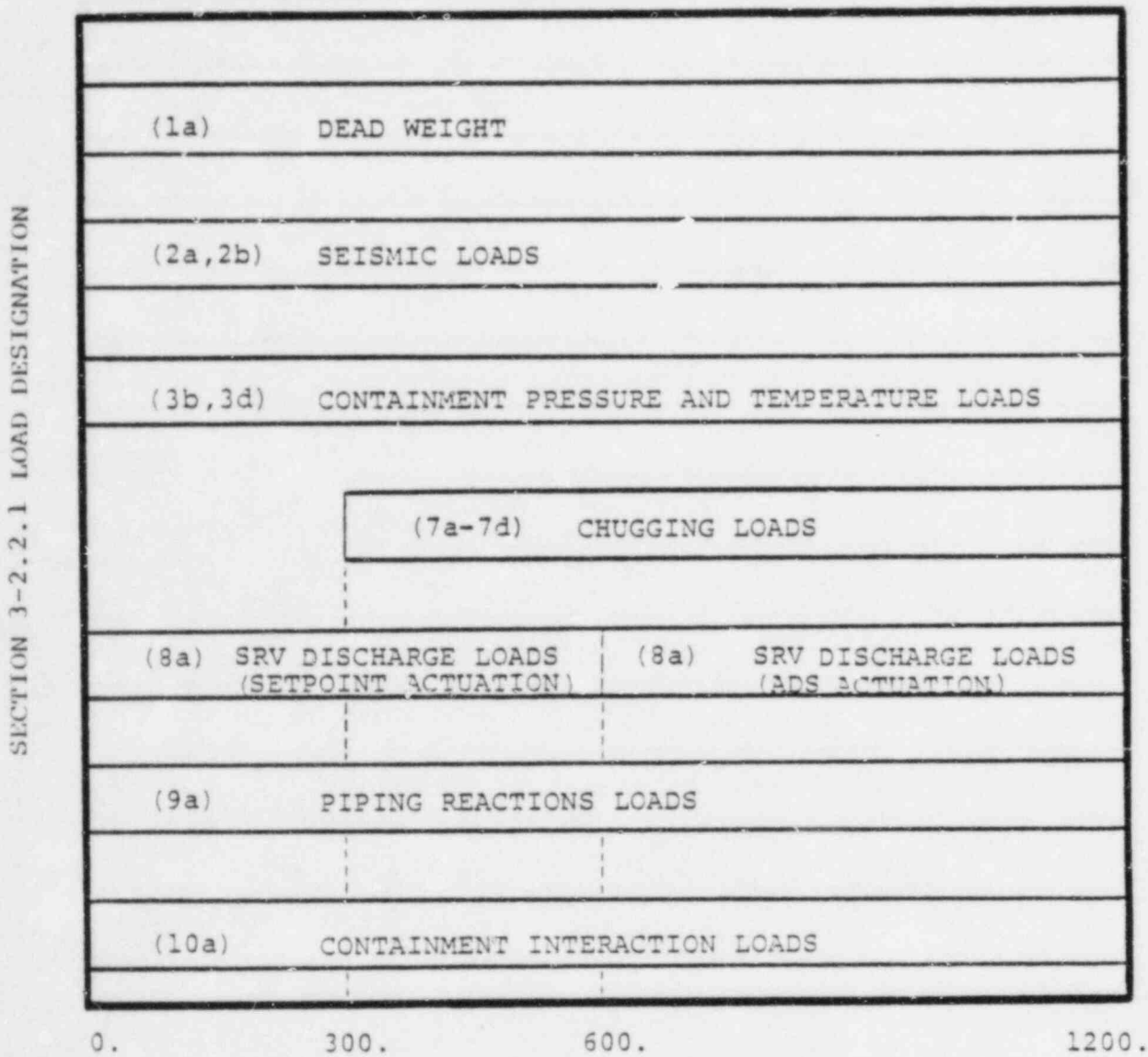

Figure 3-2.2-7

VENT SYSTEM SBA EVENT SEQUENCE

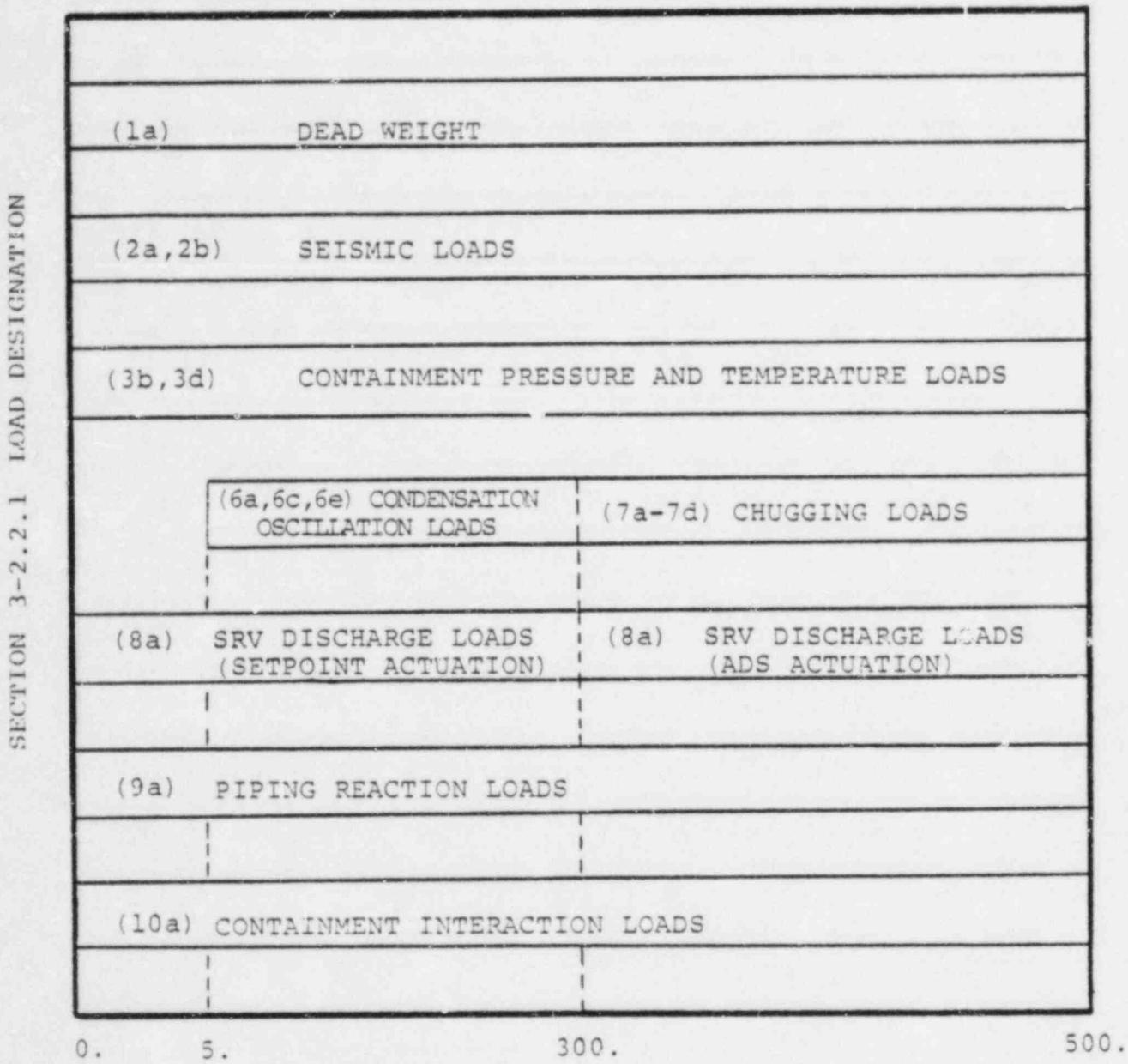

Figure 3-2.2-8

VENT SYSTEM IBA EVENT SEQUENCE

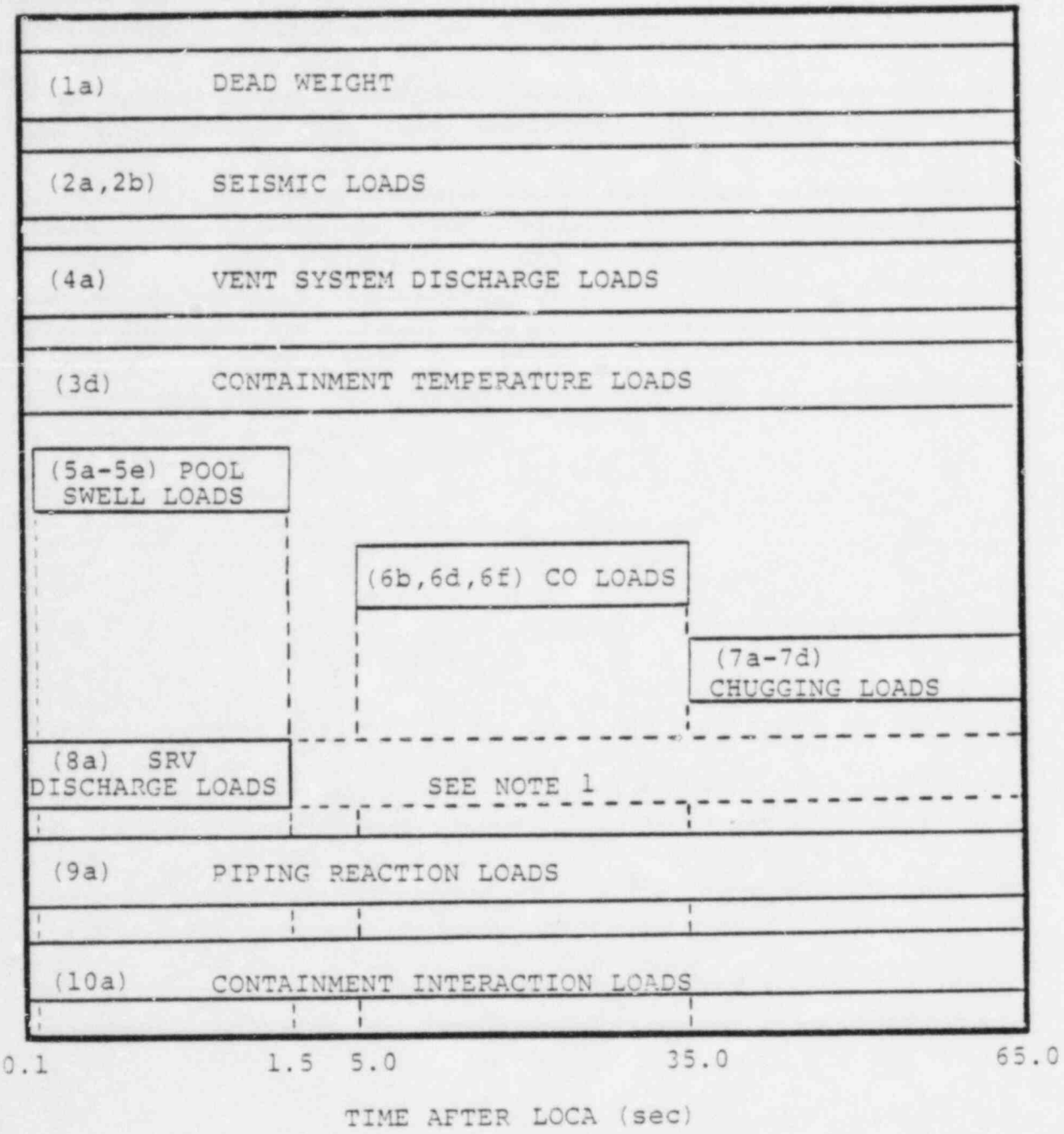

Note:

1. The SRV discharge loads which occur during this phase of the DBA event are negligible.

Figure 3-2.2-9

VENT SYSTEM DBA EVENT SEQUENCE

3-2.3 Analysis Acceptance Criteria

The acceptance criteria defined in NUREG-0661 on which the Hope Creek vent system analysis is based are discussed in Section 1-3.2. In general, the acceptance criteria follows the rules contained in the ASME Code, Section III, Division 1 including the Summer 1977 Addenda for Class MC components and component supports (Reference 6). The corresponding service limit assignments, jurisdictional boundaries, allowable stresses, and fatigue requirements are consistent with those contained in the applicable subsections of the ASME Code and the Mark I Containment Program Plant Unique Analysis Application Guide (PUAAG) (Reference 5). The acceptance criteria used in the analysis of the vent system are summarized in the paragraphs which follow.

The items examined in the analysis of the vent system include the vent lines, vent header, downcomers, the support columns and associated support elements, the overhead truss members, the drywell shell near the vent line penetrations, the downcomer-vent header intersection stiffener plates and bracing system, the vacuum breaker supports, the vent line-SRV piping penetration assembly, and the vent line bellows assembly. The specific component parts associated with each of these

items are identified in Figures 3-2.1-1 through 3-2.1-14.

The vent lines, vent header, downcomers, the support column ring plates away from the pin locations, the drywell shell, the downcomer-vent header intersection stiffener plates, the vacuum breaker support, and the vent line-SRV piping penetration assembly are evaluated in accordance with the requirements for Class MC components contained in Subsection NE of the ASME Code. Fillet welds and partial penetration welds joining these component parts or attaching other structures to these parts are also examined in accordance with the requirements for Class MC welds contained in Subsection NE of the ASME Code.

The support columns, the overhead truss members, the downcomer bracing members, and the associated connecting elements and welds are evaluated in accordance with the requirements for Class MC component supports contained in Subsection NF of the ASME Code.

As shown in Table 3-2.2-15, the SBA II, and DBA II combinations have Service Level B limits. The DBA III combination has Service Level C limits, but is evaluated against the allowables specified for DBA I as

discussed in Section 3-2.2.2. Since these load combinations have somewhat different maximum temperatures, the allowable stresses are conservatively determined at the highest temperature of the three load combinations.

The allowable stresses for all the major components of the vent system, such as the vent line, vent header and downcomers, are determined at the maximum DBA temperature of 292°F. The allowable stresses for the vent line-SRV piping nozzle and adjoining component parts are determined at 407°F. The allowable stresses for the remaining vent system component parts are determined at the maximum IBA suppression chamber temperature of 167°F. The allowable stresses for the load combinations with Service Level B limits are shown in Table 3-2.3-1.

The allowable displacements and associated number of cycles for the vent line bellows are shown in Table 3-2.3-2. These values are taken from the FSAR, as permitted by NUREG-0661 in cases where the analysis technique used in the evaluation is the same as that contained in the plant's FSAR.

The acceptance criteria described in the preceding paragraphs result in conservative estimates of the existing margins of safety and ensure that the original vent system design margins are maintained.

Table 3-2.3-1

ALLOWABLE STRESSES FOR VENT SYSTEM COMPONENTS AND COMPONENT SUPPORTS

Item	Material	(1) Material Properties (ksi)	Stress Type	(2) Allowable Stress (ksi)
C O M P O N E N T S				
Drywell Shell	SA-516 Gr. 70	S_{mc} = 19.30 S_{ml} = 22.55	Local Primary Membrane	28.95
			Primary + (5) Secondary Stress Range	67.64
Vent Line	SA-516 Gr. 70	S_{mc} = 19.30 S_{ml} = 22.55	Primary Membrane	19.30
			Local Primary Membrane	28.95
			Primary + (5) Secondary Stress Range	67.64
Vent Header	SA-516 Gr. 70	S_{mc} = 19.30 S_{ml} = 22.55	Primary Membrane	19.30
			Local Primary Membrane	28.95
			Primary + (5) Secondary Stress Range	67.64
[illegible]ncomer	SA-516 Gr. 70	S_{mc} = 19.30 S_{ml} = 22.55	Primary Membrane	19.30
			Local Primary Membrane	28.95
			Primary + (5) Secondary Stress Range	67.64
Support Column Ring Plates	SA-537 Cl. 2	S_{mc} = 22.00 S_{ml} = 26.70	Primary Membrane	22.00
			Local Primary Membrane	33.00
			Primary + (5) Secondary Stress Range	80.10
(8) SRV Piping Penetration Nozzle	SA-333 Gr. 6	S_{mc} = 16.50 S_{ml} = 19.92	Primary Membrane	16.50
			Local Primary Membrane	24.75
			Primary + (5) Secondary Stress Range	59.76

Table 3-2.3-1
(Concluded)

Item	Material	(1) Material Properties (ksi)	Stress Type	(2) Allowable Stress (ksi)
C O M P O N E N T S U P P O R T S				
Columns (6)	SA-333 Gr. 1	S_y = 28.20	Bending	18.61
			Tensile	16.92
			Combined	1.00
			Compressive (7)	14.33
			Interaction	1.00
W E L D S				
Downcomer to Vent Header	SA-516 Gr. 70	S_{mc} = 19.30	Primary	15.01
			Secondary	45.03
(8) SRV Piping Penetration Nozzle to Insert Plate	SA-516 Gr. 70	S_{mc} = 19.30	Primary	11.58
			Secondary	34.74

Notes:

1. Material properties taken at maximum event temperatures.
2. Allowables shown correspond to Service Level B stress limits. The DBA III combination is evaluated with DBA I allowables, except as noted.
3. Thermal bending stresses are excluded when evaluating primary-plus-secondary stress ranges.
4. The allowable stresses for local primary membrane stresses at penetrations are increased by 1.3 when evaluating the DBA III load combination.
5. Evaluation of primary-plus-secondary stress intensity range and fatigue are not required for the DBA III load combination.
6. Stresses due to thermal loads may be excluded when evaluating component supports.
7. Allowable compressive stress based on maximum column length.
8. For the DBA III combination, the SRV piping penetration nozzle and nozzle to insert plate weld are evaluated with the following Service Level C allowables: Nozzle - Primary Membrane = 29.88 ksi, Local Primary Membrane = 44.82 ksi, Weld - Primary = 19.48 ksi.

Table 3-2.3-2

ALLOWABLE DISPLACEMENTS AND CYCLES
FOR VENT LINE BELLOWS

Type		Allowable Value	
		Normal Operating Conditions	Accident Conditions
Axial	Compression	0.75 in.	1.25 in.
	Extension	0.75 in.	0.75 in.
Lateral	w/Axial Compression	0.50 in.	0.75 in.
	w/Axial Extension	0.75 in.	1.25 in.
Number of Cycles of Maximum Displacements		230	10

3-2.4 Method of Analysis

The governing loads for which the Hope Creek vent system is evaluated are presented in Section 3-2.2.1. The methodology used to evaluate the vent system for the overall effects of all loads, except those which exhibit asymmetric characteristics, is discussed in Section 3-2.4.1. The effects of asymmetric loads on the vent system are evaluated using the methodology discussed in Section 3-2.4.2. The methodology used to examine the local effects at the penetrations and intersections of the vent system major components is discussed in Section 3-2.4.3. The methodology used to evaluate the local effects of pool swell impact loads on the vent header is discussed in Section 3-2.4.4.

The methodology used to formulate results for the controlling load combinations, examine fatigue effects, and evaluate the analysis results for comparison with the applicable acceptance limits is discussed in Section 3-2.4.5.

3-2.4.1 Analysis for Major Loads

The repetitive nature of the vent system geometry is such that the vent system can be divided into 16 identical segments which extend from midbay of the vent line bay to midbay of the non-vent line bay, as shown in Figure 3-2.1-6. The governing loads which act on the vent system, except for seismic loads and a few chugging load cases, exhibit symmetric and/or anti-symmetric characteristics with respect to a 1/16th segment of the vent system. The analysis of the vent system for the majority of the governing loads is therefore performed for a typical 1/16th segment.

A beam and finite element model of a 1/16th segment of the vent system and suppression chamber, as shown in Figure 3-2.4-1, is used to obtain the response of the vent system to all loads except local response of the vent header to pool swell impact loads and the response of the vent system to those loads which result in asymmetric effects. The model includes the vent line, vent header, downcomers, the support columns, the overhead truss members, and the suppression chamber shell and ring beams. The model also includes the downcomer bracing system and the vacuum breaker and vacuum breaker support. The portion of the SRV piping,

T-quenchers, and their associated supports in the suppression chamber are also included to account for the interaction effects of these structures.

The local stiffness effects at the penetrations and intersections of the major vent system components, shown in Figures 3-2.1-3 and 3-2.1-7 through 3-2.1-9, are included using stiffness matrix elements of these penetrations and intersections. A matrix element for the vent line-drywell penetration, which connects the upper end of the vent line to the conical transition segment, is developed using the finite difference model of the penetration shown in Figure 3-2.4-3. The finite element model of the vent line-SRV piping penetration, shown in Figure 3-2.4-4, is used to develop a matrix element which connects the beams on the centerline of the vent line to the SRV piping penetration nozzle. A beam element which connects the vent header to the beams on the centerline of the vent line is developed using the finite element model of the vent line-vent header intersection shown in Figure 3-2.4-5.

The finite element model of the downcomer-vent header intersection, shown in Figure 3-2.4-6, is used to develop matrix elements which connect the beams on the centerline of the vent header to the upper ends of the

downcomers at the downcomer ring locations. Additional information on the analytical models used to evaluate the penetrations and intersections of major vent system components is contained in Section 3-2.4.3.

The finite element model of the SRV piping ramshead is used to develop matrix elements which connect the SRV discharge line to the T-quenchers. Additional information on the ramshead analytical model is contained in Volume 5 of this report.

The local stiffness effects at the attachments of the downcomer bracing, vacuum breaker supports, vent system support columns, overhead truss members, and SRV piping pad plates located on the vent header are also included. Beams which account for the local stiffness of the support rings and pad plates are used to connect the associated component parts to beams which model the vent line, vent header, and downcomers.

The 1/16th segment model contains 539 nodes, 441 beam elements, 264 plate bending and stretching elements, and 6 matrix elements. The node spacing used in the analytical model is refined to ensure adequate distribution of mass and determination of structural frequencies and mode shapes, and to facilitate accurate

application of loadings. Small displacement linear-elastic behavior is assumed throughout.

The analytical model includes a corrosion allowance of 1/8 inch subtracted from the nominal thicknesses and diameters of the torus shell, ring beams, downcomers, vent system support members, and T-quencher supports. A corrosion allowance of 1/16 inch is subtracted from the vent line, vent header, and SRV piping supports. The SRV piping and T-quencher are nominal size. These corrosion allowances are in accordance with the original design requirements documented in the plant's FSAR. The mass densities used in the model are adjusted to account for the weight of the vent system and suppression chamber with nominal material dimensions as shown in Figures 3-2.1-1 through 3-2.1-14.

The boundary conditions used in the 1/16th beam model are both physical and mathematical in nature. The physical boundary conditions include the elastic restraints provided at the attachment of the vent line to the drywell, and the suppression chamber attachments to the reactor building as defined in PUAR Volume 2. The associated vent line-drywell penetration stiffnesses are included as a stiffness matrix element, the development of which is discussed in the preceding

paragraphs. The mathematical boundary conditions consist of either symmetry, anti-symmetry, or a combination of both at the midcylinder planes, depending on the characteristics of the load being evaluated.

When computing the response of the suppression chamber and vent system to dynamic loadings, the fluid-structure interaction effects of the suppression chamber shell and contained fluid (water) are considered. A finite element model of the fluid is used to develop a coupled mass matrix which is added to the submerged nodes of the suppression chamber analytical model to represent the fluid. The approach used is similar to the one documented in Section 2-2.4.1 of PUAR Volume 2. Additional mass is lumped along the length of the submerged portions of the downcomers, support columns, SRV piping, and T-quenchers and supports to account for the effective mass of water which acts with these components during dynamic loadings. For all but the pool swell and condensation oscillation dynamic loadings, the mass of water inside the submerged portion of the downcomers is included. The downcomers are assumed to contain air and/or steam during pool swell and condensation oscillation, the mass of which is neglected. The mass of water inside

the submerged portion of the SRV piping and T-quenchers is also included for all dynamic loadings. An addicional mass of 600 pounds to account for the weight of the drywell/wetwell vacuum breaker is lumped at the center of gravity of the vacuum breaker.

A frequency analysis is performed using the 1/16th segment model of the vent system and suppression chamber for the case with water inside the downcomers and the case with no water inside the downcomers. All structural modes in the range of 0 to 35 hertz and 0 to 100 hertz, respectively, are extracted for these cases. The resulting frequencies and modal weights are shown in Tables 3-2.4-1 and 3-2.4-2.

A dynamic analysis is performed for the pool swell loads and condensation oscillation loads specified in Section 3-2.2-1, using the 1/16th beam and finite element model of the vent system and suppression chamber. A dynamic analysis to assess the local effects of pool swell impact loads on the vent header is also performed, using the 1/32 segment pool swell impact finite element model discussed in Section 3-2.4.4. The analysis consists of a transient analysis for pool swell loads, and a harmonic analysis for condensation oscillation loads. The modal superposition

technique, including modes to 100 hertz with 2% damping, is utilized in both the transient and harmonic analyses.

The remaining vent system load cases specified in Section 3-2.2.1 involve either static loads or dynamic loads, which are evaluated using an equivalent static approach. For the latter, conservative dynamic amplification factors are developed and applied to the maximum spatial distributions of the individual dynamic loadings.

The effects of asymmetric loads are evaluated by applying these loads to the 180° beam model. Additional information related to the vent system analysis for asymmetric loads is provided in Section 3-2.4.2.

The 1/16th segment model is also used to generate loads for the evaluation of stresses in the major vent system component penetrations and intersections. Beam end loads, distributed loads, and reaction loads are developed and applied to the analytical models of the vent system penetrations and intersections shown in

Figures 3-2.4-3 through 3-2.4-6. Additional information related to the vent system penetrations and intersection stress evaluation is provided in Section 3-2.4.3.

The specific treatment of each load in the load categories identified in Section 3-2.2.1 is discussed in the paragraphs which follow.

1. Dead Weight Loads

   a. Dead Weight of Steel: A static analysis is performed for a unit vertical acceleration applied to the weight of vent system steel.

2. Seismic Loads

   a. OBE Loads: A static analysis is performed for a vertical seismic acceleration applied to the weight of vent system steel included in the 1/16th segment model. The vertical acceleration used in the analysis is obtained from the original design basis documented in the plant's FSAR at the lowest vent system frequency of 13.9 hertz. The effects of N-S and E-W horizontal seismic accelerations are evaluated using the 180° beam model as discussed in Section 3-2.4.2. The results of

the three earthquake directions are combined using SRSS.

b. SSE Loads: The procedure used to evaluate the vertical, N-S horizontal, and E-W horizontal SSE seismic accelerations is the same as that discussed for OBE seismic loads in load case 2a.

3. Containment Pressure and Temperature Loads

a. A static analysis is performed for a 2.0 psi internal pressure applied as concentrated forces to the unreacted areas of the vent system.

b. LOCA Internal Pressure Loads: A static analysis is performed for the SBA and IBA net internal pressures applied as concentrated forces to the unreacted areas of the major components of the vent system. These pressures are shown in Table 3-2.2-2. The effects of DBA internal pressure loads are included in the pressurization and thrust loads discussed in load case 4a.

Concentrated forces are also applied at the vent line-drywell penetration location using the SBA and DBA drywell internal pressures. These forces account for the pressures acting on the vent line-drywell penetration unreacted area and for the movement of the drywell due to internal pressure.

c. A static analysis is performed for the maximum normal operating temperature listed in Table 3-2.2-2. This temperature is uniformly applied to the portion of the vent system inside the suppression chamber. Corresponding temperatures of 70°F for the drywell and vent system components outside the suppression chamber, 150°F for the suppression chamber, 380°F for the submerged portion of the wetwell SRV piping, and 407°F for the SRV piping in the suppression chamber airspace are also applied in this analysis.

d. LOCA Temperature Loads: A static analysis is performed for the SBA, IBA, and DBA temperatures, which are uniformly applied to the major components and external components of the vent system. These temperatures are shown in Table 3-2.2-2. A 380°F temperature

is uniformly applied to the submerged portion of the wetwell SRV piping, and a 407°F temperature is uniformly applied to the wetwell SRV piping in the torus airspace.

Concentrated forces are applied at the vent line-drywell penetration to account for the thermal expansion of the drywell during the SBA and DBA events.

4. Vent System Discharge Loads

   a. The DBA pressurization and thrust loads are shown in Table 3-2.2-3. These loads are enveloped by the maximum DBA pressure loads shown in Table 3-2.2-2. Therefore the maximum DBA pressure loads are used in lieu of DBA pressurization and thrust loads in the analysis.

5. Pool Swell Loads

   a. Vent System Impact and Drag Loads: A dynamic analysis is performed for the vent line, vent header, and downcomer pool swell impact loads shown in Tables 3-2.2-4 and 3-2.2-5. The local effects of pool swell impact loads on the vent header are assessed using the 1/32 segment finite element model, as discussed in Section 3-2.4.4.

b. Impact and Drag Loads on Other Structures: A dynamic analysis is performed for pool swell impact loads on the downcomer bracing members and ring plates. These loads are shown in Table 3-2.2-4. The pool swell impact loads acting on the SRV piping and supports are also applied.

c. Froth Impingement and Fallback Loads: A dynamic analysis is performed for froth impingement loads on the downcomer bracing members, overhead truss members, and the vacuum breaker and vacuum breaker support. These loads are shown in Table 3-2.2-4. Froth fallback loads are negligible. The froth impingement loads acting on the SRV piping and supports are also applied.

d. Pool Fallback Loads: A dynamic analysis is performed for pool fallback loads on the downcomer bracing members and ring plates. These loads are shown in Table 3-2.2-4. The pool fallback loads acting on the SRV piping and supports are also applied.

e. LOCA Air Clearing Submerged Structure Loads: An equivalent static analysis is performed for LOCA air clearing submerged structure loads on the downcomers. These loads are shown in Table 3-2.2-6. LOCA air clearing submerged structure loads on the support columns are negligible. The values of the loads include dynamic amplification factors which are computed using first principles and the dominant frequency of the downcomers. The dominant frequency of the downcomers without water inside is obtained from the structural frequency analysis. The resulting dominant frequency is reported in Table 3-2.4-3.

6. Condensation Oscillation Loads

a. IBA Condensation Oscillation Downcomer Loads: A dynamic analysis is performed for the IBA condensation oscillation downcomer loads shown in Table 3-2.2-7 using the most severe cases of those shown in Figure 3-2.2-4. The dominant frequency of the downcomers without water inside is reported in Table 3-2.4-3. It is apparent that the dominant downcomer frequency occurs in the frequency range of the second condensation oscillation downcomer

load harmonic. The first and third condensation oscillation downcomer load harmonics are therefore applied at frequencies equal to 0.5 and 1.5 times the value of the dominant downcomer frequency.

b. DBA Condensation Oscillation Downcomer Loads: The procedure used to evaluate the DBA condensation oscillation downcomer loads shown in Table 3-2.2-8 is the same as that discussed for IBA condensation oscillation downcomer loads in load case 6a.

c. IBA Condensation Oscillation Vent System Pressures: An equivalent static analysis is performed for IBA condensation oscillation vent system pressures on the vent line and vent header. These loads are shown in Table 3-2.2-9. The dominant vent line and vent header frequencies used in the analysis are summarized in Table 3-2.4-3. An additional static analysis is performed for a 1.5 psi internal pressure applied as concentrated forces to the unreacted areas of the vent system.

d. DBA Condensation Oscillation Vent System Pressure Loads: The procedure used to evaluate the DBA condensation oscillation vent system pressure loads shown in Table 3-2.2-9 is the same as that discussed for IBA condensation oscillation vent system pressure loads in load case 6c.

e. IBA Condensation Oscillation Submerged Structure Loads: As previously discussed, pre-chug loads described in load case 7c are specified in lieu of IBA condensation oscillation loads.

f. DBA Condensation Oscillation Submerged Structure Loads: The DBA condensation oscillation loads on the support columns are shown in Table 3-2.2-6. The loads include dynamic amplification factors which are computed using first principles and the dominant frequencies of the support columns. The dominant frequencies of the support columns are obtained using manual frequency calculations for simply supported beams. The resulting dominant frequencies are summarized in Table 3-2.4-3. The DBA condensation

oscillation submerged structure loads are bounded by post-chug submerged structure loads (Case 7d). Therefore post-chug submerged structure loads are used in lieu of DBA condensation oscillation loads in the analysis.

7. Chugging Loads

a. Chugging Downcomer Lateral Loads: The dominant downcomer frequency for use in calculating the maximum chugging load magnitude is obtained from the structural frequency analysis results for downcomers with water inside. The resulting dominant frequency is shown in Table 3-2.4-3. The resulting chugging load magnitudes are shown in Table 3-2.2-10. A static analysis using the 1/16th beam model is performed for chugging downcomer lateral load cases 4 through 9. These load cases are shown in Table 3-2.2-11. An additional static analysis using the 180° beam model is performed for load cases 1 through 3, as discussed in Section 3-2.4.2.

A static analysis is also performed for the maximum chugging load shown in Table 3-2.2-12, applied to a single downcomer in the in-plane and out-of-plane directions. The results of this analysis are used in evaluating fatigue.

b. Chugging Vent System Pressures: An equivalent static analysis is performed for the chugging vent system pressures applied to the unreacted areas of the vent system. These loads are shown in Table 3-2.2-13. The dominant vent line and vent header frequencies used in this evaluation are summarized in Table 3-2.4-3.

c. Pre-Chug Submerged Structure Loads: As discussed in Section 3-2.2.1, post-chug submerged structure loads are used in lieu of pre-chug. Therefore this load is not evaluated further.

d. Post-Chug Submerged Structure Loads: An equivalent static analysis is performed for the post-chug submerged structure loads on the support columns. These loads are shown in Table 3-2.2-6. The loads include dynamic

amplification factors which are computed using the methodology described for DBA CO submerged structure loads in load case 6f. The post-chug submerged structure loads acting on the submerged portion of the SRV piping, T-quenchers and supports are also applied.

8. Safety Relief Valve Discharge Loads

   a. SRV Discharge Air Clearing Submerged Structure Loads: An equivalent static analysis is performed for SRV discharge drag loads on the downcomers and support columns. These loads are shown in Table 3-2.2-6. The loads include a dynamic load factor as discussed in Section 1-4.2.4. The SRV discharge submerged structure loads acting on the submerged portion of the SRV piping, T-quenchers and supports are also applied.

9. Piping Reaction Loads

   a. SRV Piping Reaction Loads: As previously discussed, the wetwell SRV piping, T-quenchers, and T-quencher supports are included in the 1/16th segment model of the vent system. Loads in categories 1 through 8

which act on the vent system, wetwell SRV piping, T-quenchers and supports are applied to these structures and the interaction effects are evaluated.

Additional equivalent static loads caused by SRV discharge line clearing pressurization and by thrust loads acting on the wetwell SRV piping and T-quenchers are also applied. The conditions which cause the maximum reaction loads on the vent line-SRV piping penetration are evaluated.

10. Containment Interaction Loads

a. Containment Structure Motions: The motions of the drywell due to internal pressure and thermal expansion are applied to the 1/16th segment model. The motions caused by loads in other load categories acting on the drywell have been evaluated and found to have a negligible effect on the vent system.

The containment interaction effects of the suppression chamber on the vent system are accounted for by the finite element representation of the suppression chamber in the

1/16th segment model. Suppression chamber steel and water dead loads and vertical seismic loads, torus internal pressure and temperature loads, and pool swell, condensation oscillation, chugging, and SRV torus shell loads are included in the 1/16th segment model analysis. These loads are discussed in Volume 2 of this report.

A dynamic analysis is performed for condensation oscillation, chugging, and SRV torus shell loads. An equivalent static analysis is performed for pool swell torus shell loads using conservative dynamic load factors.

The methodology described in the preceding paragraphs results in a conservative evaluation of the vent system response and associated stresses for the governing loads.

Table 3-2.4-1

VENT SYSTEM FREQUENCY ANALYSIS RESULTS WITH WATER INSIDE DOWNCOMERS

Mode Number	Frequency (Hz)	Modal Weight (lb)		
		$X^{(1)}$	$Y^{(1)}$	$Z^{(1)}$
1	13.9	49342.31	4067.67	42876.50
2	14.7	63485.52	1608.54	108403.11
3	15.0	24.97	18.91	12.21
4	16.5	158719.14	7345.39	167888.71
5	16.9	223.80	7.59	476.47
6	17.0	295.77	6.82	7159.09
7	18.7	26.81	73.82	1216.08
8	18.7	538.00	0.02	2285.36
9	19.2	11.82	93.03	0.10
10	19.3	1759.47	160.61	4223.32
11	19.7	39.37	4.13	0.62
12	20.2	2655.43	187.09	11596.20
13	20.4	206.60	0.39	3[illegible].81
14	20.6	236.25	3305.05	9.98
15	21.4	5.53	102.84	550.26
16	22.2	154.68	476.35	11923.97
17	22.6	1146.36	1120.12	7131.61
18	22.7	46.15	61.09	163.23
19	22.8	0.43	173.58	6588.69
20	23.3	198.40	1199.04	185.19
21	23.4	40.91	257.59	17.82
22	24.0	1091.32	3.73	2746.79
23	24.5	23.47	0.99	2277.46
24	24.6	2.19	44.63	12.68
25	24.7	1.02	224.83	4.68
26	24.7	58.68	[illegible].02	1563.75
27	24.8	1123.09	18.11	25475.07
28	25.6	389.52	70.26	10.87
29	25.9	324.91	474.73	5.98
30	25.9	6.64	84.61	2383.86

Table 3-2.4-1
(Concluded)

Mode Number	Frequency (Hz)	Modal Weight (lb)		
		$X^{(1)}$	$Y^{(1)}$	$Z^{(1)}$
31	26.6	7087.28	19.12	10642.49
32	27.5	44.00	2691.27	11.44
33	27.6	3593.52	212.64	38807.91
34	27.7	319.95	51.37	370.94
35	27.9	1926.33	287.19	9390.75
36	27.9	1932.74	239.62	2079.55
37	28.2	296.83	6.44	59.07
38	28.5	5.59	153.73	13767.48
39	28.8	2626.03	25.59	49994.24
40	29.1	535.44	572.78	22072.50
41	29.7	671.61	1968.71	7883.50
42	30.3	1328.90	4.92	2376.30
43	30.4	4465.43	51.55	8441.00
44	30.6	1349.06	29.66	23183.00
45	31.1	462.91	13.11	725.51
46	31.5	15.75	75.37	45.98
47	31.6	5653.37	43.99	211.99
48	32.6	12249.00	336.32	730.29
49	33.5	160.96	402.44	831.79
50	33.7	75.31	49.72	1214.92
51	34.0	298.47	68.80	1141.85
52	34.4	0.75	5.11	24.39
53	34.8	32.17	81.60	19.66
54	35.6	154.35	14.75	278.39
55	35.8	247.75	231.40	18.19

Note:

1. See Figure 3-2.4-1 for coordinate system directions.

Table 3-2.4-2

VENT SYSTEM FREQUENCY ANALYSIS

RESULTS WITHOUT WATER INSIDE DOWNCOMER

Mode Number	Frequency (Hz)	Modal Weight (lb)		
		$X^{(1)}$	$Y^{(1)}$	$Z^{(1)}$
1	14.5	105620.43	4696.21	157063.24
2	15.0	18.92	18.53	7.40
3	16.1	31856.67	408.78	28438.84
4	16.6	132558.92	7650.07	131854.86
5	16.9	480.35	0.93	799.22
6	17.0	80.60	0.22	8479.32
7	18.7	21.90	62.08	1229.42
8	18.7	531.57	0.27	2262.19
9	19.2	24.09	40.05	0.16
10	19.3	2367.10	214.78	4717.52
11	19.7	29.65	5.74	1.46
12	20.2	2850.30	180.95	11856.41
13	20.4	270.74	4.38	296.95
14	20.6	267.52	3044.55	12.56
15	21.4	26.05	147.43	531.61
16	22.3	137.96	111.08	21830.82
17	22.7	0.27	0.57	42.26
18	22.8	41.41	40.27	4792.77
19	22.9	252.45	9.83	143.98
20	23.4	23.69	141.40	32.14
21	24.5	13.40	0.01	2262.47
22	24.5	37.27	0.67	56.87
23	24.6	1.39	3.35	151.08
24	24.7	68.79	3.89	1788.51
25	24.8	1135.55	69.54	26115.92
26	25.6	397.44	277.96	59.86
27	25.9	0.99	24.23	2314.42

Table 3-2.4-2
(Continued)

Mode Number	Frequency (Hz)	Modal Weight (lb)		
		$X^{(1)}$	$Y^{(1)}$	$Z^{(1)}$
28	26.6	2405.16	0.72	2721.01
29	27.1	140.40	1283.96	15777.09
30	27.7	12.36	223.45	18754.40
31	27.8	137.06	157.67	25476.54
32	28.1	9082.14	57.57	257.59
33	28.2	860.26	22.17	24.63
34	28.6	1111.18	432.37	27896.49
35	28.8	891.05	14.68	36215.49
36	29.5	9184.05	775.33	551.09
37	29.5	458.34	18.42	34801.83
38	29.9	148.45	2209.11	730.35
39	30.4	15.56	0.36	63.72
40	30.6	4663.20	55.05	3215.11
41	30.6	310.87	107.83	21717.91
42	31.1	193.60	0.33	1909.14
43	31.4	3020.39	90.54	0.50
44	31.5	458.77	133.99	0.22
45	31.9	761.20	126.74	145.39
46	32.7	10749.45	653.99	683.09
47	33.5	102.72	270.49	808.01
48	33.8	185.48	28.66	1372.06
49	34.2	428.85	0.04	1026.38
50	34.5	109.14	1958.58	341.21
51	34.8	32.66	153.02	56.76
52	35.1	54.67	0.25	96.94
53	35.8	369.18	250.64	174.50
54	35.9	28.16	313.91	45.78

Table 3-2.4-2
(Continued)

Mode Number	Frequency (Hz)	Modal Weight (lb)		
		$X^{(1)}$	$Y^{(1)}$	$Z^{(1)}$
55	36.3	4657.98	130.38	130.31
56	36.6	3.51	0.09	862.99
57	37.1	8.84	17.04	72.04
58	37.7	18.96	300.71	1.19
59	38.8	6934.50	651.28	39.13
60	39.1	24.40	342.94	43.18
61	39.5	410.13	13.06	232.30
62	39.6	379.18	1928.59	2.93
63	39.9	2953.26	609.59	77.66
64	40.9	161.11	224.17	4.92
65	41.5	979.91	1.92	95.34
66	41.7	7112.19	86.79	370.73
67	42.3	1.03	22.29	3.13
68	42.4	247.19	2625.21	8.77
69	43.2	54.39	37.43	511.73
70	43.6	2.56	0.13	448.55
71	43.8	77.07	92.90	17708.89
72	44.1	1805.77	51.67	105.81
73	44.9	2654.88	167.55	683.04
74	45.2	149.38	12.68	172.16
75	45.3	821.75	2.72	12.17
76	45.8	13.99	462.33	530.19
77	46.1	54.50	187.50	581.28
78	46.1	26.99	45.55	436.15
79	46.2	33.94	165.64	331.53
80	46.2	265.97	222.07	331.73
81	46.5	387.82	2466.27	1991.08

Table 3-2.4-2

(Continued)

Mode Number	Frequency (Hz)	Modal Weight (lb)		
		$X^{(1)}$	$Y^{(1)}$	$Z^{(1)}$
82	47.1	207.55	141.49	1157.66
83	48.2	0.06	29.02	37.66
84	49.0	7.00	11.88	5.59
85	49.5	49.77	5.63	31.60
86	50.2	13.74	798.07	0.44
87	50.6	93.05	99.11	37.43
88	51.5	663.79	180.59	5.86
89	52.0	933.91	21.16	77.07
90	52.6	102.95	81.19	283.46
91	53.0	149.14	72.68	62.25
92	54.1	28.20	635.88	16.76
93	54.1	46.49	855.43	1.05
94	54.2	2.12	11.25	13.18
95	54.2	0.00	0.00	639.57
96	54.2	0.00	0.00	639.57
97	54.3	17.20	1.24	8.07
98	54.5	2.97	114.11	39.17
99	55.1	38.91	480.01	125.40
100	55.8	1.17	383.32	2.15
101	57.4	163.92	328.41	28.50
102	57.6	588.49	95.05	44.43
103	60.1	2.33	20.05	129.83
104	60.4	45.34	122.75	1778.10
105	61.6	0.03	0.11	35.40
106	62.1	0.70	2.84	6.20
107	62.5	33.80	14.04	163.04
108	63.3	63.98	322.23	0.08

Table 3-2.4-2
(Continued)

Mode Number	Frequency (Hz)	Modal Weight (lb)		
		$X^{(1)}$	$Y^{(1)}$	$Z^{(1)}$
109	63.9	1.12	100.41	147.14
110	64.4	44.20	17.89	694.94
111	64.7	1.24	3.40	314.51
112	65.0	87.88	290.09	1462.63
113	65.2	10.94	13.44	250.90
114	65.7	225.93	200.10	120.91
115	66.2	29.29	307.51	8.43
116	66.7	42.81	14.15	254.53
117	67.2	1.13	1292.01	9.65
118	67.8	0.01	1404.02	57.79
119	68.2	0.57	956.14	125.02
120	71.6	69.37	43.25	1850.05
121	72.6	86.57	240.37	397.08
122	72.9	0.20	1.32	1340.95
123	73.6	7.15	172.93	0.62
124	74.7	17.57	107.29	380.90
125	76.0	49.96	218.07	149.35
126	76.4	63.40	22.31	8246.23
127	77.4	3.99	57.05	15.35
128	78.8	18.30	50.10	30.00
129	79.5	63.12	15.44	233.49
130	79.8	14.15	2.86	7.96
131	80.8	19.28	60.54	3.32
132	80.9	49.55	27.17	10.31
133	81.3	14.77	106.00	133.48
134	82.5	401.07	9.79	0.21
135	83.4	151.82	7.10	6193.34

Table 3-2.4-2
(Concluded)

Mode Number	Frequency (Hz)	Modal Weight (lb)		
		$X^{(1)}$	$Y^{(1)}$	$Z^{(1)}$
136	84.4	40.53	226.88	369.81
137	85.4	0.03	96.64	1440.60
138	87.1	19.97	39.22	1484.18
139	88.4	69.50	8.04	2724.94
140	89.7	11.21	24.77	1025.43
141	90.1	2.06	0.17	351.24
142	90.5	0.03	84.91	15.26
143	92.1	7.14	85.09	390.39
144	92.5	0.01	29.73	23.15
145	94.2	1.70	100.69	78.34
146	95.9	3.94	8.06	0.01
147	97.5	4.03	3.16	0.35
148	98.6	34.48	195.46	21.51
149	98.9	4.40	78.20	47.56
150	99.2	13.16	225.76	100.63

Note:

1. See Figure 3-2.4.1 for coordinate system directions.

Table 3-2.4-3

STRUCTURAL FREQUENCIES FOR
HARMONIC LOADS ANALYSIS

Vent System Component	Type of Load	Dominant Frequency (Hz)
Downcomer (with water)	Lateral	13.92
Downcomer (without water)	Lateral	16.06
Vent Line	Internal Pressure	13.92 (1)
Vent Header	Internal Pressure	13.92 (1)
Midcylinder NVB Support Column	Submerged Drag	39.63
Mitered Joint Support Column	Submerged Drag	23.85
Midcylinder VB Support Column	Submerged Drag	38.22

Note:

1. Dominant frequency for vent system pressure load is taken as the lowest structural frequency obtained from the 1/16th segment model frequency analysis.

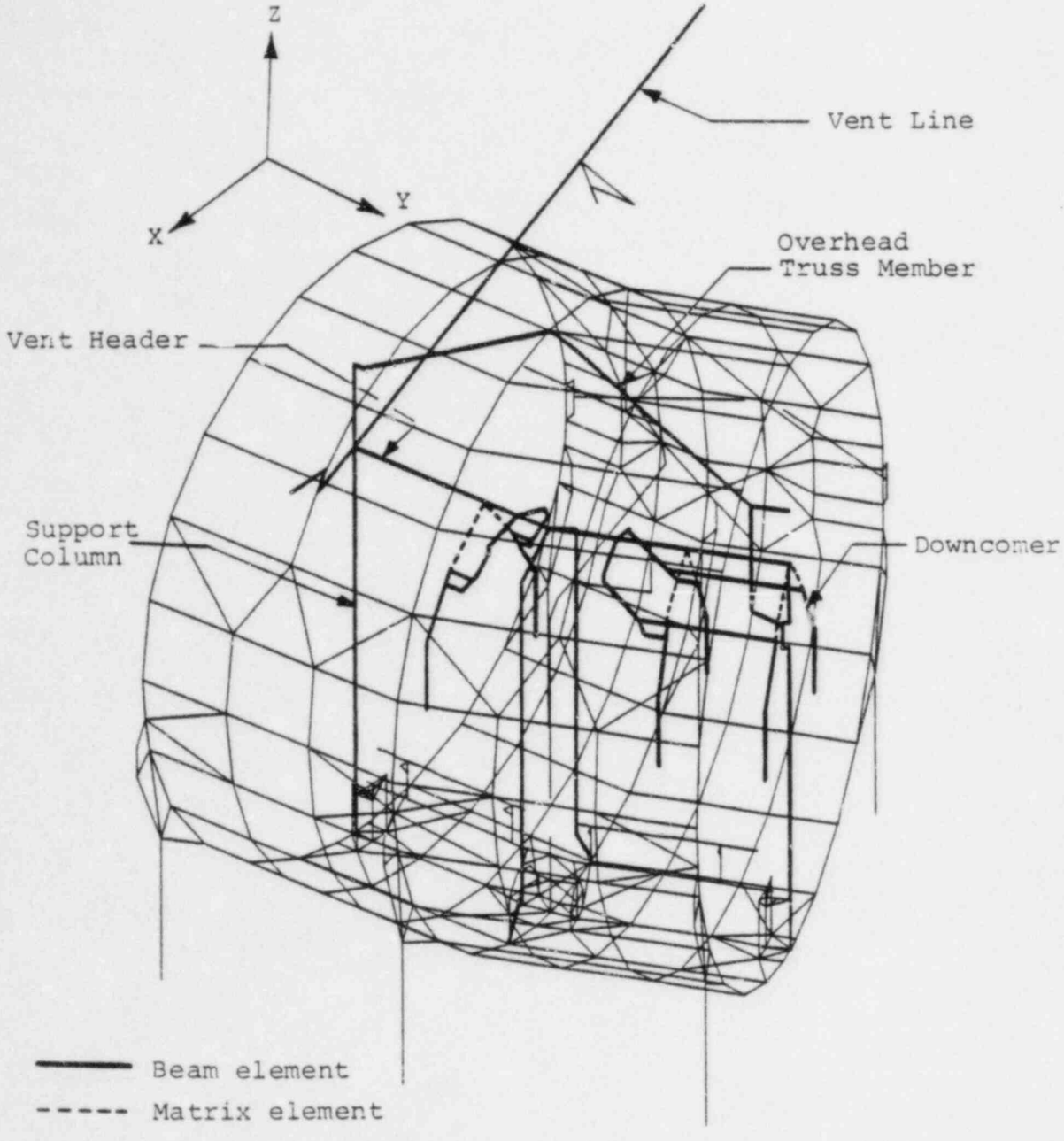

Figure 3-2.4-1

VENT SYSTEM 1/16th SEGMENT BEAM AND FINITE ELEMENT MODEL - ISOMETRIC VIEW

3-2.4.2 Analysis for Asymmetric Loads

The analysis of the vent system for asymmetric loads is performed for a typical 180° segment of the vent system cut along the plane of a principal azimuth. A beam model of a 180° segment of the vent system, shown in Figure 3-2.4-2, is used to obtain the response of the vent system to asymmetric loads. The model includes the vent line, vent header, downcomers, support columns, and overhead truss members.

Many of the modeling techniques used in the 180° beam model, such as those used for local mass and stiffness determination, are the same as those utilized in the 1/16th segment model of the vent system discussed in Section 3-2.4.1. The local stiffness effects at the vent line-drywell penetrations are included using stiffness matrix elements for these penetrations. The local stiffness effects of the vent line-vent header intersections and vent header-downcomer intersections are included using beams which account for these local stiffnesses. The local stiffness effects at the attachments of the support columns and overhead truss members to the vent system are included using beams which account for the local stiffnesses at the attachment locations.

The 180° beam model contains 302 nodes, 325 beam elements, and 4 matrix elements. The model is less refined than the 1/16th segment model of the vent system, and is used to characterize the overall response of the vent system to asymmetric loadings. It includes those component parts and local stiffnesses which have an effect on the overall response of the vent system. The mass properties used in the model are based on the nominal dimensions and densities of the materials used to construct the vent system. The stiffness properties are based on corroded thicknesses. Small displacement linear-elastic behavior is assumed throughout.

The boundary conditions used in the 180° beam model are both physical and mathematical in nature. The physical boundary conditions include elastic restraints which represent the suppression chamber stiffnesses at the attachments of the support columns and overhead truss members to the ring beams. Additional physical boundary conditions include the elastic restraints provided at the attachment of the vent line to the drywell. The mathematical boundary conditions used in the model consist of a symmetry boundary at the 0°-180° plane.

Additional mass is lumped along the length of the submerged portion of the downcomers and support columns in a manner similar to that used in the 1/16th segment model. The mass of water inside the submerged portion of the downcomers is also included. An additional mass of 600 pounds is lumped at the center of gravity of the drywell/wetwell vacuum breaker. The masses of other vent system component parts are also lumped at the appropriate locations in the model.

The asymmetric loads which act on the vent system include horizontal seismic loads and asymmetric chugging loads as specified in Section 3-2.2.1. An equivalent static analysis is performed for each of the loads using the 180° beam model.

The magnitudes and characteristics of governing asymmetric loads on the vent system are presented and discussed in Section 3-2.2.1. The overall effects of asymmetric loads on the vent system are evaluated using the 180° beam model and the general analysis techniques discussed in the preceding paragraphs. The specific treatment of each load which results in asymmetric loads on the vent system is discussed in the paragraphs which follow.

2. Seismic Loads

a. OBE Loads: A static analysis is performed for a N-S horizontal and an E-W horizontal seismic acceleration applied to the weight of steel and water included in the 180° beam model. The horizontal accelerations used in the analysis is obtained from the original design basis documented in the plant's FSAR at the dominant suppression chamber horizontal frequency of 12.15 hertz.

b. SSE Loads: The procedure used to evaluate N-S horizontal and E-W horizontal SSE accelerations is the same as that discussed for OBE loads in load case 2a.

7. Chugging Loads

a. Chugging Downcomer Lateral Loads: A static analysis is performed for chugging downcomer lateral load cases 1 through 3, shown in Table 3-2.2-11.

Use of the methodology described in the preceding paragraphs results in a conservative evaluation of vent system response to the asymmetric loads defined in NUREG-0661.

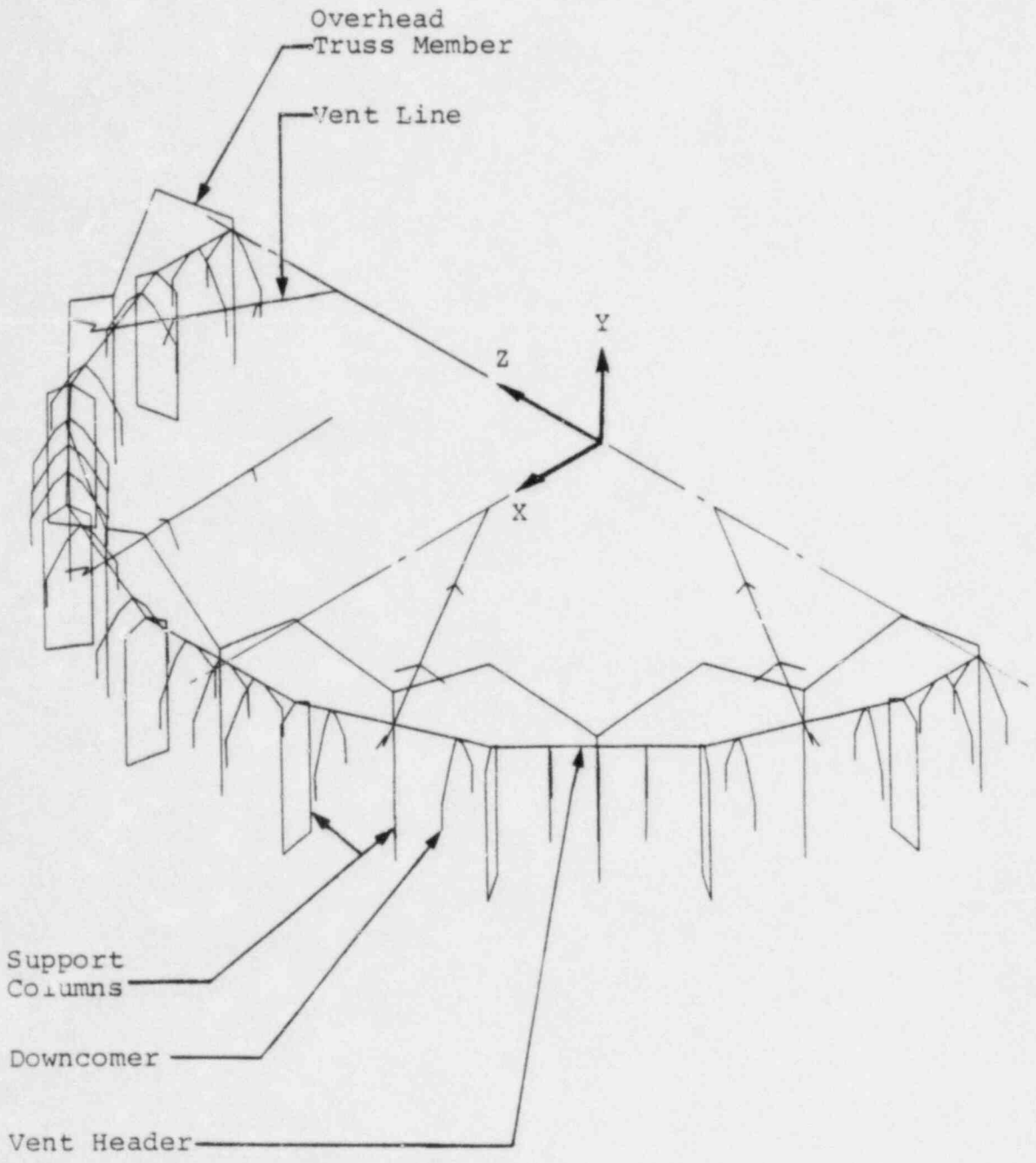

Figure 3-2.4-2

VENT SYSTEM 180° BEAM MODEL - ISOMETRIC VIEW

3-2.4.3 Analysis for Local Effects

The penetrations and intersections of the major components of the vent system are evaluated using refined analytical models of each penetration and intersection. These include the vent line-drywell penetration, the vent line-SRV piping penetration, the vent line-vent header intersection, and the downcomer-vent header intersection. The analytical models used to evaluate these penetrations and intersections are shown in Figures 3-2.4-3 through 3-2.4-6. An additional analysis is performed to evaluate local effects of pool swell impact loads on the vent header, which is discussed in detail in Section 3-2.4.4.

Each of the penetration and intersection analytical models includes mesh refinement near discontinuities to facilitate evaluation of local stresses. The stiffness properties used in the model are based on corroded thicknesses of the materials used to construct the penetrations and intersections. Small displacement linear-elastic theory is assumed throughout.

The analytical models are used to generate local stiffnesses of the penetrations and intersections for use in the 1/16th segment model and the 180° beam model as

discussed in Sections 3-2.4.1 and 3-2.4.2. Local stiffnesses are developed which represent the stiffness of the entire penetration or intersection in terms of a few local degrees of freedom on the penetration or intersection. This is accomplished either by applying unit forces or displacements to the selected local degrees of freedom, or by performing a matrix condensation to reduce the total stiffness of the penetration or intersection to those of the selected local degrees of freedom. The results are used to formulate stiffness matrix elements or beam elements which are added to the 1/16th beam model and the 180° beam model at the corresponding penetration or intersection locations.

The analytical models are also used to evaluate stresses in the penetrations and intersections. The applied loads, which are extracted from the 1/16th model and 180° beam model results, consist of loads acting on the penetration and intersection model boundaries and of loads acting on the interior of penetration and intersection models. The loads acting on the penetration and intersection model boundaries are the beam end loads taken from the 1/16th segment model and 180° beam model analyses at locations coincident with the penetration or intersection model boundary locations. The distributed loads include the pressures

and acceleration loads applied to penetration and intersection models to account for internal pressure loads, thrust loads, pool swell loads, and inertia loads.

Loads which act on the shell segment boundaries are applied to the penetration and intersection models through a system of radial beams. The radial beams extend from the middle surface of each of the shell segments to a node located on the centerline of the corresponding shell segment. The beams have large bending stiffnesses, zero axial stiffness and are pinned in all directions at the shell segment middle surface. Boundary loads applied to the centerline nodes cause only axial and shear loads to be transferred to the shell segment middle surface with no local bending effects. Use of this boundary condition minimizes end effects on penetration and intersection stresses in the local areas of interest. The system of radial beams constrains the boundary planes to remain plane during loading, which is consistent with the assumption made in small deflection beam theory.

A description of each vent system penetration and intersection analytical model and its use is provided in the paragraphs which follow.

- Vent Line-Drywell Penetration Axisymmetric Finite Difference Model: The vent line-drywell penetration model shown in Figure 3-2.4-3 includes a segment of the drywell shell, the jet deflector and gusset plates, the insert plate, the conical transition piece, and the vent line. The analytical model contains 9 segments with 126 mesh points. The reaction loads applied to the model include those computed at the upper end of the vent line. The distributed loads applied to the model include internal pressure loads.

- Vent Line-SRV Piping Penetration Finite Element Model: The vent line-SRV piping penetration model shown in Figure 3-2.4-4 includes a segment of the vent line, the penetration insert plate, the penetration nozzle, and the associated nozzle stiffener plates. The model contains 822 nodes, 86 beam elements, and 925 plate bending and stretching elements. Each end of the vent line shell segment is effectively restrained against translation and rotation. Both symmetric and antisymmetric boundary conditions on the vertical plane through the vent line centerline are used in the analysis. The boundary loads applied to the

analytical model include the drywell and wetwell SRV piping reaction loads.

- Vent Line-Vent Header Intersection Finite Element Model: The vent line-vent header intersection finite element model shown in Figure 3-2.4-5 includes a segment of the vent line, a segment of the vent header, and the vacuum breaker support. The model contains 864 nodes, 87 beam elements, and 1114 plate bending and stretching elements. The end of the vent line shell segment is restrained against translation and rotation. Boundary loads are applied at each end of the vent header shell segment, at the end of the vacuum breaker support, and at the vent system support column and overhead truss member attachment locations. The distributed loads applied to the analytical model include internal pressure loads, thrust loads, and inertia forces from dynamic loadings.

- Downcomer-Vent Header Intersection Finite Element Model: The downcomer vent header intersection finite element model shown in Figure 3-2.4-6 includes a segment of the vent header, a segment of each downcomer, the crotch plate, the downcomer

rings, the outer stiffener plates, the vent header ring plates, and the upper and lower longitudinal plates. The analytical model contains 1137 nodes, 161 beam elements, and 1400 plate bending and stretching elements. Restraints are provided at each end of the vent header shell segment. Boundary loads are applied at the ends of the downcomer segments, and at the vent system support column, the overhead truss, and the downcomer bracing attachment locations. The distributed loads applied to the model include internal pressure loads and thrust loads.

For the SBA II combination, stresses in the downcomer-vent header intersection due to SRV discharge loads, chugging downcomer lateral loads, and seismic loads are combined using the SRSS method. Use of SRSS is appropriate since the combination of the maximum chugging downcomer lateral load, which is impulsive in nature, with the maximum SRV discharge loads and seismic loads is a low-probability event.

Use of the methodology described in the preceding paragraphs results in a conservative evaluation of vent system local stresses due to the loads defined in NUREG-0661.

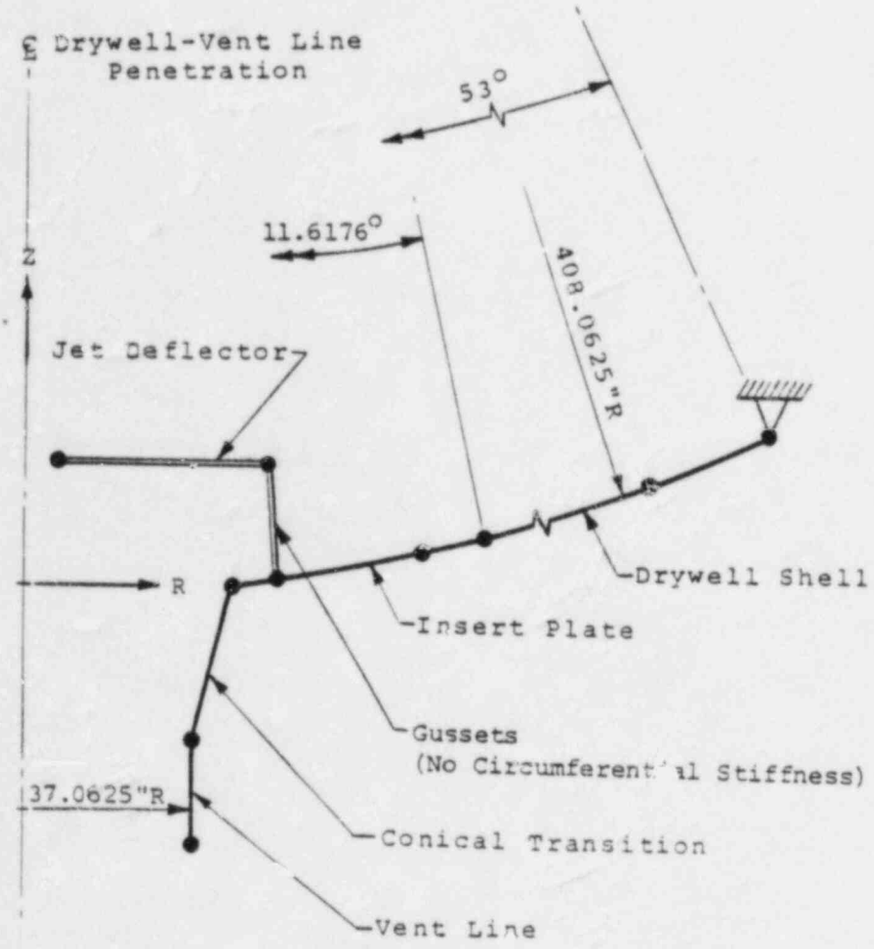

Figure 3-2.4-3

VENT LINE-DRYWELL PENETRATION AXISYMMETRIC FINITE DIFFERENCE MODEL - VIEW OF TYPICAL MERIDIAN

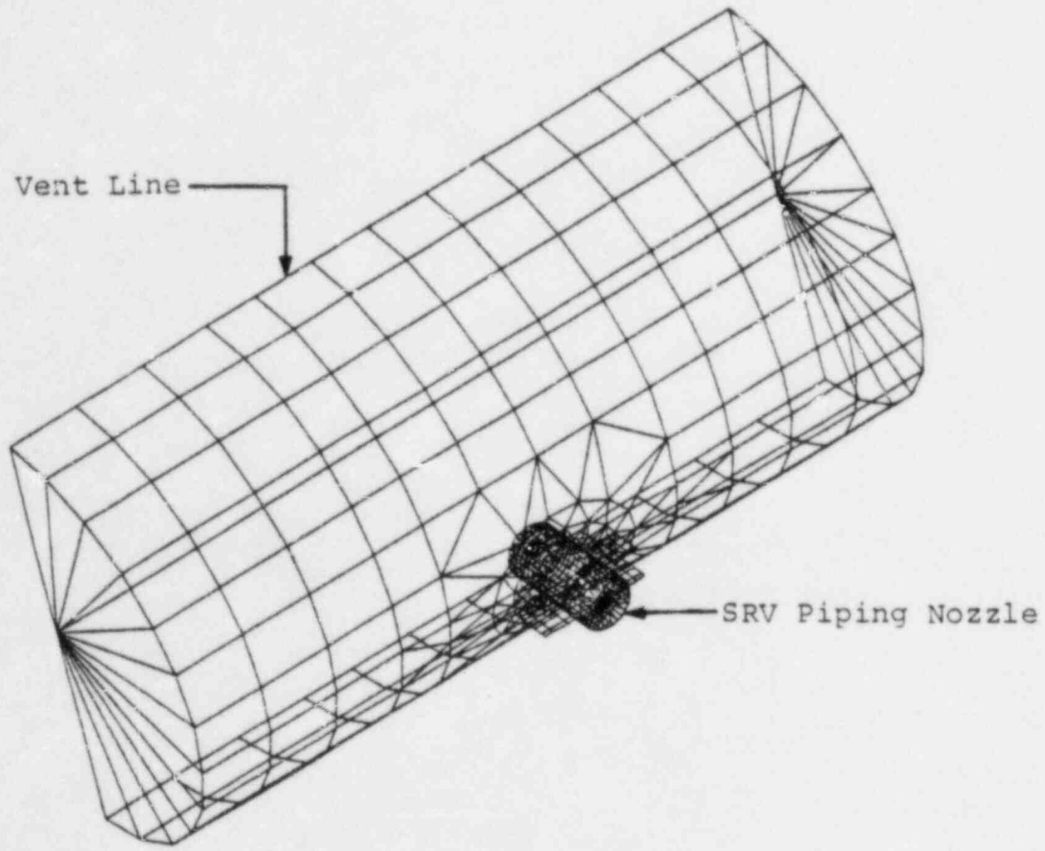

Figure 3-2.4-4

SRV PIPING-VENT LINE PENETRATION FINITE ELEMENT MODEL - ISOMETRIC VIEW

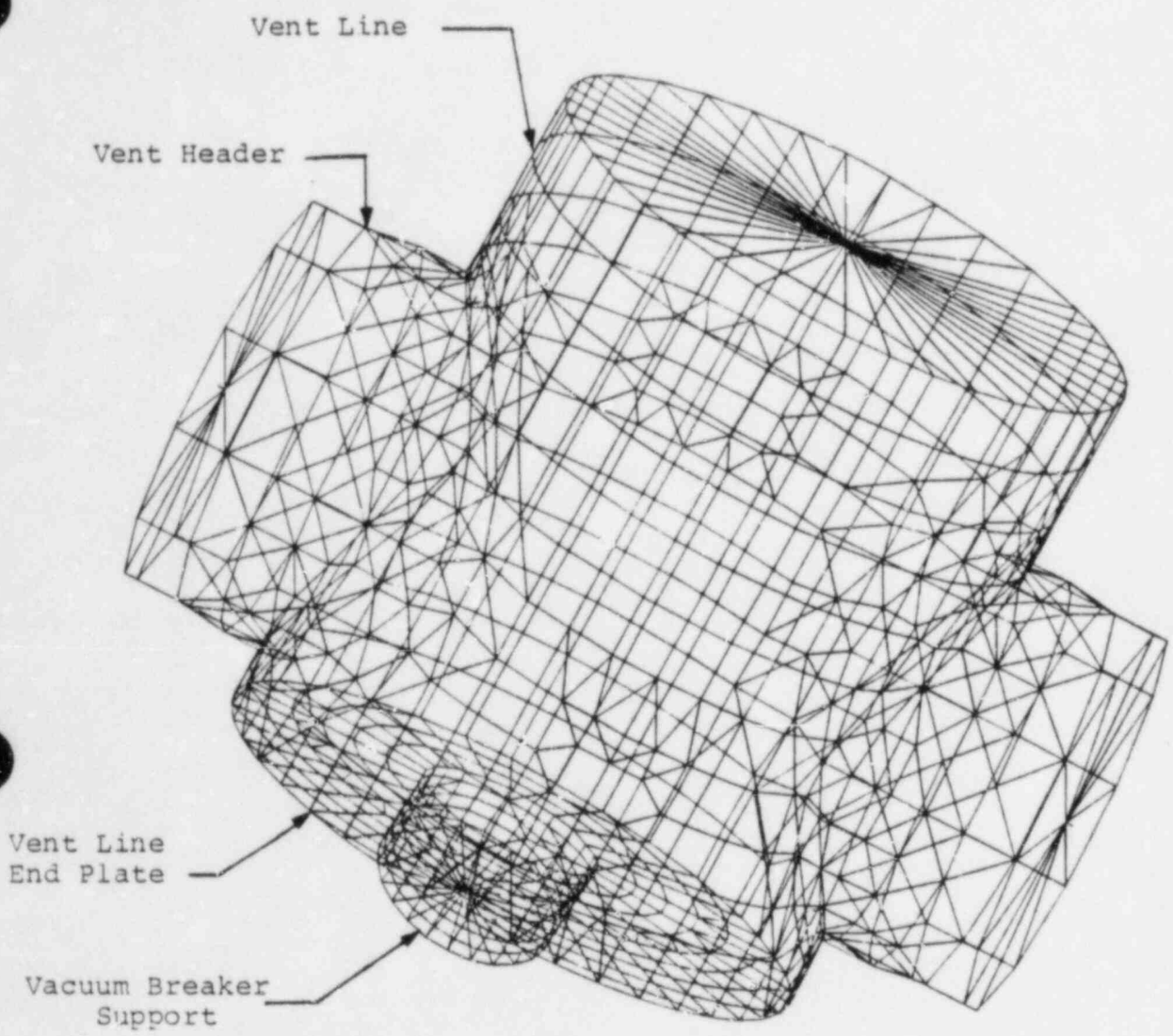

Figure 3-2.4-5

VENT LINE-VENT HEADER INTERSECTION
FINITE ELEMENT MODEL - ISOMETRIC VIEW

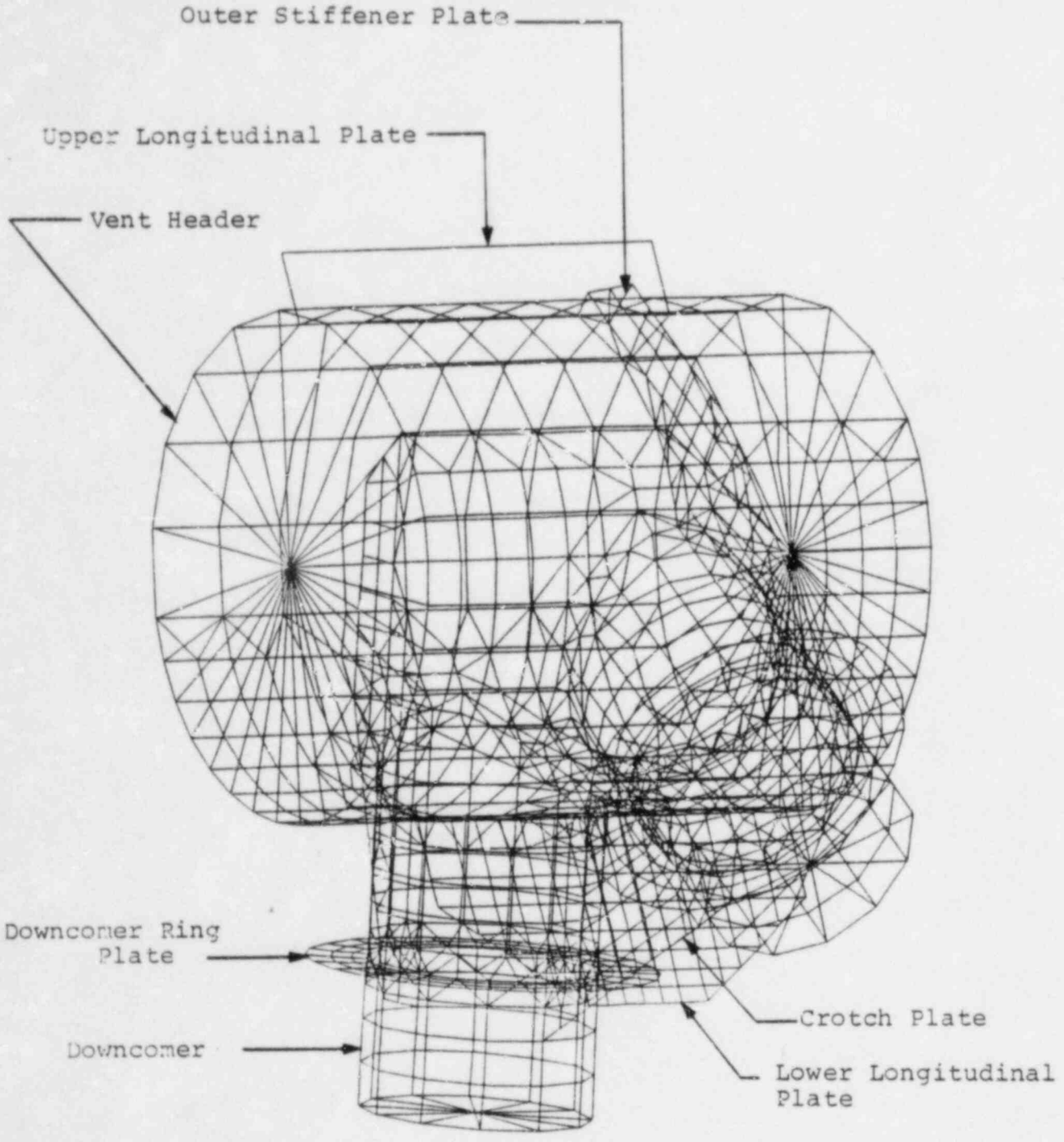

Figure 3-2.4-6

DOWNCOMER-VENT HEADER INTERSECTION
FINITE ELEMENT MODEL - ISOMETRIC VIEW

3-2.4.4 Analysis of Vent Header for Local Effects of Pool Swell Impact Loads

The analysis for the overall effects of pool swell impact loads on the vent system is performed using the 1/16 segment model discussed in Section 3-2.4.1. The analysis of the vent header for local effects of pool swell impact loads is performed using a detailed 1/32 segment finite element model of the vent header in the non-vent bay. The 1/32 segment model is shown in Figure 3-2.4-7.

The 1/32 segment model contains 1684 nodes, 163 beam elements, and 1812 plate bending and stretching elements. The vent header, the angled segments of the downcomers, the downcomer ring plates, the crotch plates, the outer gusset plates, the vent header ring plates, and the lower longitudinal plate are modeled using finite elements. Beam elements are used to model the upper longitudinal plate, the support columns, the overhead truss member, and the vertical segments of the downcomers. The stiffness properties used in the model are based on corroded thicknesses. The mass densities used in the model are adjusted to simulate the weight of the structure with nominal material dimensions.

Small displacement linear - elastic behavior is assumed throughout.

The boundary conditions used in the 1/32 segment model are both physical and mathematical in nature. The physical boundary conditions include a beam model representation of the vent line bay, which includes the vent header, vent line, and supports, attached to the 1/32 model at the vent header mitered joint. This beam representation of the vent bay accounts for both mass and stiffness effects. The flexibility of the drywell is included at the vent line penetration location. The mathematical boundary conditions consist of symmetry boundaries imposed at the centerlines of the vent bay and non-vent bay. The support columns and overhead truss members are assumed to be fixed at the suppression chamber.

Additional mass is lumped along the length of the submerged portions of the downcomers and support columns to account for the effective mass of water which acts with these structures during dynamic loadings.

A frequency analysis is performed using the 1/32 segment model and the first 100 structural modes, up to

342 hertz, are computed. A dynamic transient analysis is performed for the pool swell impact loads on the vent header. The maximum pool swell impact pressures applied to the vent header at bottom dead center are shown in Figure 3-2.2-2. Selected pool swell impact pressure transients are provided in Table 3-2.2-5. A total of 99 independent vent header loading transients are used in the analysis.

An equivalent static analysis is performed for the pool swell impact loads on the downcomer ring plates and the angled portions of the downcomers. These loads are defined in Table 3-2.2-4.

The methodology described in the preceeding paragraphs results in a conservative evaluation of the local response of the vent header to the pool swell impact loads defined in NUREG-0661.

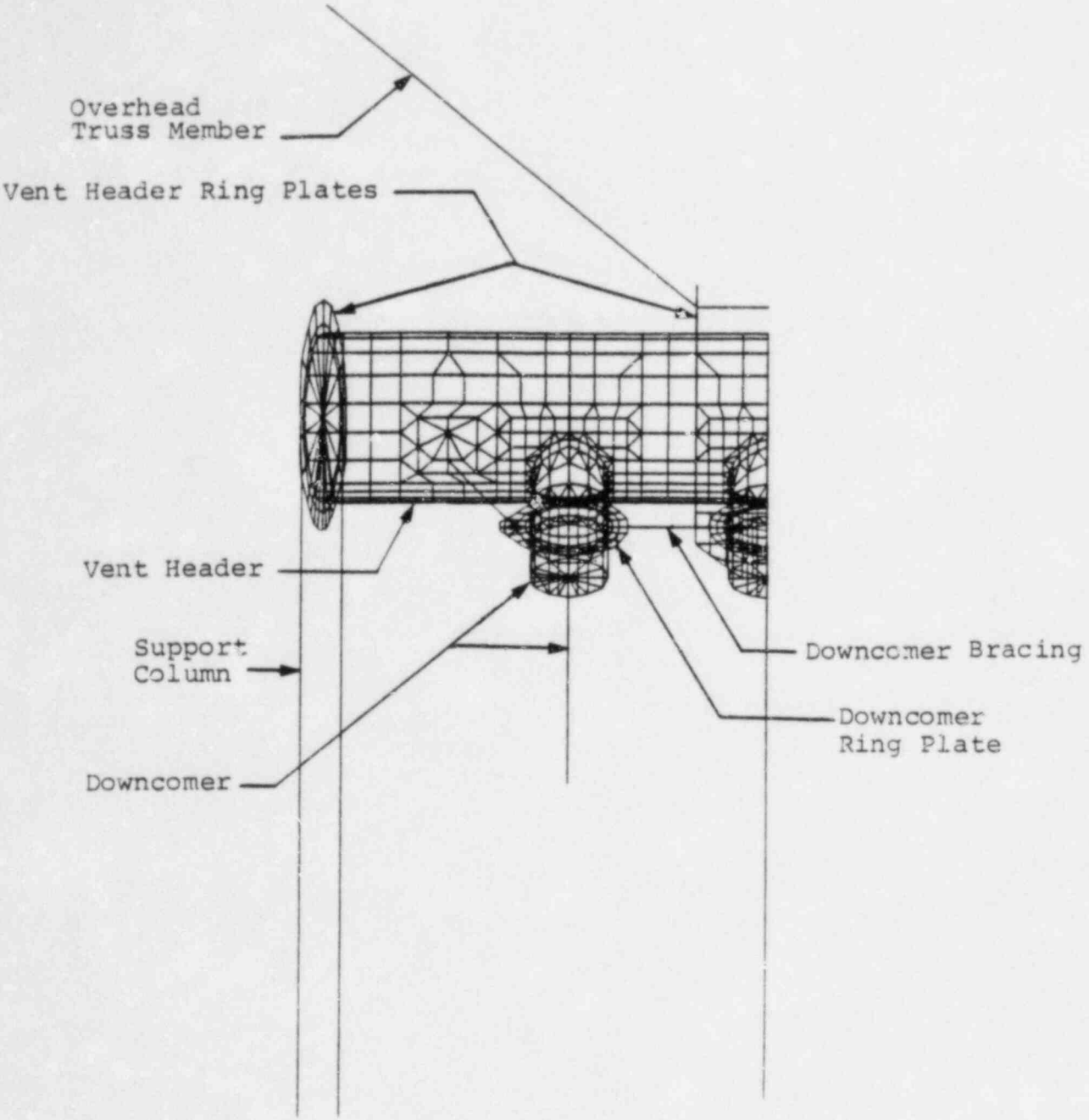

Figure 3-2.4-7

VENT SYSTEM 1/32 SEGMENT FINITE ELEMENT MODEL
FOR POOL SWELL IMPACT ANALYSIS
- ELEVATION VIEW

3-2.4.5 Methods for Evaluating Analysis Results

The methodology discussed in Sections 3-2.4.1 and 3-2.4.2 is used to determine element forces and component stresses in the vent system component parts. The methodology used to evaluate the analysis results, determine the controlling stresses in the vent system components parts, and examine fatigue effects is discussed in the paragraphs which follow.

To evaluate analysis results for the vent system Class MC components, membrane and extreme fiber stress intensities are computed. The values of the membrane stress intensities away from discontinuities are computed using 1/16th segment model and 180° beam model results. These stresses are compared with the primary membrane stress allowables contained in Table 3-2.3-1. The values of membrane stress intensities near discontinuities are computed using results from the penetration and intersection analytical models. These stresses are compared with local primary membrane stress allowables contained in Table 3-2.3-1. Primary stresses in vent system Class MC component welds are computed using maximum principal stresses or the resultant forces acting on the weld throat. The results are compared to primary weld stress allowables

contained in Table 3-2.3-1. Secondary weld stresses are computed in a similar manner, and include the effects of thermal loads. The results are compared to the secondary weld stress allowables contained in Table 3-2.3-1.

Many of the loads contained in each of the controlling load combinations are dynamic loads which result in stresses which cycle with time and are partially or fully reversible. The maximum stress intensity ranges for all vent system Class MC components are calculated using the maximum values of the extreme fiber stress differences which occur near discontinuities in the penetration and intersection analytical models. These stresses are compared to the secondary stress range allowables contained in Table 3-2.3-1.

To evaluate the vent system Class MC component supports, beam end loads obtained from the 1/16th segment model and 180° beam model results are used to compute stresses. The results are compared with the corresponding allowable stresses contained in Table 3-2.3-1. Stresses in vent system Class MC component support welds are obtained using the 1/16th segment model and 180° beam model results to compute the maximum resultant force acting on the associated

weld throat. The results are compared to weld stress limits discussed in Section 3-2.3.

The controlling vent system load combinations are defined in Section 3-2.2.2. During load combination formulation, the maximum stress components in a particular vent system part at a given location are combined for the individual loads contained in each combination. The stress components for dynamic loadings are combined so as to obtain the maximum stress intensity.

The maximum differential displacements of the vent line bellows are determined using results from the 1/16 segment model and the 180° beam model. The displacements of the attachment points of the bellows to the suppression chamber and to the vent line are determined for each load case. The differential displacement is computed from these values. The results for each load are combined to determine the total differential displacements for the controlling load combinations. These results are compared to the allowable bellows displacements in Table 3-2.3-2.

To evaluate fatigue effects in the vent system Class MC components and associated welds, extreme fiber alternating stress intensity histograms for each load in each event or combination of events are determined. Fatigue effects for chugging downcomer lateral loads are evaluated using the stress reversal histrograms shown in Table 3-2.2-11. Stress intensity histograms are developed for the vent system major components and welds with the highest stress intensity ranges. Fatigue strength reduction factors of 2.0 for major component stresses and 4.0 for component weld stresses are conservatively used to account for peak stresses at all locations. For each combination of events, a load combination stress intensity histogram is formulated and the corresponding fatigue usage factors are determined using che curve shown in Figure 3-2.4-8. The usage factors for each event are then summed to obtain the total fatigue usage.

Use of the methodology described above results in a conservative evaluation of the vent system design margins.

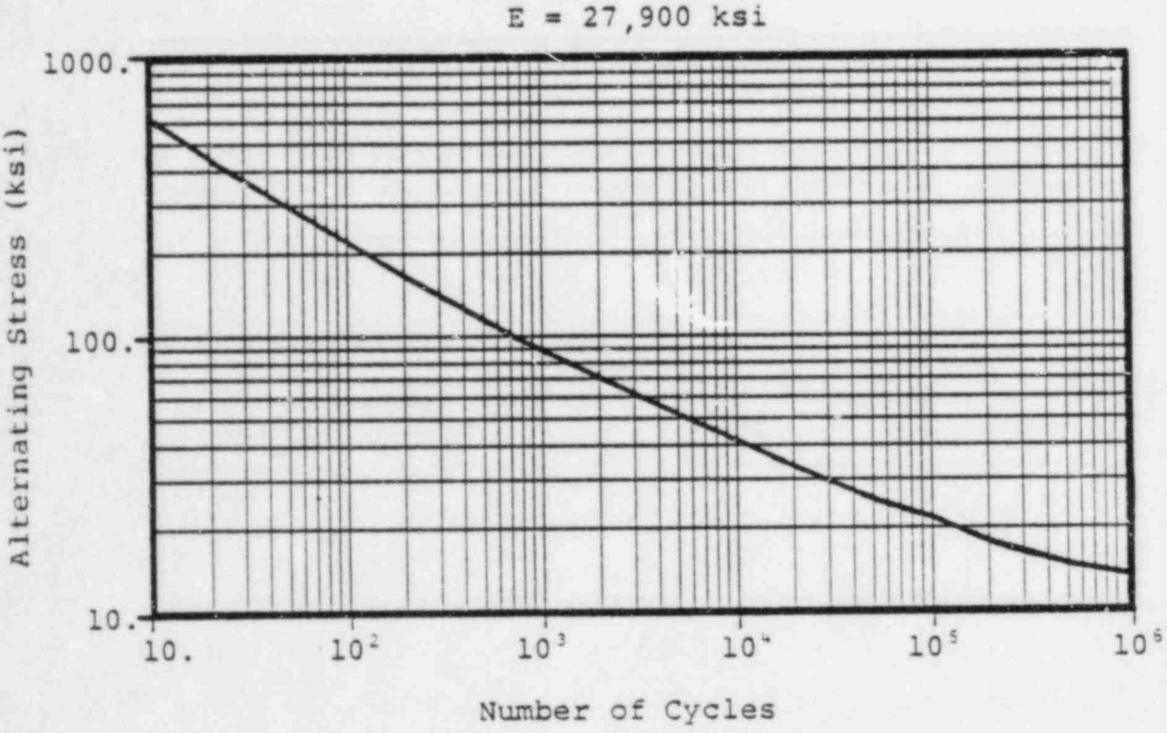

Figure 3-2.4-8

ALLOWABLE NUMBER OF STRESS CYCLES FOR VENT SYSTEM

FATIGUE EVALUATION

3-2.5 Analysis Results and Conclusions

The geometry, loads and load combinations, acceptance criteria, and analysis methods used in the evaluation of the Hope Creek vent system are presented and discussed in the preceding sections. The results and conclusions derived from the evaluation of the vent system are presented in the paragraphs and sections which follow.

The maximum primary membrane stresses for the major components of the vent system are shown in Table 3-2.5-1 for each of the governing loads. The corresponding loads for the vent system support columns are shown in Table 3-2.5-2. The transient response of selected vent system support columns for pool swell loads are shown in Figures 3-2.5-1 and 3-2.5-2.

The maximum stresses and associated design margins for the major vent system components, component supports, and welds for the SBA II, DBA II, and DBA III load combinations are shown in Table 3-2.5-3. The maximum stresses and associated design margins for the components and welds of the vent line-SRV piping penetration for the SBA II and DBA III load combinations are shown in Table 3-2.5-4. The maximum differential

displacements and design margins for the vent line bellows for the SBA II, DBA II, and DBA III load combinations are shown in Table 3-2.5-5. The fatigue usage factors for the controlling vent system component and weld for the Normal Operating plus SBA events are shown in Table 3-2.5-6. The maximum vacuum breaker accelerations due to dynamic loads on the vent system and suppression chamber shell are summarized in Table 3-2.5-7.

The vent system evaluation results presented in the preceding paragraphs are discussed in Section 3-2.5.1.

Table 3-2.5-1

MAJOR VENT SYSTEM COMPONENT MAXIMUM MEMBRANE STRESSES

FOR GOVERNING LOADS

Section 3-2.2.1 Load Designation		Primary Membrane Stress (ksi)[1]		
Load Type	Load Case Number	Vent Line	Vent Header	Downcomer
Dead Weight	1a	.51	.94	.16
Seismic	2a	.21	.40	.17
	2b	.32	.61	.23
Pressure and Temperature	3b	4.53	2.79	2.82
	3d	N/A	N/A	N/A
Vent System Discharge	4a[3]	4.53	2.79	2.82
Pool Swell	5a-5d	0.68	2.56	2.65
	5e	.01	0.12	0.92
Condensation Oscillation	6a+6c	0.56	0.57	0.57
	6b+6d	0.74	2.41	3.18
	6f[2]	0.21	1.62	0.02
Chugging	7a	0.33	2.73	12.00
	7b	0.46	0.45	0.81
	7c(6e)	-	-	-
	7d	0.21	1.62	0.02
SRV Discharge	8a	0.41	1.90	11.61

Notes:

1. Values shown are maximums irrespective of time and location for individual load types and may not be added to obtain load combination results.
2. Post-chug loads substituted for condensation oscillation loads.
3. DBA internal pressure loads are substituted for vent system discharge loads.

Table 3-2.5-2

MAXIMUM COLUMN LOADS FOR GOVERNING VENT SYSTEM LOADINGS

Section 3-2.2.1 Load Designation				Maximum Support Load (kips)
Load Type		Load Case Number[1]	Direction	
Dead Weight		1a	Compression	6.84
Seismic	OBE	2a	Tension/ Compression	4.60
	SSE	2b	Tension/ Compression	11.80
Internal Pressure		3b	Tension	33.97
Temperature		3d	Compression	83.06
Vent System Discharge		4a[2]	Tension	33.97
Pool Swell		5a-5d	Tension	107.40
			Compression	31.10
Condensation Oscillation	IBA	6a+6c	Tension	27.94
			Compression	27.94
	DBA	6b+6d	Tension	27.94
			Compression	27.94
Chugging		7a+7b	Tension	64.45
			Compression	64.45
SRV Discharge		8a	Tension	60.54
			Compression	60.54

Notes:

1. The effects of containment interaction are included.
2. DBA internal pressure loads are substituted for vent system discharge loads.

Table 3-2.5-3

MAXIMUM VENT SYSTEM STRESSES FOR CONTROLLING LOAD COMBINATIONS

Item	Stress Type	Load Combination Stresses (ksi)					
		SBA II[1]		DBA II[1]		DBA III[1]	
		Calc. Stress	Calc.[2] / Allow.	Calc. Stress	Calc.[2] / Allow.	Calc. Stress	Calc.[2] / Allow.
COMPONENTS							
Drywell Shell	Local Primary Membrane	23.40	0.81	25.00	0.86	24.80	0.86
	Prim. + Sec. Stress Range	63.85	0.94	65.85	0.97	N/A	N/A
Vent Line	Primary Membrane	5.13	0.27	6.69	0.35	9.21	0.48
	Local Primary Membrane	6.59	0.22	6.19	0.21	8.55	0.23
	Prim. + Sec. Stress Range	15.95	0.24	14.34	0.21	N/A	N/A
Vent Header	Primary Membrane	14.05	0.73	10.58	0.55	17.83	0.92
	Local Primary Membrane	26.17	0.90	15.56	0.54	37.66	1.00
	Prim. + Sec. Stress Range	60.42	0.89	30.41	0.45	N/A	N/A
Downcomer	Primary Membrane	17.60	0.91	8.94	0.46	18.28	0.95
	Local Primary Membrane	25.90	0.89	16.25	0.56	28.10	0.75
	Prim. + Sec. Stress Range	56.47	0.83	33.20	0.49	N/A	N/A
COMPONENT SUPPORTS							
Support Columns	Bending	10.41	0.56	9.20	0.50	7.01	0.38
	Tensile	6.00	0.36	2.24	0.13	8.05	0.48
	Combined	0.92	0.92	0.63	0.63	0.86	0.86
	Compressive	5.83	0.41	2.24	0.15	5.79	0.38
	Interaction	0.97	0.97	0.65	0.65	0.76	0.76
WELDS							
Downcomer to Vent Header	Primary	9.16	0.61	5.75	0.38	9.94	0.66
	Secondary	19.97	0.44	11.74	0.26	N/A	N/A

Notes:

1. Reference Table 3-2.2-15 for load combination designations.
2. Reference Table 3-2.3-1 for allowable stresses.
3. Allowable compressive stress based on length of most highly stressed column.

Table 3-2.5-4

MAXIMUM VENT LINE-SRV PIPING PENETRATION STRESSES
FOR CONTROLLING LOAD COMBINATIONS

Item	Stress Type	SBA II[1]		DBA III[1]	
		Calc. (ksi)	Calc./Allow.[2]	Calc. (ksi)	Calc./Allow.[3]
C O M P O N E N T					
Penetration Nozzle	Primary Membrane	15.35	0.93	27.63	0.93
	Local Primary Membrane	24.39	0.99	43.90	0.98
	Primary + Secondary Stress Range	60.01	1.00	N/A	-
W E L D S					
Nozzle to Insert Plate	Primary	9.30	0.80	16.74	0.86
	Secondary	28.93	0.83	N/A	-

Notes:

1. Reference Table 3-2.2-15 for load combination designations.
2. Reference Table 3-2.3-1 for allowable stresses.
3. Service Level C allowables used. Reference Table 3-2.3-1 for allowable stresses.

Table 3-2.5-5

MAXIMUM VENT LINE BELLOWS DIFFERENTIAL DISPLACEMENTS
FOR CONTROLLING LOAD COMBINATIONS

Displacement Component		SBA II (1)		DBA II (1)		DBA III (1)	
		Calc. (in)	Calc. / Allow. (2)	Calc. (in)	Calc. / Allow. (2)	Calc. (in)	Calc. / Allow. (2)
Axial	Compression	0.63	0.50	0.66	0.53	0.67	0.54
	Extension	N/A	N/A	N/A	N/A	N/A	N/A
Lateral	w/Axial Compression	0.18	0.24	0.12	0.16	0.15	0.20
	w/Axial Extension	N/A	N/A	N/A	N/A	N/A	N/A

Notes:

1. Reference Table 3-2.2-15 for load combination designations.
2. Reference Table 3-2.2-2 for allowable displacements.

Table 3-2.5-6

MAXIMUM FATIGUE USAGE FACTORS FOR VENT SYSTEM COMPONENTS AND WELDS

Event Sequence	Load Case Cycles				Condensation Oscillation (sec.)	Chugging[4] (sec.)	Event Usage Factor	
	Seismic	Pressure	Temperature	SRV[3] Discharge			Vent[5] Header	Weld[6]
NOC w/SRV Discharge	0	150[2]	150[2]	596	N/A	N/A	.207	.285
SBA 0. to 600. sec	0	0	0	50	N/A	300.	.215	.265
SBA 600. to 1200 sec	1000[2]	1	1	2	N/A	600.	.208	.241
Maximum Cumulative Usage Factors					NOC + SBA		.629	.791

Notes:

1. See Table 3-2.2-15 and Figure 3-2.2-7 for load cycles and event sequencing information.
2. Entire number of load cycles conservatively assumed to occur during time of maximum event usage.
3. Total number of SRV actuations shown are conservatively assumed to occur in same suppression chamber bay.
4. Each chug-cycle has a duration of 1.4 sec. See Table 3-2.2-12 for chugging downcomer load histogram. The maximum fatigue usage factor for chugging downcomer loads at the downcomer-vent header intersection is .054.
5. The maximum cumulative usage for a vent system component occurs in the downcomer at the downcomer-vent header intersection.
6. The maximum cumulative usage for a vent system component weld occurs at the downcomer-vent header intersection.

Table 3-2.5-7

MAXIMUM VACUUM BREAKER ACCELERATIONS
DUE TO DYNAMIC LOADS

Load	Maximum Acceleration (g's)	
	Vertical	Resultant
Pool Swell Vent System Impact	2.19	2.25
Condensation Oscillation Torus Shell	1.35	1.65
Post-Chug Torus Shell	0.36	0.44
SRV Discharge Torus Shell	2.66	2.76

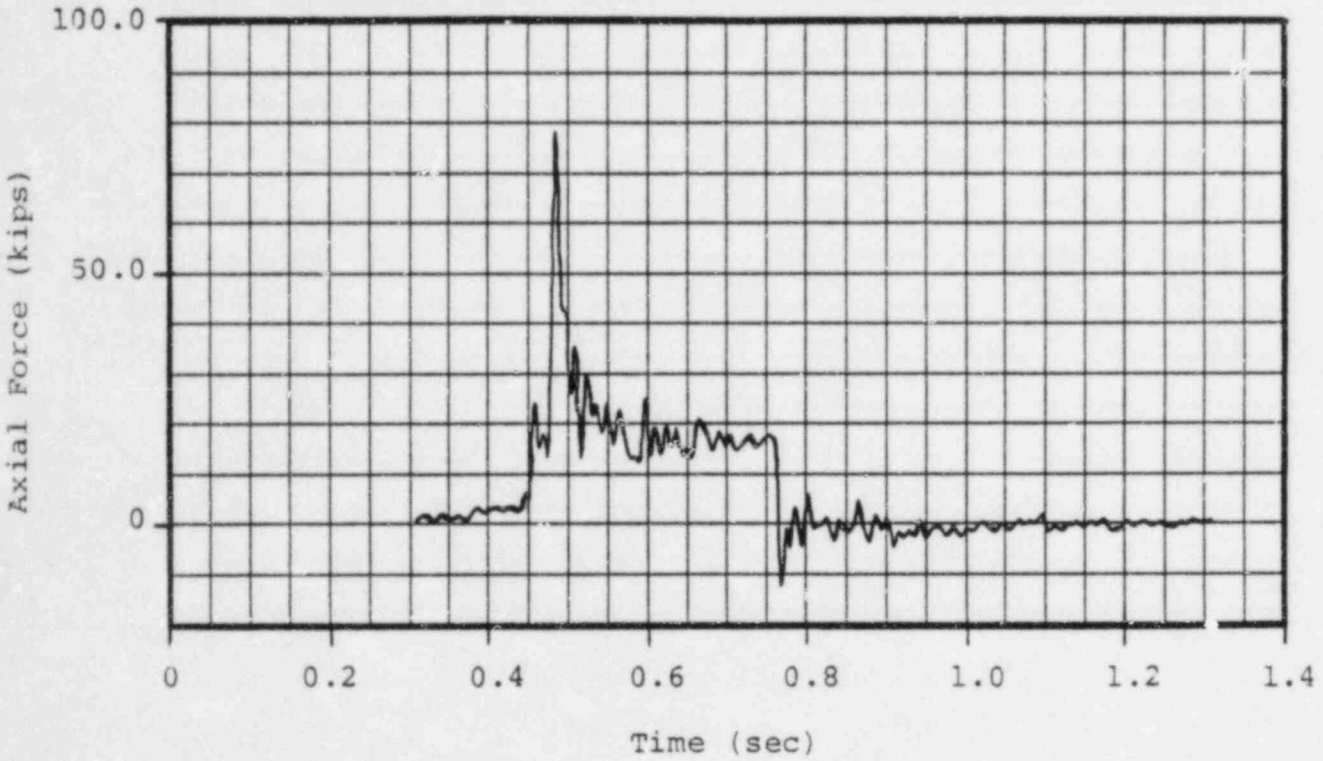

Figure 3-2.5-1

VENT SYSTEM SUPPORT COLUMN RESPONSE DUE TO POOL SWELL IMPACT LOADS - COLUMN AT MIDCYLINDER NON-VENT BAY

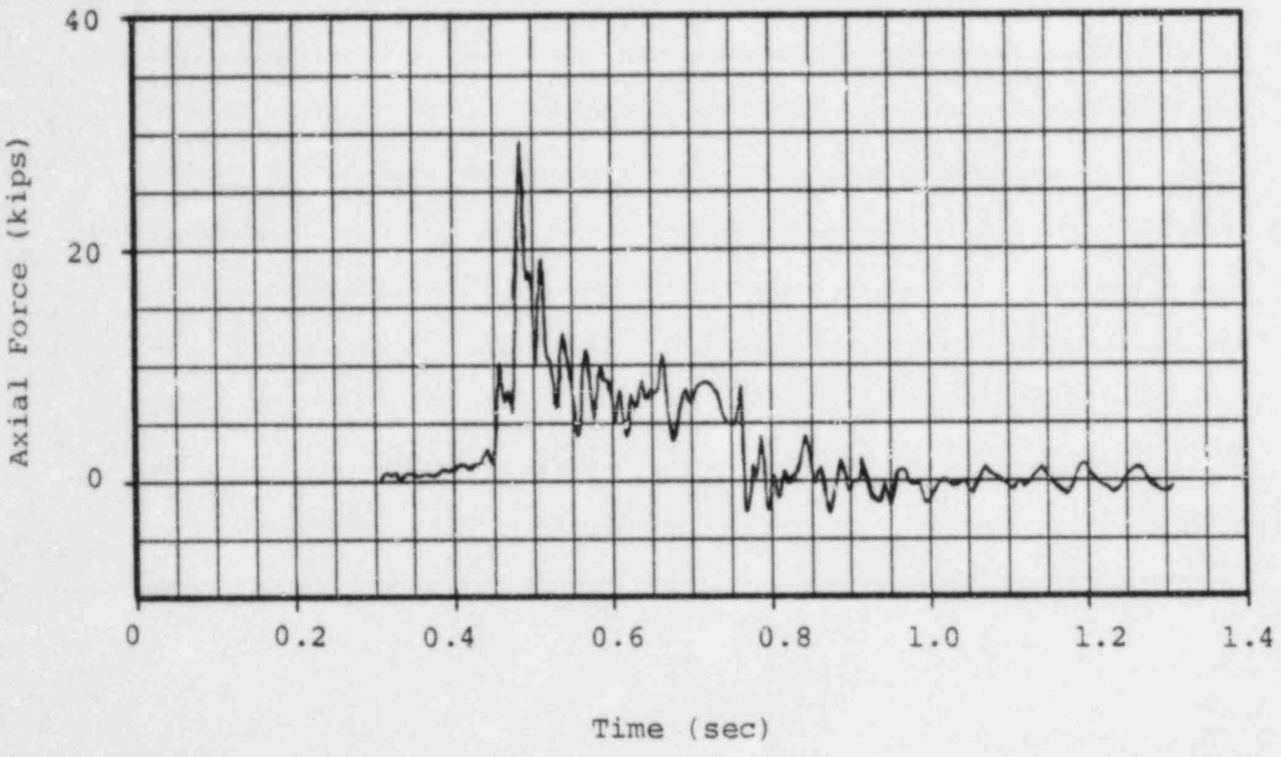

Figure 3-2.5-2

VENT SYSTEM SUPPORT COLUMN RESPONSE DUE TO POOL SWELL IMPACT LOADS - OUTSIDE COLUMN AT MITERED JOINT

3-2.5.1 Discussion of Analysis Results

The results shown in Table 3-2.5-1 indicate that the largest vent system primary membrane stresses occur for internal pressure loads, vent system discharge loads, pool swell impact loads, DBA condensation oscillation downcomer loads, and chugging downcomer lateral loads. The remaining loadings result in small primary stresses in the vent system major components. Table 3-2.5-2 shows that the largest vent system support column reactions occur for thermal loads, pool swell impact loads, chugging loads, and SRV discharge loads.

The results shown in Table 3-2.5-3 indicate that the highest stresses in the vent system components, component supports, and associated welds occur for the SBA II and the DBA III load combinations. The vent line, vent header, and downcomer stresses for the SBA II and DBA III load combinations are less than the allowable limits with stresses in other vent system components, component supports, and welds well within the allowable limits. The stresses in the vent system components, component supports, and welds for the DBA II load combination are also well within the allowable limits.

The results shown in Table 3-2.5-5 indicate that the vent line bellows differential displacements are all well within allowable limits. The maximum displacement occurs for the DBA III load combination.

The loads which cause the highest number of displacement cycles at the vent line bellows are seismic loads, SRV loads, and LOCA related loads such as pool swell, condensation oscillation, and chugging. The bellows displacements for these loads are small compared to the maximum allowable displacement and their effect on fatigue is negligible. Thermal loads and internal pressure loads are the largest contributors to bellows displacements. The specified number of thermal load and internal pressure load cycles is 150. Since the bellows have a rated capacity of 230 cycles at maximum displacement for Normal Operating conditions, their adequacy for fatigue is assured.

The vent system fatigue usage factors shown in Table 3-2.5-6 are computed for the controlling Normal Operating plus SBA events. The governing vent system component for fatigue is the vent header at the downcomer-vent header intersection. The governing vent system weld for fatigue is the downcomer to vent header weld. The magnitudes and cycles of downcomer lateral

loads are the primary contributors to fatigue at this location.

Fatigue effects at other locations in the vent system are less severe than at those described above, due primarily to lower stresses and a lesser number of stress cycles.

3-2.5.2 Conclusions

The vent system loads described and presented in Section 3-2.2.1 are conservative estimates of the loads postulated to occur during an actual LOCA or SRV discharge event. Applying the methodology discussed in Section 3-2.4 to examine the effects of the governing loads on the vent system results in bounding values of stresses and reactions in vent system components and component supports.

The load combinations and event sequencing defined in Section 3-2.2.2 envelop the actual events postulated to occur during a LOCA or SRV discharge event. Combining the vent system responses to the governing loads and evaluating fatigue effects using this methodology results in conservative values of the maximum vent system stresses, support reactions, and fatigue usage factors for each event or sequence of events postulated to occur throughout the life of the plant.

The acceptance limits defined in Section 3-2.3 are at least as restrictive, and in many cases more restrictive, than those used in the original containment design documented in the plant's FSAR. Comparing the resulting maximum stresses and support reactions to

these acceptance limits results in a conservative evaluation of the design margins present in the vent system and vent system supports. As is demonstrated from the results discussed and presented in the preceding sections, all of the vent system stresses and support reactions are within these acceptance limits.

As a result, the components of the vent system described in Section 3-2.1, which are specifically designed for the loads and load combinations used in this evaluation, exhibit the margins of safety inherent in the original design of the primary containment as documented in the plant's FSAR. The intent of the NUREG-0661 requirements, as it relates to the design adequacy and safe operation of the Hope Creek vent system, is therefore considered to be met.

3-3.0 LIST OF REFERENCES

1. "Mark I Containment Long-Term Program," Safety Evaluation Report, NRC, NUREG-0661, July 1980.

2. "Mark I Containment Program Load Definition Report," General Electric Company, NEDO-21888, Revision 2, December 1981.

3. "Mark I Containment Program Plant Unique Load Definition," Hope Creek Generating Station Unit 1, General Electric Company, NEDO-24579, Revision 1, January 1982.

4. "Final Safety Analysis Report (FSAR)," Hope Creek Generating Station, Public Service Electric and Gas Company, Section 3.8, October 1983.

5. "Mark I Containment Program Structural Acceptance Criteria Plant Unique Analysis Application Guide, Task Number 3.1.3," General Electric Company, NEDO-24583-1, October 1979.

6. ASME Boiler and Pressure Vessel Code, Section III, Division 1, 1977 Edition with Addenda up to and including Summer 1977.